World Health Organization
Western Pacific Region

WPSAR
Western Pacific Surveillance and Response Journal

Volume 17, Number 1, 2026, Pages 1–60
p-ISSN: 2094-7321 e-ISSN: 2094-7313

wpsar@who.int | https://ojs.wpro.who.int/

IN THIS ISSUE

Western Pacific Surveillance and Response

WHO Western Pacific Surveillance and Response (WPSAR) is an open access journal dedicated to the surveillance of and response to public health events. The goal of the journal is to create a platform for timely information sharing within our region and globally to enhance surveillance and response activities. WPSAR is a publication managed by the World Health Organization Regional Office for the Western Pacific.

To contact us:

Western Pacific Surveillance and Response
World Health Organization
Office for the Western Pacific Region
United Nations Avenue
1000 Manila, Philippines
wpsar@who.int
https://ojs.wpro.who.int/

p-ISSN: 2094-7321
e-ISSN: 2094-7313

Development and utilization of an open-data, web-based geographic information system to support the response to the 2024 Noto Peninsula earthquake, Japan

Ryo Horiike,[a] Tomoya Itatani,[b] Hisao Nakai[c] and Kentaro Tanaka[d]

Correspondence to Ryo Horiike (email: ryo.horiike@naramed-u.ac.jp)

On 1 January 2024, an earthquake of magnitude 7.6 struck the Noto Peninsula in Japan, causing over 500 deaths and damaging about 160 000 houses.[1] Eight months later, torrential rains in the same area caused a further 14 fatalities and extensive flooding.[2] During the first 4 months of the response, 15 489 people, including public health nurses (PHNs) and Disaster Health Emergency Assistance Teams, were dispatched to Ishikawa Prefecture.[3] Aggregated, real-time disaster data are available to support disaster response via the Shared Information Platform for Disaster Management and the Disaster Digital Information System for Health and Wellbeing, but they are rarely accessible to front-line personnel before their deployment to disaster-affected areas.[4] In early January 2024, we developed an open-data Public Health Nursing map (PHN-Map) on Web-based Geographic Information Systems (WebGIS) architecture, to support public health nursing activities by providing up-to-date situational information and training resources before deployment to the Noto Peninsula. This report describes the development of the WebGIS system and the subsequent addition of 360° images to PHN-Map in September 2024, as well as the results of a user survey.

METHODS

Data integration

Between 2 and 7 January 2024, we downloaded data from National Land Numerical Information, a database of the Geospatial Information Authority of Japan. The extracted data included administrative areas, emergency transport roads, and medical and public facilities.[5] Additional data sets, namely 2020 census grid statistics (the 250-m population mesh from the Statistics Bureau via e-Stat portal[6]) and municipal open data on evacuees, isolated hamlets and temporary housing, were downloaded from public web sites (**Table 1**). Data sets were used to create thematic layers including administrative boundaries, emergency transport roads, medical facilities, shelters, evacuee counts, populations of isolated hamlets and temporary housing.

Several layers required trimming or reformatting before being added to the WebGIS platform and were edited in the Quantum Geographic Information System (QGIS).[7] To maximize speed of deployment, we used Felt,[8] a cloud-based collaborative mapping platform

[a] School of Medicine, Department of Nursing, Nara Medical University, Nara, Japan.
[b] Division of Home Care Nursing, Department of Fundamental and Community Nursing Science, School of Nursing, Faculty of Medicine, University of Miyazaki, Miyazaki, Japan.
[c] Faculty of Nursing, University of Kochi, Kochi, Japan.
[d] Graduate School of Nursing, Department of Nursing, Osaka Metropolitan University, Osaka, Japan.
Published: 16 March 2026
doi: 10.5365/wpsar.2026.17.1.1277

Table 1. **Layers of the PHN-Map**

No.	Data publication period	Type of disaster	Data name	Source	URL
1	Post-disaster	Earthquake and torrential rain	Number of people in isolated settlements	Ishikawa Prefecture Disaster Response headquarters meeting materials	https://www.pref.ishikawa.lg.jp/saigai/202401jishin-taisakuhonbu.html#honbu
2	Post-disaster	Earthquake and torrential rain	Number of evacuees in shelters (Nanao City)	raokiey and Nanao City web site	https://github.com/raokiey/R06-Noto-Peninsula-EQ-open-shelter-Nanao/blob/main/README.md
3	Post-disaster	Earthquake and torrential rain	Number of emergency temporary housing	MASAMURA Akinobu, Tokyo Metropolitan University	https://github.com/a-masumura/R06-Noto-Peninsula-EQ-temporary-housing/
4	Post-disaster	Earthquake	DHEAT, number of dispatched public health nurses	Ministry of Health, Labour and Welfare web site	https://www.mhlw.go.jp/stf/newpage_37198.html
5	Post-disaster	Earthquake and torrential rain	Landslide and deposition distribution	Geospatial Information Authority of Japan	https://www.gsi.go.jp/BOUSAI/20240101_noto_earthquake.html#6-1
6	Post-disaster	Earthquake	Tsunami inundation area	Geospatial Information Authority of Japan	https://www.gsi.go.jp/BOUSAI/20240101_noto_earthquake.html#7
7	Post-disaster	Earthquake and torrential rain	Inundation area by heavy rainfall	National Research Institute for Earth Science and Disaster Resilience	https://mizu.bosai.go.jp/wiki2/wiki.cgi?page=%CE%E1%CF%C26%C7%AF9%B7%EE21%C6%FC%A4%AB%A4%E9%A4%CE%C2%E7%B1%AB
8	Post-disaster	Earthquake	Open building footprints	Google	https://data.humdata.org/dataset/open_buildings_v3_west_japan_earthquake_epicenter? (English)
9	Post-disaster	Earthquake and torrential rain	Aerial photographs (orthoimages)	GSI tiles (Geospatial Information Authority of Japan)	https://maps.gsi.go.jp/development/ichiran.html#t20240102noto_suzu_0114do
10	Post-disaster	Earthquake and torrential rain	Emergency restored road sections	Ministry of Land, Infrastructure, Transport and Tourism road restoration visualization map	https://www.mlit.go.jp/road/r6noto/index2.html (Japanese and English)
11	Post-disaster	Earthquake and torrential rain	Damaged road locations	Ministry of Land, Infrastructure, Transport and Tourism road restoration visualization map	https://www.mlit.go.jp/road/r6noto/index2.html (Japanese and English)
12	Post-disaster	Earthquake	CS stereographic map	Forestry and Forest Products Research Institute, National Research and Development Agency	https://www2.ffpri.go.jp/soilmap/data-src.html
13	Post-disaster	Earthquake and torrential rain	360° imagery	First author	https://gisphn.github.io/360-image-viewer/
14	Normal times	ND	Administrative districts	National Land Numerical Information, Japan	https://nlftp.mlit.go.jp/ksj/gml/datalist/KsjTmplt-N03-v3_1.html

No.	Data publication period	Type of disaster	Data name	Source	URL
15	Normal times	ND	Peninsula circulatory roads	Digital National Land Information	https://nlftp.mlit.go.jp/ksj/gml/datalist/KsjTmplt-A37.html
16	Normal times	ND	Sediment disaster alert areas	Digital National Land Information	https://nlftp.mlit.go.jp/ksj/gml/datalist/KsjTmplt-A33-v2_0.html
17	Normal times	ND	Tsunami inundation anticipation areas	Digital National Land Information	https://nlftp.mlit.go.jp/ksj/gml/datalist/KsjTmplt-A40-v2_1.html
18	Normal times	ND	Schools	Digital National Land Information	https://nlftp.mlit.go.jp/ksj/gml/datalist/KsjTmplt-P29-v2_0.html
19	Normal times	ND	Medical facilities	Digital National Land Information	https://nlftp.mlit.go.jp/ksj/gml/datalist/KsjTmplt-P04-v3_0.html
20	Normal times	ND	Emergency transport roads	Digital National Land Information	https://nlftp.mlit.go.jp/ksj/gml/datalist/KsjTmplt-N10-v2_0.html
21	Normal times	ND	National and prefectural agencies	Digital National Land Information	https://nlftp.mlit.go.jp/ksj/gml/datalist/KsjTmplt-P28-v2_0.html
22	Normal times	ND	Municipal offices and public assembly facilities	Digital National Land Information	https://nlftp.mlit.go.jp/ksj/gml/datalist/KsjTmplt-P05-v3_0.html
23	Normal times	ND	Population (250-m mesh)	The Portal Site of Official Statistics of Japan (e-Stat)	https://www.e-stat.go.jp/gis/statmap-search?type=1 (Japanese and English)
24	Normal times	ND	Disaster base hospitals	Ishikawa Prefecture Open Data Catalogue	https://ckan.opendata.pref.ishikawa.lg.jp/dataset/170003_saigai_hospital
25	Normal times	ND	Public facilities	Ishikawa Prefecture Open Data Catalogue	https://ckan.opendata.pref.ishikawa.lg.jp/dataset/170003_public_facility
26	Normal times	ND	Designated shelters	Ishikawa Prefecture Open Data Catalogue	https://ckan.opendata.pref.ishikawa.lg.jp/dataset/170003_evacuation_space

ND: not determined.

that connects spatial data sets and allows users to build interactive maps accessible from any device, including laptops used by PHNs in the field. The system also enables users to view their own location while exploring the map, facilitating situational awareness during disaster response. The use of WebGIS and the Felt software facilitated the integration of heterogeneous data sets into one platform, making it possible to visualize the distribution of evacuation centres, hazard areas and the population in a single image. The map was released publicly on 8 January 2024. After the torrential rains on 20–23 September 2024, inundation and landslide polygons plus new shelters were added; currently, 26 thematic layers are updated as needed.

360° imagery

In March 2024 and March 2025 (2 and 14 months post-quake, respectively), Insta360 X3 cameras recorded 360° photos at key sites in the Noto Peninsula. Images were published through an open-source viewer.[9] The URL for each photo was linked to its coordinates in PHN-Map pop-ups, enabling users to view the images in either a web browser or a head-mounted display, while 360° imagery provided spatial context beyond the 2D maps, enabling PHNs to virtually assess disaster conditions. Precautions included shooting when only a few people were present, avoiding non-researcher faces, and obscuring vehicle licence plates.

User feedback

With support from the National Association of Chief Public Health Nurses, an online questionnaire comprising three 10-point Likert-type questions was e-mailed to 5549 PHNs nationwide. The questionnaire was open from 11 April to 14 June 2024. It contained three questions:

1. How easy was PHN-Map to use?
2. How useful was PHN-Map for your work during the Noto Peninsula earthquake?
3. How necessary will PHN-Map be for future disaster PHN activities?

Respondents could also add free-text comments.

RESULTS

Analytics recorded 301 visits on launch day (8 January 2024) and a weekday mean of 84 visits from 9 to 30 January 2024. After flood layers were added, visits peaked at 212 on 24 September 2024. **Fig. 1** shows the PHN-Map of the Noto Peninsula that was made publicly available on 8 January 2024. The figure presents the version updated as of January 2025, incorporating additional data sets accumulated since the initial release. The map was generated from government aerial imagery and OpenStreetMap tiles and overlaid with symbols indicating damage status, shelters, PHN team bases, populated areas and temporary housing.

Reported field uses, derived from both web site analytics and survey comments, included:

- pre-deployment triage: matching shelter density and road status to PHN specialties;
- flood-risk reassessment: overlapping flood polygons and earthquake damage zones to anticipate waterborne risks;
- home visit routing: identifying isolated households by intersecting population and building footprint data (**Fig. 2**); and
- training and debriefing: using 360° imagery to simulate field conditions for non-deployed PHNs.

The PHN-Map was created by the authors as a ready-made interactive WebGIS integrating multiple data layers; however, users could freely select which layers to display depending on their needs.

User survey

The questionnaire received 48 responses (response rate: 0.9%).[10] Survey results were: usability 5.5/10 (95% CI: 5.1–6.0), usefulness for earthquake response 5.5/10 (4.9–6.1) and need for future disasters 7.7/10 (7.2–8.3). PHNs who were inexperienced with GIS valued future need as highly as experienced peers. Free-text comments included requests for tutorials and lighter data formats.

Fig. 1. **Public health nursing activity-support WebGIS (PHN-Map), as of January 2025**

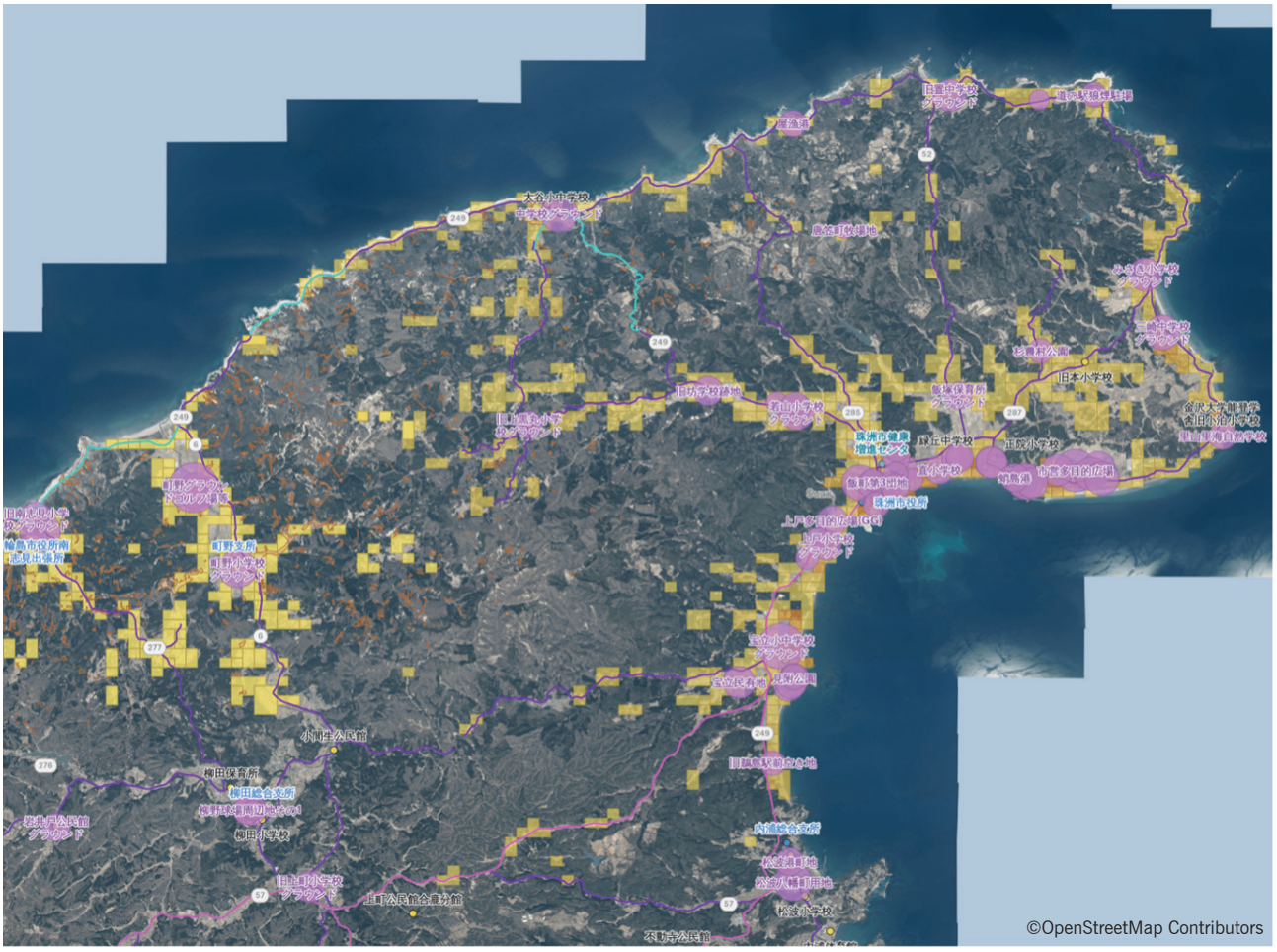

The figure shows the Noto Peninsula tip area.

Aerial photographs show the damage on the ground, and the 250-metre population mesh is shown in yellow, with purple bubbles indicating the location and names of temporary housing.

Disaster base hospitals and evacuation centres, such as elementary schools, are indicated by small, coloured dots. Road openings are indicated by purple or light blue lines.

Sources: National Land Information,[5] e-Stat,[6] QGIS Geographic Information System.[7]

DISCUSSION

PHN-Map, constructed entirely from open data, reduced the "land-knowledge gap" among outside responders deployed to the Noto Peninsula earthquake, aligning with prior evidence that rapid GIS visualization can improve the efficiency of disaster resource allocation.[11] Integrating 360° media also provided an engaging educational tool for pre-service PHN students and disaster-naïve PHNs, who could virtually experience the affected area and rehearse response scenarios with high immersion.[9]

The main system development challenges included the need for manual geocoding of municipal PDF reports without coordinates; this work is labour-intensive, time-consuming and risks misplacing features. Large file sizes were also identified by both developers during implementation and users in survey responses, as a technical limitation that slowed transfers on low-bandwidth disaster networks and could exceed laptop capacity. Ongoing work includes developing automated PDF parsing and vector-tile conversion to address these issues. The survey's very low response rate likely reflected fatigue among PHNs engaged in disaster response and the use of a broad mailing list, making invitations easy to overlook. This represents a limitation in the evaluation process rather than of the system itself. Further studies are needed to evaluate the system's effectiveness in disaster exercises, assess PHN training needs, and explore the integration of real-time or crowd-sourced data.

Fig. 2. **Home-visit routing**

Inhabited buildings in an isolated hamlet are identified by overlaying the 250-m population mesh (yellow) with open building-footprint outlines (red) on aerial imagery.

Yellow squares denote census grid cells in which at least one resident is recorded.

Red polygons mark all detected buildings.

Where a yellow square overlaps a red outline, the structure is inferred to be an inhabited house, while red outlines outside the yellow mesh suggest unoccupied facilities (for example, warehouses).

The magenta line shows a restored road used for home-visit routing.

Sources: e-Stat,[6] QGIS Geographical Survey Institute.[7]

Conclusion

An open-source WebGIS enriched with 360° imagery furnished PHNs with actionable, up-to-date information during a dual disaster of earthquake and floods. The system also addressed previous problems by enabling pre-deployment overview, the integration of multiagency data, and improved spatial understanding via 360° imagery, which also served as training material for non-deployed PHNs. Routine GIS use in everyday PHN work

is recommended, as everyday use will increase PHNs' and other responders' proficiency with GIS tools when a disaster occurs.

Acknowledgements

The authors thank the National Association of Chief Public Health Nurses for disseminating the WebGIS survey and the GIS team at the Ministry of Land, Infrastructure, Transport and Tourism for advice on layers that used National Land Numerical Information data.

Conflicts of interest

The authors have no conflicts of interest to declare.

Ethics statement

Ethical review was deemed unnecessary under the Nara Medical University Research Ethics Committee Guidelines because no personal information was included and the report was not a study but a practical report.

Funding

None.

References

1. [Damage caused by the 2024 Noto Peninsula earthquake and the response of fire departments, etc.]. Tokyo: Fire and Disaster Management Agency; 2024 (in Japanese). Available from: https://www.fdma.go.jp/disaster/info/items/ed651f44b96482e107b093fd844f4b82796814f8.pdf, accessed 1 May 2025.
2. [Damage to the Noto Peninsula caused by the 2024 Oku-Noto heavy rain] [website]. Kanazawa: Government of Ishikawa Prefecture; 2024 (in Japanese). Available from: https://www.pref.ishikawa.lg.jp/saigai/202409ooame-higai.html,accessed 1 May 2025.
3. [Public health nurse deployment after the Noto Peninsula earthquake]. Tokyo: Ministry of Health, Labour and Welfare; 2024 (in Japanese). Available from: https://www.mhlw.go.jp/content/11907000/001282849.pdf, accessed 1 May 2025.
4. Suzuki K. [Report on DMAT activities in the Noto Peninsula earthquake]. The 43rd Kanto-Koshinetsu Block Association of Physical Therapists and the 30th Chiba Prefecture Physical Therapy Academic Conference; 2024 (in Japanese). Available from: https://doi.org/10.14901/ptkanbloc.43.0_247_247, accessed 1 May 2025.
5. [National Land Numerical Information download service] [website]. Tokyo: Ministry of Land, Infrastructure, Transport and Tourism; 2024 (in Japanese). Available from: https://nlftp.mlit.go.jp/ksj/, accessed 1 May 2025.
6. E-Stat: portal site of official statistics of Japan [website]. Tokyo: The National Statistics Center; 2025. Available from: https://www.e-stat.go.jp/en, accessed 1 May 2025.
7. QGIS Development Team. QGIS Geographic Information System. Available from: https://qgis.org/, accessed 1 May 2025.
8. Felt. Collaborative mapping platform. Available from: https://felt.com/, accessed 1 May 2025.
9. Horiike R. [360-image-viewer: Noto disaster scenes] [website]. GitHub.io; 2025 (in Japanese). Available from: https://gisphn.github.io/360-image-viewer/, accessed 1 May 2025.
10. Horiike R. [WebGIS user survey report] [website]. Japanese Association of Public Health Nurse Directors; 2024 (in Japanese). Available from: https://www.nacphn.jp/02/saigai/index.html, accessed 1 May 2025.
11. Shao W, Jackson NP, Ha H, Winemiller T. Assessing community vulnerability to floods and hurricanes along the Gulf Coast of the United States. Disasters. 2020;44(3):518–47. doi:10.1111/disa.12383 pmid:31251410

Description of events reported to the Australian National Focal Point, 2014–2023

Amish Talwar[a] and Martyn D Kirk[a]

Correspondence to Amish Talwar (email: amish.talwar@anu.edu.au)

The 2005 revision of the International Health Regulations (IHR; 2005) requires States Parties of the World Health Organization (WHO) to designate National Focal Points (NFPs) to serve as defined points of contact to communicate with WHO (Article 6: IHR notification) and other States Parties (Article 44: Collaboration and assistance) on IHR matters, particularly the mandatory reporting of significant public health events, including public health emergencies of international concern (PHEICs).[1] Although previous studies have evaluated the timeliness of event reporting from the start of an event to when the event information was disseminated through WHO's *Disease Outbreak News*,[2,3] it remains less clear what types of events are reported to the NFPs and how those events are adjudicated, including whether to notify WHO of the event. WHO has recently promoted the 7-1-7 targets for detecting infectious disease threats within 7 days, notifying public health authorities within 1 day and initiating response activities within 7 days after being notified.[4,5] Ideally, to align with these targets, event information should include the times of event start, NFP notification and response initiation.

In Australia, the NFP function is hosted under the auspices of the Australian Government Department of Health, Disability and Ageing's National Incident Centre (NIC), which supports national coordination of health sector emergencies. For diseases on the National Notifiable Disease List (NNDL),[6] the primary role of the Australian NFP for most domestic events is to provide notifications to Australian states and territories (or Responsible Bodies, which have constitutional authority for health responses), who may take appropriate public health action as per their legislative obligations or guidelines. Additionally, the NFP manages IHR (2005)-related communications between Australia and WHO as well as other governments. Following the COVID-19 pandemic and subsequent amendments to the IHR (2005), including a new requirement for a National IHR Authority to coordinate IHR (2005) implementation,[7] it is an opportune time for Australia to review events reported to its NFP and to describe its event information management system. In this Brief Report, we summarize events reported to the Australian NFP from 2014 to 2023.

METHODS

In Australia, information about events reported to the NFP is uploaded, stored and categorized in a dedicated incident management system (IMS). The main events are categorized as being reported from within Australia or by international NFPs, associated with flights or ships travelling domestically or internationally, or not otherwise classified. For our analysis, we used the following event information: date the NFP was notified; event category; type of associated hazard; registration of the event in the NNDL; name of the original notifying body; international NFPs notified; and domestic Responsible Bodies notified. Other event information, including date of event start, date of event detection, date of response initiation, place of event start and number of cases, was not directly available (or provided) through the IMS. Additionally, it was unclear which events were communicated to the WHO Regional Office for the Western Pacific. From the information made available, we determined the number of events by year and hazard type. Within these categories, we also reported the number of events according to whether they were reported from within or outside Australia. Among the events reported from within Australia, we determined whether these events were reported to other country NFPs.

[a] National Centre for Epidemiology and Population Health, The Australian National University, Canberra, Australian Capital Territory, Australia.
Published: 25 March 2026
doi: 10.5365/wpsar.2026.17.1.1335

RESULTS

From 2014 to 2023, 967 events were reported to the Australian NFP. Excluding two consolidated entries for international reporting for the COVID-19 pandemic and the monkeypox virus (mpox) multicountry epidemic, six events of unknown origin and eight non-notifications, 951 events were reported. From within Australia, 340/951 (35.8%) events were reported. These included events reported by an Australian state or territory that were associated with domestic flights and international flights originating in Australia. From outside Australia, 611/951 (64.2%) events were reported, including those reported from overseas or associated with flights originating and departing overseas, as well as flights and ships arriving in Australia. The greatest number of events was reported in 2020 (171/951, 18.0%) and the least in 2021 (19/951, 2.0%). The top three hazards reported from within Australia included tuberculosis (112/340, 32.9%), legionellosis (69/340, 20.3%) and measles (53/340, 15.6%) (**Table 1**).

DISCUSSION

This report presents the first extended description of events received or reported by an NFP. Among all hazards reported, tuberculosis, legionellosis and measles were the most reported by a substantial margin, both from within and outside Australia. This high reporting is likely a product of overseas acquisition of these diseases among people who travelled to Australia (with disease detection either at the point of origin, at a place of transit or upon arrival) and also reflects the NFP's role in assisting with contact tracing of exposed travellers, indicating heightened concern over transmission of these particular diseases.[8–10] On the other hand, the decline in reporting from 2020 to 2021 is likely attributable to international travel and trade restrictions and the imposition of lockdowns during the COVID-19 pandemic.[11]

Although the Australian IMS provides an accurate ledger of events based on the type of event, when the Australian NFP was notified and whether other NFPs were notified, it does not consistently provide crucial information to evaluate the event reporting system in Australia, including the dates of event start, detection and response initiation. This makes it challenging to assess the efficacy of the reporting system in relation to the 7-1-7 standard and to compare it with other countries. Also, it is unclear from the IMS data why certain events were reported to NFPs in other countries while others were not. While the most recent version of the IHR (2005) Annex 2 lists a handful of diseases always requiring notification, NFPs must use the Annex 2 decision algorithm for all other potential PHEICs.[1] A 2011 study revealed that, when presented with fictitious public health events, NFPs did not necessarily agree with each other or an expert panel on which events required notification.[12] Finally, it is unclear from the available IMS data which events were communicated to the Regional Office and the rationale for doing so. These data would have been a clearer signal of events that the NFP adjudged as meeting the Annex 2 criteria for notification to WHO.

For a better understanding of why NFPs might have different reporting behaviours, NFPs should strive to document their rationale for reporting certain events and routinely compare their reporting behaviours to identify best practices and areas requiring remediation. The establishment of National IHR Authorities represents an opportune moment for NFPs to revisit how public health events are reported and tracked, and to update their data management systems to ensure accurate and comprehensive information gathering in line with State Parties' IHR (2005) obligations. For a federal system like Australia, this would be an opportunity to examine how best to facilitate outbreak data centralization to comply with these practices amidst the devolution of public health responsibilities to states and territories, including the prerogative for what and when to report to the Australian NFP. Such an effort would represent a significant step forward for future pandemic prevention, preparedness and response.

Acknowledgements

The Department of Health, Disability and Ageing provided the raw data used in the development of this report. In accordance with the provisions of the Privacy Act 1988, the data supplied did not contain any personal or identifiable information. All interpretations, conclusions and recommendations presented herein are solely those of the authors. The Department of Health, Disability and Ageing did not participate in the analytical process or in the formulation of the findings contained in this document.

Table 1. **Hazards associated with events reported to the Australian NFP by hazard type, location of event origin and overseas NFP notification status for events of domestic origin, 2014–2023 (*N* = 951)**

Hazard	Events reported from within Australia[a] (% of hazard events reported)	Events reported from outside Australia[b] (% of hazard events reported)	Overseas NFP(s) notified for domestic events[c] (% of hazard events reported from within Australia)	Total events reported to Australian NFP[a,b]	Comment
Arbovirus	0 (0.0)	1 (100.0)	N/A	1	Unspecified pathogen
Botulism	1 (100.0)	0 (0.0)	0 (0.0)	1	–
Chikungunya	1 (33.3)	2 (66.7)	0 (0.0)	3	–
Cholera	9 (69.2)	4 (30.8)	6 (66.7)	13	–
Coronavirus	0 (0.0)	2 (100.0)	N/A	2	Unspecified pathogen
Cryptosporidiosis	0 (0.0)	1 (100.0)	N/A	1	–
Diphtheria	1 (33.3)	2 (66.7)	0 (0.0)	3	–
Flavivirus	5 (50.0)	5 (50.0)	2 (40.0)	10	Includes Zika virus, dengue virus and unspecified pathogen
Gastrointestinal disease	2 (66.7)	1 (33.3)	0 (0.0)	3	Unspecified pathogen
Gonococcal infection	3 (100.0)	0 (0.0)	2 (66.7)	3	–
Hepatitis	14 (48.3)	15 (51.7)	4 (28.6)	29	Includes hepatitis A, hepatitis B, hepatitis E and unspecified hepatitis
Human immunodeficiency virus	1 (100.0)	0 (0.0)	1 (100.0)	1	–
Influenza	4 (57.1)	3 (42.9)	1 (25.0)	7	Unspecified subtype
Japanese encephalitis virus	2 (50.0)	2 (50.0)	0 (0.0)	4	–
Legionellosis	69 (28.4)	174 (71.6)	32 (46.4)	243	–
Leprosy	0 (0.0)	1 (100.0)	N/A	1	–
Listeriosis	3 (75.0)	1 (25.0)	0 (0.0)	4	–
Lyssavirus	1 (100.0)	0 (0.0)	1 (100.0)	1	–
Malaria	1 (100.0)	0 (0.0)	0 (0.0)	1	–
Measles	53 (29.3)	128 (70.7)	22 (41.5)	181	–
Meningococcal disease	20 (38.5)	32 (61.5)	6 (30.0)	52	–
Mpox	1 (50.0)	1 (50.0)	1 (100.0)	2	–
Murray Valley encephalitis virus	1 (100.0)	0 (0.0)	0 (0.0)	1	–
Nipah virus	0 (0.0)	2 (100.0)	N/A	2	–
Norovirus	2 (66.7)	1 (33.3)	0 (0.0)	3	–
Other diseases	5 (62.5)	3 (37.5)	3 (60.0)	8	–
Paratyphoid fever	0 (0.0)	1 (100.0)	N/A	1	–
Pertussis	3 (75.0)	1 (25.0)	2 (66.7)	4	–
Pneumococcal disease	1 (100.0)	0 (0.0)	0 (0.0)	1	–
Poliovirus	3 (50.0)	3 (50.0)	1 (33.3)	6	–
Psittacosis (ornithosis)	0 (0.0)	2 (100.0)	N/A	2	–
Q fever	0 (0.0)	3 (100.0)	N/A	3	–
Rabies	5 (31.3)	11 (68.8)	4 (80.0)	16	–
Ross River virus	0 (0.0)	2 (100.0)	N/A	2	–

Hazard	Events reported from within Australia[a] (% of hazard events reported)	Events reported from outside Australia[b] (% of hazard events reported)	Overseas NFP(s) notified for domestic events[c] (% of hazard events reported from within Australia)	Total events reported to Australian NFP[a,b]	Comment
Rotavirus	2 (100.0)	0 (0.0)	2 (100.0)	2	–
Salmonellosis	1 (14.3)	6 (85.7)	0 (0.0)	7	–
Shewanella	1 (100.0)	0 (0.0)	1 (100.0)	1	–
Shiga toxin-producing *Escherichia coli*	4 (57.1)	3 (42.9)	1 (25.0)	7	–
Shigellosis	4 (50.0)	4 (50.0)	2 (50.0)	8	–
Streptococcus	1 (100.0)	0 (0.0)	1 (100.0)	1	Unspecified pathogen
Syphilis	2 (66.7)	1 (33.3)	1 (50.0)	3	–
Tuberculosis	112 (38.1)	182 (61.9)	76 (67.9)	294	–
Typhoid fever	1 (14.3)	6 (85.7)	0 (0.0)	7	–
Varicella zoster	1 (50.0)	1 (50.0)	1 (100.0)	2	Includes chickenpox, shingles and unspecified pathogen
Viral haemorrhagic fever	0 (0.0)	4 (100.0)	N/A	4	Includes Lassa virus and unspecified pathogen
Totals	**340 (35.8)**	**611 (64.2)**	**173**	**951**	–

NFP: national focal point; N/A: not applicable.

[a] Includes events reported by an Australian state, events associated with domestic flights and events associated with international flights originating in Australia.

[b] Includes events reported from overseas, events associated with flights originating and departing overseas, events associated with flights arriving to Australia and events associated with ships arriving to Australia.

[c] Events reported from within Australia that were reported to one or more overseas NFPs.

Conflicts of interest

MDK worked with the Australian Government Department of Health, Disability and Ageing from 2020 to 2024 as part of the Australian COVID-19 response. AT has no conflicts of interest to declare.

Ethics statement

This study was approved by the Australian National University's Human Research Ethics Committee (protocol H/2024/0849).

Funding

None.

References

1. International Health Regulations (2005), 3rd ed. Geneva: World Health Organization; 2016. Available from: https://iris.who.int/handle/10665/246107, accessed 4 October 2024.
2. Kluberg SA, Mekaru SR, McIver DJ, Madoff LC, Crawley AW, Smolinski MS, et al. Global capacity for emerging infectious disease detection, 1996–2014. Emerg Infect Dis. 2016;22(10):E1–6. doi:10.3201/eid2210.151956 pmid:27649306
3. Chan EH, Brewer TF, Madoff LC, Pollack MP, Sonricker AL, Keller M, et al. Global capacity for emerging infectious disease detection. Proc Natl Acad Sci U S A. 2010;107(50):21701–6. doi:10.1073/pnas.1006219107 pmid:21115835
4. Frieden TR, Lee CT, Bochner AF, Buissonnière M, McClelland A. 7-1-7: an organising principle, target, and accountability metric to make the world safer from pandemics. Lancet. 2021;398(10300):638–40. doi:10.1016/S0140-6736(21)01250-2 pmid:34242563
5. Guidance and tools for conducting an early action review (EAR): rapid performance improvement for outbreak detection and response, 31 August 2023. Geneva: World Health Organization; 2023. Available from: https://iris.who.int/handle/10665/372579, accessed 4 October 2024.
6. Nationally Notifiable Diseases Surveillance System (NNDSS) [website]. Canberra: Australian Centre for Disease Control, Government of Australia; 2026. Available from: https://www.cdc.gov.au/diseases/surveillance-systems-and-networks/national-notifiable-diseases-surveillance-system-nndss, accessed 1 March 2026.
7. International Health Regulations (2005). Geneva: World Health Organization; 2025. Available from: https://apps.who.int/gb/bd/pdf_files/IHR_2014-2022-2024-en.pdf, accessed 1 March 2026.

8. Department of Health annual report 2014–15. Canberra: Department of Health, Government of Australia; 2015. Available from: https://www.health.gov.au/resources/publications/department-of-health-annual-report-2014-15, accessed 29 September 2025.
9. Department of Health annual report 2015–16. Canberra: Department of Health, Government of Australia; 2016. Available from: https://www.health.gov.au/sites/default/files/department-of-health-annual-report-2015-16.pdf, accessed 29 September 2025.
10. Department of Health annual report 2018–19. Canberra: Department of Health, Government of Australia; 2019. Available from: https://www.health.gov.au/sites/default/files/documents/2019/10/department-of-health-annual-report-2018-19_0.pdf, accessed 29 September 2025.
11. Department of Health annual report 2020–21. Canberra: Department of Health, Government of Australia; 2021. Available from: https://www.health.gov.au/sites/default/files/documents/2021/10/department-of-health-annual-report-2020-21.pdf, accessed 29 September 2025.
12. Haustein T, Hollmeyer H, Hardiman M, Harbarth S, Pittet D. Should this event be notified to the World Health Organization? Reliability of the international health regulations notification assessment process. Bull World Health Organ. 2011;89(4):296–303. doi:10.2471/BLT.10.083154 pmid:21479094

Detection of a *Serratia sarumanii* outbreak in neonatal intensive care units using SaTScan and whole genome sequencing, Philippines, 2022

Giselle V Godin,[a*] Sonia B Sia,[b*] Ferissa B Ablola,[b*] June M Gayeta,[b*] Marietta L Lagrada,[b*] Polle Krystle V Macaranas,[b] Agnettah M Olorosa,[b] Janziel Fiel Palarca,[b] Manuel C Jamoralin Jr,[b] June Janice Borlasa,[b] Ma Fe Laren B Gacho,[a] Rica Marie B Andico,[a] Ida Marrione Q Arriola,[a] Jo-Anne J Lobo,[a,c,d*] Melanie B Adolfo,[a,d,e] Jessica Anne A Dumalag,[a,d,e] Joel T Gallardo,[a,e] Ma Delta S Aguilar,[a,c,d] Allyne M Aguelo,[a,c,d] Charlotte V Bañes[a,d,e,f] and Genelynne J Beley[a,d,f]

Correspondence to Sonia B Sia (email: sonia.sia@ritm.gov.ph)

Objective: This study aimed to demonstrate the benefits of using SaTScan (Boston, MA, USA), a cluster-detection software programme, and whole genome sequencing to investigate a suspected outbreak of *Serratia marcescens* infections in a tertiary government hospital in the southern Philippines. The hospital is part of the national Antimicrobial Resistance Surveillance Program's network of sentinel sites.

Methods: The investigation followed national outbreak investigation protocols. In May 2022, when evaluation of daily hospital laboratory census data revealed an increase in the number of *Serratia* species in the hospital, an alert was triggered. A concurrent, routine SaTScan analysis of the hospital's surveillance data by the Antimicrobial Resistance Surveillance Reference Laboratory confirmed a cluster of cases. The Reference Laboratory requested isolates from clinical specimens from the hospital for confirmation of bacterial identification, antimicrobial susceptibility testing and whole genome sequencing.

Results: Six isolates were submitted for genomic analysis, two of which were from the identified cluster. Although originally identified as *S. marcescens*, five of the isolates were subsequently confirmed as *S. sarumanii*. Phylogenetic analysis showed that the two isolates from the cluster were closely related and belonged to the same clade, which may suggest a common source. Three antimicrobial resistance genes were identified, but their phenotypic expression was limited, with one isolate exhibiting resistance mechanisms.

Discussion: This study highlighted the utility of SaTScan for the early detection of potential disease outbreaks. The use of whole genome sequencing enhanced the investigation by enabling the analysis of potential transmission pathways at the genetic level, identification of the outbreak source and the detection of novel species.

Serratia species are aerobic, Gram-negative bacilli in the Enterobacteriaceae family that occur naturally in soil and water. Some strains produce prodigiosin, a red pigment, giving colonies a distinctive colouration.[1] *Serratia* infections give rise to a wide range of clinical manifestations,[2] and outbreaks have led to significant morbidity and mortality, most commonly in patients in intensive care units and most notably in low-birthweight neonates.[3] Asymptomatic infections have also been reported. Outbreaks have been traced to contaminated medical equipment, such as bronchoscopes, nebulizers and basins used to collect urine.[4] Outbreaks have also been associated with disruptions in infection control techniques caused by overcrowding, understaffing and problems with maintaining nursery routines, particularly hand hygiene.[5] In the Philippines, only a few cases have

[a] Department of Pediatrics, Southern Philippines Medical Center, Davao City, Philippines.
[b] Antimicrobial Resistance Surveillance Reference Laboratory, Research Institute for Tropical Medicine, Department of Health, Muntinlupa City, Philippines.
[c] Section of Infectious Diseases, Southern Philippines Medical Center, Davao City, Philippines.
[d] Department of Pediatrics, College of Medicine, Davao Medical School Foundation, Davao City, Philippines.
[e] Section of Newborn Medicine, Southern Philippines Medical Center, Davao City, Philippines.
[f] Department of Biochemistry, College of Medicine, Davao Medical School Foundation, Davao City, Philippines.
[*] These authors contributed equally.
Published: 26 January 2026
doi: 10.5365/wpsar.2026.17.1.1092

been reported, the most recent of which was in a neonate with a congenital malformation, described by Lappay et al. in 2022.[6]

An important characteristic of *Serratia* species is their ability to secrete protein factors such as deoxyribonuclease (or DNAse), lipase and haemolysin, which confer resistance to a number of antibiotics, including cephalosporins, such as cefoxitin and cefotaxime, and penicillins, such as ampicillin and amoxicillin–clavulanic acid.[7] Their ability to persist in hospital environments and infect various hosts, coupled with a propensity to act as a reservoir for resistant genes and with evidence of increasing prevalence, means that *Serratia* species pose a significant and growing threat to public health, placing increasing importance on ensuring robust investigations of outbreaks involving these species.

Traditional approaches to detecting and investigating outbreaks of infectious disease have involved demographic case review coupled with laboratory testing of biological specimens from suspected cases or environmental samples, or both, to identify the responsible pathogen. However, phenotypic typing methods often lack the resolution required to accurately pinpoint the source of an outbreak and to trace chains of transmission, especially when isolates cluster together as indistinguishable members of the same organism.

Advances in molecular biology have given rise to genotypic typing methods that overcome some of the limitations of traditional phenotypic methods. Whole genome sequencing (WGS), for example, makes it possible to identify all the genomic characteristics of a bacterium. Moreover, this technique has the capacity to identify functionally important variants in DNA sequences that affect gene expression.

At the same time, SaTScan (Boston, MA, USA), a free-to-access software application available from within WHONET,[8] is increasingly being used by epidemiologists globally to detect and describe temporal and spatial clusters of infectious and chronic disease, as well as disease vectors and risk factors. SaTScan can identify whether an infection is randomly distributed over space, over time, or over space and time. Moreover, it allows for evaluation of the statistical significance of disease cluster alarms.[9] This combination of technologies – SaTScan and WGS – is emerging as a valuable tool for investigating outbreaks.

In the Philippines, surveillance for antimicrobial resistance (AMR) is the responsibility of the Department of Health. Its Antimicrobial Resistance Surveillance Program operates a network of 28 hospital surveillance sites, located in all 18 administrative regions of the country. Laboratory testing of clinical samples is conducted by the Antimicrobial Resistance Surveillance Reference Laboratory (ARSRL), which is housed at the Research Institute for Tropical Medicine. In 2019, laboratory services were expanded to include WGS for selected isolates, supplementing routine services for bacterial identification and antimicrobial susceptibility testing, and providing enhanced capacity for identifying the genomic characteristics of isolates with emerging AMR. In 2021, as an additional service for the Antimicrobial Resistance Surveillance Program, the ARSRL started to routinely analyse daily microbiological data provided by the programme's surveillance sites via WHONET, using SaTScan to aid in detecting outbreaks caused by pathogens with potential AMR. Currently, the ARSRL runs SaTScan weekly, and alerts are issued if the software detects groups of bacterial isolates of the same species with a similar resistance profile. Pre-set criteria determine whether any detected clusters are investigated using WGS and assessment of epidemiological data.

On 26 May 2022, the bacteriology department of one of the Antimicrobial Resistance Surveillance Program's surveillance sites, the Southern Philippines Medical Center, observed an increase in the number of *Serratia* species in the facility. This was promptly communicated to the ARSRL. On 27 May 2022, the Reference Laboratory ran its weekly SaTScan analysis on data routinely submitted by the Medical Center. The SaTScan report confirmed the presence of a potential cluster of *Serratia* species, which met the pre-set criteria for further investigation. The first isolate belonging to this cluster was identified on 10 May 2022.

This study describes the investigation and reporting of the outbreak of *Serratia* infections that occurred in the neonatal intensive care units (NICUs) of the Medical Center. This investigation showcases the strengths of employing SaTScan software in combination with WGS

to facilitate prompt outbreak detection and targeted, control-focused responses.

METHODS

Study design and setting

This investigation of a suspected outbreak of *Serratia* infections at the Medical Center, a sentinel site in the national AMR surveillance programme, utilized a prospective cohort study design. The Medical Center is a 1200-bed tertiary hospital in Davao City with 70 NICU beds. It is situated in one of the most populous Philippine cities, within an administrative region comprising six cities and 43 municipalities. As an end-referral centre with several highly specialized clinical services, the Medical Center also caters to the health needs of patients from different parts of Mindanao and the country.

Routine SaTScan analysis

In accordance with protocols for national outbreak investigations, the Data Management Unit of the ARSRL ran its weekly SaTScan analysis in WHONET[8,9] on 27 May 2022 on daily AMR surveillance data transferred by sentinel sites during the preceding week, initially with the term "resistance profile" as the summary row input. The analysis was then set to run on "resistance profile" with the term "include cluster alerts". The SaTScan analysis method used was the "space-time permutation model – simulated prospective". The "maximum cluster length" and "baseline data" fields were set to 100 days and 365 days, respectively, while the "recurrence interval" was set to 365 days and "Monte Carlo simulations" to 9999.

The SaTScan analysis verified the presence of a potential cluster of *Serratia* species isolates exhibiting similar AMR profiles that met pre-set criteria for close spatial, temporal and space-time relationships.[9] The identified cluster also met the criteria for further investigation using WGS (**Supplementary Material**). The outcome of the line list of cluster isolates, together with a notification letter, were sent via email to the hospital, addressed to the head of the laboratory and the Infection Prevention and Control Committee.

Laboratory and environmental analysis

The sentinel site was requested to send the six isolates in the identified cluster to the ARSRL, as well as any environmental samples collected. The Reference Laboratory conducted confirmatory bacterial identification using an automated system (Vitek 2, bioMérieux, Marcy-l'Étoile, France) and conventional biochemical tests.

The isolates included in this study were all tested against nine antibiotics: amikacin, cefepime, cefotaxime, ceftriaxone, ertapenem, gentamicin, imipenem, meropenem and tetracycline. The zone of inhibition and minimum inhibitory concentration were interpreted following the guidelines of the Clinical and Laboratory Standards Institute.[7]

Whole genome sequencing and bioinformatics analysis

DNA was extracted from a single colony in each of the six isolates using a DNA extraction kit (Nexttec Biotechnologie, Hilgertshausen, Germany). DNA libraries were prepared using the Illumina Nextera DNA Flex Library Prep Kit (Illumina, San Diego, CA, USA), which employs bead-linked transposome technology to simultaneously fragment and tag DNA with adapter sequences. Following tagmentation, a magnetic bead-based clean-up was performed, and indexed primers were used for polymerase chain reaction amplification. The quality and concentration of the amplified libraries were assessed using fluorometric quantification. Pooled libraries were then subjected to sequencing on the Illumina MiSeq platform.

The study utilized the Bactopia pipeline (v. 3.1)[10] for genomic analysis. Genome assembly was performed using Shovill (v. 1.1)[11] with SPAdes (v. 4.1; St Petersburg genome assembler),[12] targeting a genome size of 5.2 Mb and coverage of 100x. Multilocus sequence typing (MLST) was conducted using MLST software (v. 2.23), which uses PubMLST[13] schemes. Phylogenetic analysis employed the Snippy (v. 4.6)[14] workflow; the reference genome (US National Library of Medicine, Reference Sequence collection: GCF_002264285.1) was selected

based on the closest genome identified by Mash (v. 2.3)[15] from the two clustered isolates.

A maximum likelihood phylogenetic tree was generated with IQ-TREE (v. 2.2.2.7)[16] using the general time-reversible + invariant sites + γ distribution substitution model, and single nucleotide polymorphism (SNP) distances between isolates were calculated with snp-dists (v. 0.8.2).[17] AMR was predicted using AMRFinderPlus (v. 4.0.19),[18] with database version 2024-12-18.1, specifying the options -p, -n and -g for *S. marcescens*, and considering AMR determinants and mutations with at least 90% coverage and 90% identity. Raw sequence data were deposited in the United States National Center for Biotechnology Information under project accession identification PRJNA1023302.

RESULTS

The sentinel site submitted six isolates. Two of these isolates were from the identified cluster; the other four were convenience samples. It was not possible to retrieve and forward other cluster isolates to the Reference Laboratory because the site had discarded them by the time the ARSRL informed it of the clustering of *Serratia* species. Moreover, no environmental sampling had been conducted at the site before or after notification, so no environmental isolates were available for analysis. The results of the genomic characterization and analyses of the six isolates included in this study were concluded by 9 July 2022.

Three of the six isolates were from NICUs 1 and 2; two were from the Medicine Burn Center and one was from Medicine Ward 4 (**Table 1**). The isolates from the two NICU samples were presumed to be nosocomial isolates (i.e. the specimens were collected ≥72 hours after admission). The two cluster isolates (22ARS_DMC0256 and 22ARS_DMC0258) and one non-cluster isolate (22ARS_DMC0257) were susceptible to all tested antibiotics. One non-cluster isolate (22ARS_DMC0255) showed resistance to cephalosporins and gentamicin; two non-cluster isolates (22ARS_DMC0259 and 22ARS_DMC0260) demonstrated resistance to tetracycline (**Table 2**).

All isolates were initially molecularly identified as *S. marcescens*. However, ribosomal MLST identified five of the isolates as *S. sarumanii*; the exception was the non-cluster isolate 22ARS_DMC0259, which was confirmed as *S. marcescens* (**Table 3**). PubMLST sequencing further revealed that the two isolates in the cluster (22ARS-DMC0256 and 22ARS-DMC0258) belonged to sequence type 595, whereas the other isolates had distinct sequence types. Additionally, the genome comparator tool in PubMLST generated a phylogenetic tree that grouped the two cluster isolates together with 42 available *S. sarumanii* sequences from China. The differences between these isolates were minimal, with 33–48 SNP differences.

Phylogenetic analysis of the sequencing data from the five *S. sarumanii* and one *S. marcescens* isolates showed five distinct clades (**Fig. 1**). The isolate (22ARS-DMC0259) in clade 1 was from a wound sample collected on 5 June 2022 from a 63-year-old male in the Medicine Burn Center. This isolate was considered an outlier, given the high SNP difference between it and the five other isolates (**Fig. 1**, **Table 4**). The second clade comprised isolate 22ARS-DMC0260; it was likewise grown from a wound sample and was collected on 3 June 2022 from a 35-year-old male patient in the Medicine Burn Center. Isolate 22ARS-DMC0255 in clade 3 was from a tracheal sample collected on 7 June 2022 from a 1-month-old patient in NICU 1. Isolates in clades 2 and 3 exhibited distinct antimicrobial susceptibility profiles for cefepime, ceftriaxone and gentamicin (**Table 2**). Furthermore, isolate 22ARS-DMC0259 (clade 2) harboured the tet_41 AMR gene, which was absent in isolate 22ARS-DMC0255 (clade 3) (**Table 3**). Clade 4 included isolate 22ARS-DMC0257 from the tracheal specimen of a 42-year-old patient from Medicine Ward 4.

The two cluster isolates genotypically belonged to clade 5: 22ARS-DMC0258 was recovered from a tracheal aspirate sample collected on 27 May 2022 from a 2-month-old male in NICU 2, and 22ARS-DMC0256 was recovered from a sample collected on 23 May 2022 from a 4-day-old female in NICU 1. Furthermore, the SNP difference between these two isolates, at 41 units (**Table 4**), was minimal, and they exhibited identical phenotypic antimicrobial susceptibility testing results.

Three AMR genes were identified across the six *Serratia* isolates (**Table 3**), but their phenotypic expression was limited, with only one isolate exhibiting resistance mechanisms. The aac(6′) gene (aminoglycoside 6′-N-acetyltransferase), which confers resistance to

Table 1. **Demographic data of patients with Serratia sarumanii or Serratia marcescens isolates, southern Philippines, 2022 (*N* = 6)**

Accession no.	Age	Ward	Specimen type	Admission date	Specimen date
22ARS_DMC0255	1 month	NICU1	Tracheal aspirate	20 April 2022	7 June 2022
22ARS_DMC0256[a]	4 days	NICU1	Tracheal aspirate	20 May 2022	23 May 2022
22ARS_DMC0257	42 years	Medicine Ward 4	Tracheal aspirate	26 May 2022	28 May 2022
22ARS_DMC0258[a]	2 months	NICU2	Tracheal aspirate	23 May 2022	27 May 2022
22ARS_DMC0259	63 years	Medicine Burn Center	Wound	21 May 2022	5 June 2022
22ARS_DMC0260	35 years	Medicine Burn Center	Wound	19 April 2022	3 June 2022

NICU1: neonatal intensive care unit 1; NICU2: neonatal intensive care unit 2.

[a] Isolates included in the cluster.

Table 2. **Results of antimicrobial susceptibility testing of Serratia sarumanii and Serratia marcescens isolates, southern Philippines, 2022 (*N* = 6)**

Accession no.	Tetracycline	Cephalosporins			Aminoglycosides		Carbapenems		
		Cefotaxime	Cefepime	Ceftriaxone	Amikacin	Gentamicin	Imipenem	Meropenem	Ertapenem
22ARS_DMC0255	S	R	R	R	S	R	S	S	S
22ARS_DMC0256[a]	S	S	S	S	S	S	S	S	S
22ARS_DMC0257	S	S	S	S	S	S	S	S	S
22ARS_DMC0258[a]	S	S	S	S	S	S	S	S	S
22ARS_DMC0259	R	S	S	S	S	S	S	S	S
22ARS_DMC0260	R	S	S	S	S	S	S	S	S

R: resistant; S: susceptible.

[a] Isolates included in the cluster.

Table 3. **Antimicrobial resistance genes detected in Serratia sarumanii and Serratia marcescens isolates, southern Philippines, 2022 (*N* = 6)**

Accession no.	Species identification		Sequence type	Gene		
	Bactopia pipeline[10]	PubMLST[13]		aac(6')-Ib	blaSRT or blaSST	tet_41
22ARS_DMC0255	*S. marcescens*	*S. sarumanii*	521	aac(6')-Ib	bla_{SRT}	–
22ARS_DMC0256[a]	*S. marcescens*	*S. sarumanii*	595	aac(6')-Ib	bla_{SRT}	–
22ARS_DMC0257	*S. marcescens*	*S. sarumanii*	506	aac(6')-Ib	bla_{SRT}	–
22ARS_DMC0258[a]	*S. marcescens*	*S. sarumanii*	595	aac(6')-Ib	bla_{SRT}	–
22ARS_DMC0259	*S. marcescens*	*S. marcescens*	1035	aac(6')-Ib	bla_{SST}	*tet_41*
22ARS_DMC0260	*S. marcescens*	*S. sarumanii*	406	aac(6')-Ib	bla_{SRT}	–

MLST: multilocus sequence typing.

[a] Isolates included in the cluster.

aminoglycosides, was phenotypically expressed only in isolate 22ARS_DMC0255 (**Table 2**). Similarly, the bla_{SRT} resistance gene, which confers resistance to cefepime and ceftriaxone, was also expressed only in this same isolate.

DISCUSSION

In May 2022, the Southern Philippines Medical Center, a sentinel site for AMR, alerted the Philippines ARSRL about a potential outbreak of infections caused by

Fig. 1. **Phylogenetic tree of *Serratia sarumanii* and *Serratia marcescens* isolates, southern Philippines, 2022 (*N* = 6)**

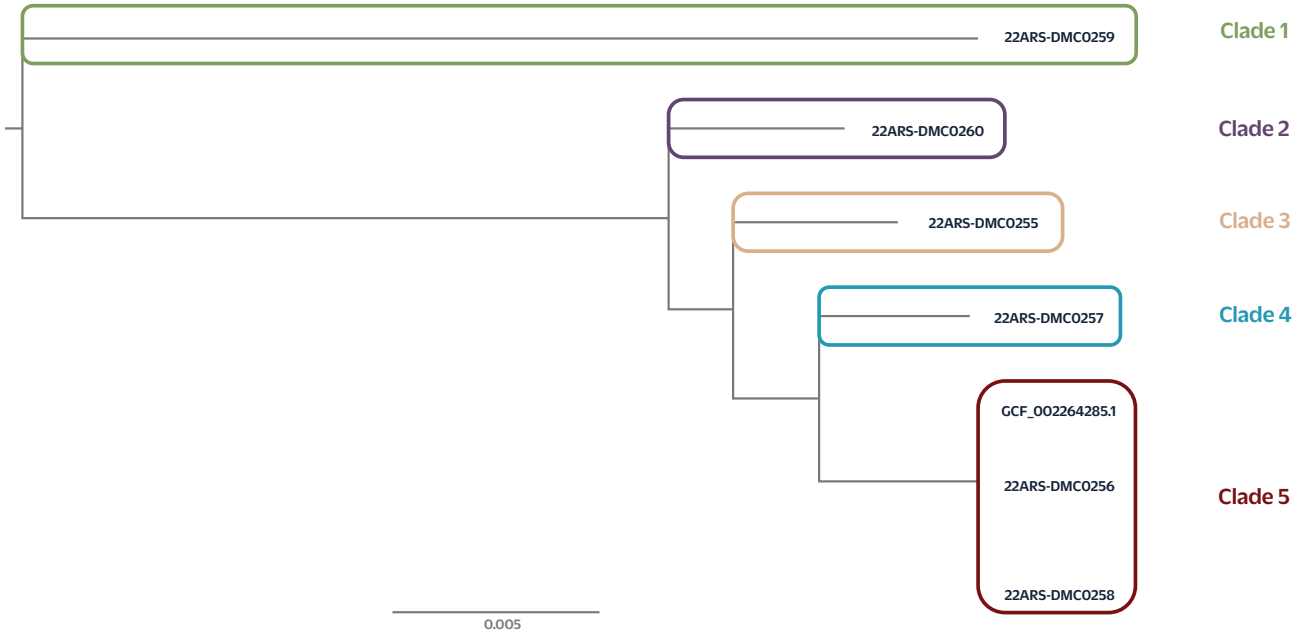

GCF: reference genome.

Serratia species. Subsequent investigations, involving the tandem use of SaTScan and WGS molecular testing, confirmed the presence of a cluster of *S. marcescens* and *S. sarumanii* at the site. The latter had recently been described as a novel species, based on evidence of phenotypic differences from *S. marcescens*, including differences in colony colour, haemolysis on blood agar and antibiotic susceptibility.[19] Most notably, the two species have demonstrably different antimicrobial susceptibility profiles, with *S. sarumanii* generally showing resistance to ampicillin, piperacillin, piperacillin–tazobactam and cefotaxime, while *S. marcescens* is typically susceptible to these.

This study showcases the capability of WGS to differentiate closely related organisms and update species identification. Initial phenotyping of the isolates from the sentinel site identified the pathogen as *S. marcescens*, one of the most common agents involved in hospital-acquired bacterial infections. However, subsequent molecular analyses confirmed that five of the six isolates were *S. sarumanii*. Moreover, WGS was able to provide granular evidence of genetic relatedness among the isolates from the identified cluster. The large SNP differences among the four isolates in clades 1–4 and also between isolates in clades 1–4 and those in clade 5 suggested that isolates from clades 1–4 were genetically distinct from one another and thus unlikely to be from a single source. Conversely, given that the two NICU cluster isolates (22ARS-DMC0256 and 22ARS-DMC0258) were presumed to be nosocomial isolates and exhibited only minimal SNP differences, this pointed to a potential hospital-acquired outbreak of *S. sarumanii* infection. It is also interesting that the SNP differences between the two cluster isolates were less than those reported by an investigation of a confirmed outbreak of *S. marcescens* infections in the NICU of a hospital in Australia (41 vs 48).[4] Finally, phylogenetic analysis indicated a likely single transmission source for the two *S. sarumanii* isolates recovered from the patients in NICU 1 and NICU 2.

Antibiotic resistance genes (i.e. specific DNA sequences that confer resistance to antimicrobial agents) are expected to be expressed in the presence of an antibiotic or in the presence of harmful bacterial species. However, not every gene for AMR is necessarily expressed.[20] Therefore, it is possible that the acc(6′) gene identified in this study was expressed only in isolate 22ARS_DMC0255 and not in the other five isolates, which were susceptible to both amikacin and gentamicin. Only isolate 22ARS_DMC0255 also showed resistance to cefepime and ceftriaxone, raising the further possibility of non-expression of bla_{SRT} in the remaining isolates.

Table 4. **Single nucleotide polymorphism analysis of *Serratia sarumanii* and *Serratia marcescens* isolates, southern Philippines, 2022 (*N* = 6)**

Accession no.	SNP analysis						
	22ARS-DMC0255	22ARS-DMC0256	22ARS-DMC0257	22ARS-DMC0258	22ARS-DMC0259	22ARS-DMC0260	GCF_002264285.1
22ARS-DMC0255	0	44 625	41 351	45 114	169 474	45 554	45 742
22ARS-DMC0256[a]	44 625	0	36 355	**41**	173 220	50 938	93
22ARS-DMC0257	41 351	36 355	0	36 688	162 457	47 433	37 197
22ARS-DMC0258[a]	45 114	**41**	36 688	0	175 793	51 706	87
22ARS-DMC0259	169 474	173 220	162 457	175 793	0	172 931	177 931
22ARS-DMC0260	45 554	50 938	47 433	51 706	172 931	0	52 439
GCF_002264285.1	45 742	93	37 197	87	177 931	52 439	0

GCF: reference genome; SNP: single nucleotide polymorphism.

[a] Isolates included in the cluster. The numbers in bold highlight the minimum SNP difference between the two isolates included in the cluster.

Nevertheless, the presence of these AMR genes among these isolates poses a potential public health risk, since the transfer of these genes from one organism to another can be mediated by mobile genetic elements, such as plasmids.

Following detection of the cluster of *S. sarumanii* infections, a multidisciplinary team composed of staff from the Infection Prevention and Control Unit, paediatric infectious diseases specialists and neonatologists was convened to implement immediate control measures to prevent and mitigate further transmission. These measures included targeted cleaning and daily thorough disinfection in the NICUs; environmental swabbing, water analysis and limiting of human traffic in the NICUs; and enhanced monitoring of procedures in the microbiology laboratory, from specimen receipt to result release. Subsequently, multiple meetings were held to review and refine the implementation of these measures.

While this study demonstrated the benefits of using SaTScan and WGS to detect and investigate possible outbreaks of bacterial infections in vulnerable hospital patients, it also identified challenges and potential barriers to wider adoption of these methods for AMR surveillance. While not a major concern in this particular study, occasional operational lapses may cause disruptions to the routine uploading of laboratory data about AMR from surveillance sites to the ARSRL, resulting in delays in detecting and verifying potential clusters using SaTScan. The limited storage capacity for biological samples at sentinel sites is another potential risk, as this can impact the availability of isolates for WGS once a potential outbreak has been identified by SaTScan. In this investigation, only two cluster isolates (out of six) were available for sequencing by the time the site was notified. Nevertheless, in this setting, the inclusion of four non-cluster isolates provided valuable spatial and temporal context for the outbreak investigation itself, while also demonstrating the value of genomic analysis in distinguishing a potential outbreak from a coincidental increase in cases. However, the unavailability of environmental samples and swabs from staff was a noted limitation of this investigation, as these may have helped pinpoint the source of the outbreak. From a broader operational perspective, the cost of performing WGS is high, limiting its application in routine purposes, such as surveillance. Sequencing services in many low- and middle-income countries will

likely be limited due to constraints on resources and access to hard-to-procure reagents.

Conclusions

This study highlights the potential advantages of combining WHONET's SaTScan feature with WGS for detecting and investigating outbreaks of potentially resistant bacterial infections in health-care facilities. In this case, the use of SaTScan prompted a timely investigation of an increase in *Serratia* infections detected in routine laboratory census data, while WGS provided granular evidence of the genetic relatedness of two cluster isolates, indicating that the infections may have come from a single source within the hospital's NICUs. The use of such tools has the potential to assist in delivering a more focused and efficient response by providing insights for effective outbreak management and resource optimization in health-care settings.

Acknowledgements

The authors thank the residents and consultants of the Department of Pediatrics, the NICU nurses, and the staff and consultants of the laboratory at the Southern Philippines Medical Center, and all the staff at the Antimicrobial Resistance Surveillance Reference Laboratory of the Research Institute for Tropical Medicine at the Department of Health.

Conflicts of interest

The authors have no conflicts of interest to declare.

Ethics statement

This study was evaluated and approved by the Institutional Review Board of the Research Institute for Tropical Medicine at the Department of Health, with reference number 2023-25.

Funding

None.

References

1. Braun V. Iron uptake mechanisms and their regulation in pathogenic bacteria. Int J Med Microbiol. 2001;291(2):67–79. doi:10.1078/1438-4221-00103 pmid:11437341
2. Cristina ML, Sartini M, Spagnolo AM. *Serratia marcescens* infections in neonatal intensive care units (NICUs). Int J Environ Res Public Health. 2019;16(4):610. doi:10.3390/ijerph16040610 pmid:30791509
3. Maragakis LL, Winkler A, Tucker MG, Cosgrove SE, Ross T, Lawson E, et al. Outbreak of multidrug-resistant *Serratia marcescens* infection in a neonatal intensive care unit. Infect Control Hosp Epidemiol. 2008;29(5):418–23. doi:10.1086/587969 pmid:18419363
4. Howard-Jones AR, Janto C, Jennings Z, Branley J, Wang Q, Sintchenko V, et al. Prompt control of a *Serratia marcescens* outbreak in a neonatal intensive care unit informed by whole-genome sequencing and comprehensive infection control intervention package. Antimicrob Steward Healthc Epidemiol. 2022;2(1):e104. doi:10.1017/ash.2022.234 pmid:36483351
5. Pena SJ, Fabay XC. Outbreak of *Serratia marcescens* in the newborn care unit in a local tertiary hospital. Pediatr Infect Dis Soc Philipp. 2012;13(2):39–46.
6. Lappay JI, Gaddi MJ, Calotes-Castillo LV. *Serratia marcescens* healthcare-associated ventriculitis and cerebral abscess in a neonate with Chiari II malformation: a case report and systematic review. Acta Med Philipp. 2022;56(10):829. doi:10.47895/amp.vi0.829
7. Performance standards for antimicrobial susceptibility testing, thirty-first edition. Wayne (PA): Clinical and Laboratory Standards Institute; 2021. Available from: https://clsi.org/about/news/clsi-publishes-m100-performance-standards-for-antimicrobial-susceptibility-testing-31st-edition, accessed 1 October 2025.
8. O'Brien TF, Stelling JM. WHONET: an information system for monitoring antimicrobial resistance. Emerg Infect Dis. 1995;1(2):66. doi:10.3201/eid0102.950209 pmid:8903165
9. Kulldorff M. SaTScan: software for the spatial, temporal, and space-time scan statistics [website]. Boston (MA): SaTScan; 2005. Available from: https://www.satscan.org, accessed 1 October 2025.
10. Petit RA 3rd, Read TD. Bactopia: a flexible pipeline for complete analysis of bacterial genomes. mSystems. 2020;5(4):e00190-20. doi:10.1128/mSystems.00190-20 pmid:32753501
11. Seemann T. Shovill: assemble bacterial isolate genomes from Illumina paired-end reads [software program]. In: GitHub. San Francisco (CA): Microsoft; 2019. Available from: https://github.com/tseemann/shovill, accessed 1 October 2025.
12. Bankevich A, Nurk S, Antipov D, Leven E, Prjibelski A, Korobeynikov A, et al. SPAdes: a new genome assembly algorithm and its applications to single-cell sequencing. J Comput Biol. 2012;19(5):455–77. doi:10.1089/cmb.2012.0021 pmid:22506599
13. Jolley KA, Bray JE, Maiden MCJ. Open-access bacterial population genomics: BIGSdb software, the PubMLST.org website and their applications. Wellcome Open Res. 2018;3:124. doi:10.12688/wellcomeopenres.14826.1 pmid:30345391
14. Seemann T. Snippy: rapid haploid variant calling and core genome alignment [software program]. In: GitHub. San Francisco (CA): Microsoft; 2015. Available from: https://github.com/tseemann/snippy, accessed 1 October 2025.
15. Ondov BD, Treangen TJ, Melsted P, Mallonee AB, Bergman NH, Koren S, et al. Mash: fast genome and metagenome distance estimation using MinHash. Genome Biol. 2016;17(1):132. doi:10.1186/s13059-016-0997-x pmid:27323842
16. Ceparano M, Capitani V, Migliara G, Rondon S, Baccolini V, Carattoli A, et al. Diversity versus clonality in carbapenem-resistant *A. baumannii*: a two-year surveillance study in four intensive care units at a large teaching hospital in Rome, Italy. Antimicrob Resist Infect Control. 2025;14(1):84. doi:10.1186/s13756-025-01605-7 pmid:40629400

17. Minh BQ, Schmidt HA, Chernomor O, Schrempf D, Woodhams MD, von Haeseler A, et al. IQ-TREE 2: new models and efficient methods for phylogenetic inference in the genomic era. Mol Biol Evol. 2020;37(5):1530–4. doi:10.1093/molbev/msaa015 pmid:32011700

18. Feldgarden M, Brover V, Gonzalez-Escalona N, Frye JG, Haendiges J, Haft DH, et al. AMRFinderPlus and the Reference Gene Catalog facilitate examination of the genomic links among antimicrobial resistance, stress response, and virulence. Sci Rep. 2021;11(1):12728. doi:10.1038/s41598-021-91456-0 pmid:34135355

19. Klages LJ, Kaup O, Busche T, Kalinowski J, Rückert-Reed C. Classification of a novel *Serratia* species, isolated from a wound swab in North Rhine–Westphalia: proposal of *Serratia sarumanii* sp. nov. Syst Appl Microbiol. 2024;47(5):126527. doi:10.1016/j.syapm.2024.126527 pmid:38959748

20. Stasiak M, Maćkiw E, Kowalska J, Kucharek K, Postupolski J. Silent genes: antimicrobial resistance and antibiotic production. Pol J Microbiol. 2021;70(4):421–9. doi:10.33073/pjm-2021-040 pmid:35003274

Investigation of the first carbon monoxide poisoning cluster associated with a hotpot restaurant in Thailand, 2023

Siriyakorn Thanasitthichai,[a] Oranut Srihadom,[b] Tanaporn Thongsim,[b] Pasika Nonluecha,[b] Kriangkrai Kampaiboon,[c] Chuthamat Bodnok[d] and Pawinee Doungngern[e]

Correspondence to Siriyakorn Thanasitthichai (email: s.thanasitthichai@gmail.com)

Objective: On 27 June 2023, the Thailand Department of Disease Control was notified of an incident of carbon monoxide poisoning related to a Thai-style hotpot restaurant. An outbreak investigation was performed to describe the incident, confirm its cause and sources of exposure, and provide preventive measures.

Methods: The restaurant owner, restaurant guests and waiting staff were interviewed, and the medical records of hospitalized cases were reviewed. In an environmental survey, air quality parameters were measured, including temperature, relative humidity, carbon dioxide and carbon monoxide. Additionally, a simulation of the incident was conducted, and data were reviewed from previous poisoning incidents in Thailand.

Results: There were 11 cases, all of whom were guests who dined in the same private dining room. The median age of cases was 28 years (range 2–62 years). Three cases were hospitalized and received hyperbaric oxygen therapy. The air changes in the dining rooms were below the recommended level. The incomplete combustion of charcoal in a poorly ventilated room led to carbon monoxide build-up, which caused the incident. The simulation experiment showed a high concentration of carbon monoxide (mean 183.16 ± 55.15 parts per million), above the standard level. Ten similar poisoning incidents occurred between 2019 and June 2023, totalling 23 cases and 2 deaths; none occurred in a restaurant.

Discussion: Charcoal use in poorly ventilated areas poses a health risk, especially for children. The use of charcoal stoves for hotpot cooking indoors is prohibited. Public health policy should mandate regular restaurant inspections to ensure compliance with occupational and environmental health standards.

Carbon monoxide (CO) is an odourless, colourless, non-irritant gas produced from an incomplete combustion of hydrocarbon fuels and substances. When inhaled, CO becomes toxic by binding and altering the functions of heme proteins in the haemoglobin, myoglobin and other components of oxygen-carrying pathways. The formation of carboxyhaemoglobin (COHb) severely impairs the oxygen-carrying capacity of blood and reduces oxygen release to the tissues. The primary targets of CO-induced injuries are the brain and heart, the organs with the highest oxygen demand.[1] Symptoms of CO toxicity include headache, dizziness, confusion, nausea, blurred vision, rhabdomyolysis, arrhythmias, myocardial infarction, loss of consciousness, seizure and coma.[2] Delivery of 100% oxygen is the mainstay treatment for CO poisoning. In addition, hyperbaric oxygen therapy should be considered in patients at high risk of severe symptoms to improve long-term neurological outcomes and survival.[3] Children, older adults, pregnant women and people with anaemia are more susceptible to CO toxicity, as are those with chronic respiratory, cerebrovascular or coronary heart diseases.[4]

Unintentional, non-fire related (UNFR) CO poisoning is a public health concern. While highly preventable, it is the leading cause of poisoning morbidity and mortality in many countries.[5] In 2007, an estimated 21 000 emergency department visits and 2300 hospitalizations

[a] Field Epidemiology Training Program, Ministry of Public Health, Nonthaburi, Thailand.
[b] Division of Occupational and Environmental Diseases, Department of Disease Control, Ministry of Public Health, Nonthaburi, Thailand.
[c] Pathum Thani Hospital, Pathum Thani, Thailand.
[d] Pathum Thani Provincial Public Health Office, Ministry of Public Health, Pathum Thani, Thailand.
[e] Division of Epidemiology, Department of Disease Control, Ministry of Public Health, Nonthaburi, Thailand.
Published: 25 March 2026
doi: 10.5365/wpsar.2026.17.1.1110

in the United States of America were attributed to UNFR CO poisoning.[6] They mainly occur in domestic settings and are more common during the autumn and winter months.[7,8] Fuel-burning appliances such as heating systems are responsible for the majority of incidents.[9–11] However, no previous studies have investigated the incidence or characteristics of CO poisoning in Thailand.

On 27 June 2023, the Division of Occupational and Environmental Diseases, Department of Disease Control, Ministry of Public Health, was notified of an incident of CO poisoning among restaurant guests who had dined in the same dining room of a Thai-style hotpot restaurant on the previous day in a province in the central region of Thailand. The Department of Disease Control, the Office of Disease Prevention and Control Region 4 Saraburi, Pathum Thani Hospital, and the local health-care team jointly investigated the incident on 28 June and 4 July 2023. In this report, we describe the incident, confirm the cause and sources of exposure, and provide recommendations for CO poisoning prevention.

METHODS

For the epidemiological investigation, active case-finding was initiated, and those who were in the restaurant at the time of the event were interviewed, including the restaurant guests and waiting staff who were in the private dining room on the day of the event, as well as the restaurant owner. The medical records of those who visited hospitals were reviewed.

Data on patients' demographic characteristics, medical history, time and manner of CO exposure, clinical symptoms, laboratory results and treatments received were collected using a semi-structured questionnaire. Case definitions were adapted from the 2019 case definition of CO poisoning by the United States Centers for Disease Control and Prevention.[12] Suspected cases were defined as restaurant guests or staff who had been in the dining room on 26 June 2023 and who had at least one of the following symptoms: fatigue, nausea, vomiting, chest pain, difficulty breathing, blurred vision, headache, dizziness, confusion, light-headedness, loss of consciousness and a history of CO exposure. Confirmed cases were suspected cases who had a COHb level over 6% for non-smokers or over 12% for smokers.

A walk-through survey of the restaurant facilities was conducted. The air quality of the indoor and outdoor dining areas was monitored. The targeted parameters were temperature, relative humidity, carbon dioxide (CO_2) and CO. Each sampling point was placed 1.1 m above the floor and away from potential sources of air pollution. The ventilation rate of dining rooms was determined by the number of air changes per hour, which equals the volumetric air flow rate divided by the volume of space.[13]

A 60-minute simulation was conducted using data from the cases to further analyse the air quality of the dining room at the time of the incident. Details on the types and number of possible sources of pollutants and the environmental conditions during which the CO poisoning occurred were obtained through interviews. Air temperature, relative humidity, CO_2 and CO were measured using the Q-Trak™ Indoor Air Quality Monitor Model 7575 and a model IAQ Probe 982 (TSI Inc., Shoreview, MN, USA). For air velocity measurement, the Testo 400 - Universal IAQ Instrument and a 100-mm vane probe head (Testo SE & Co. KGaA, Titisee-Neustadt, Germany) were used. Devices were calibrated, and pre- and post-zero checks were done. Air quality data were recorded at each sampling point at an interval of 10 seconds for at least 15 minutes. The data were calculated as mean and standard deviation.

We also reviewed UNFR CO poisoning incidents recorded in the event-based surveillance system of the Thai Department of Disease Control from January 2019 to June 2023 to determine the number and characteristics of UNFR CO poisoning incidents in Thailand, using the same case definitions as in our epidemiological investigation.

RESULTS

The restaurant

The hotpot restaurant has an outdoor dining area and a dining room (Dining Room A), as well as two private rooms (Private Rooms B and C). The CO poisoning incident took place in Private Room B. The restaurant had been open for 10 months at the time and serves a variety of Thai-Esan cuisine, including Thai-style hotpots cooked on burning charcoal stoves. Typically, no more than three hotpots are served in a private dining room at a time.

Description of the incident

The restaurant did not have a record of guests' names or contact numbers; therefore, we were only able to interview the affected guests and the waiting staff. There were 11 restaurant guests and four waiting staff in Private Room B on 26 June 2023. All restaurant guests were family members. Eleven restaurant guests met our case definitions (8 suspected and 3 confirmed cases), whereas none of the waiting staff were symptomatic. The median age of cases was 28 years (range 2–62 years). Three cases had underlying diseases (chronic hypertension, diabetes mellitus, asthma). None were pregnant. Demographic, treatment and outcome data of cases are shown in **Table 1**. The median duration of CO exposure was 140 minutes (range 90–140 minutes) among restaurant guests and 18 minutes (range 10–70 minutes) among waiting staff. The median time to symptom onset was 90 minutes (range 45–300 minutes) after first exposure. Dizziness (82%), headache (46%) and light-headedness (46%) were the most common symptoms.

The guests arrived at the restaurant around 19:00 and ordered five Thai-style hotpots. Four were served at the beginning and one was served an hour later. At 20:00, a 2-year-old girl started crying and vomiting, and her parents took her home at 20:30. Around that time, other guests in the room reported experiencing symptoms such as fatigue, headache and dizziness. At 21:00, three restaurant guests (11-year-old boy, 19-year-old woman, 58-year-old woman) fainted, so the family left for the hospital. No other guests entered Private Room B on that day (**Fig. 1**).

On arrival, the three patients with light-headedness were sent to the emergency department. Their COHb levels were 25%, 31% and 33%. They received hyperbaric oxygen therapy and were hospitalized for 24-hour observation. Two of them developed grade II middle ear barotrauma after treatment. Other cases had mild symptoms and were treated as outpatients. At 1-week follow-up, two cases had lingering headache and fatigue and nine had fully recovered (**Table 1**).

Indoor air quality of the dining areas

The restaurant is in an urban area with moderate traffic intensity. No other sources of air pollution (for example, open chimneys) were observed nearby. All indoor dining rooms have mini-split air conditioning systems. There are 1–2 wall exhaust fans in each room.

During the environmental survey, the weather was cloudy with light rainfall. Daytime temperatures were up to 33°C with a relative humidity of 55–89%. The air quality parameters of the dining rooms were measured while air conditioners and exhaust fans were on. The measurements were performed during the restaurant's closing hours (13:00–16:00) at the request of the restaurant owner. The mean values of temperature, relative humidity, CO and CO_2 of the dining rooms were within acceptable ranges according to the Notification of the Department of Health regarding Indoor Air Quality Monitoring Standards in Public Building B.E. 2565 (2022), except for the temperature of Private Room B, which was slightly higher than the recommendation.[14] However, the ventilation rates of the dining rooms were below the required 10 air changes per hour, ranging from 0.25 to 4.19 air changes per hour (**Table 2**).

Simulation of CO poisoning incident

A 60-minute simulation of the CO poisoning incident was conducted in Private Room B. Four charcoal stoves were lit, the air conditioner and wall exhaust fans were operating, and the door was closed. During the simulation, the mean CO was 183.16 ± 55.15 parts per million (ppm) and the mean CO_2 was 1502.54 ± 283.61 ppm (**Fig. 2**). The concentrations of CO and CO_2 in the air were both above the acceptable limits set by the Thai Department of Health for indoor air quality.[14] Moreover, the CO concentrations exceeded the World Health Organization air quality guideline value (<26 ppm in 1 hour) and the Acute Exposure Guideline Level 2 (AEGL-2) value (<83 ppm in 1 hour) for CO.[15,16]

Public health response

The restaurant owner was notified of the results of the analysis of the incident and advised that the use of indoor charcoal stoves was strictly prohibited. A visible sign has been posted at the restaurant's entrance to inform patrons of this policy. The floor plans of the restaurant were reviewed by municipal officials, and the restaurant was temporarily closed to undergo renovations to ensure compliance with environmental standards. A food hygiene and safety training course for local restaurant owners and staff was conducted,

Table 1. **Demographic, treatment and outcome data of carbon monoxide poisoning cases in Private Room B of a hotpot restaurant, central Thailand, 2023**

ID	Sex	Age (years)	Underlying diseases	Case status	Visit type	COHb level (%)	Treatment	Outcome at 1-week follow-up
1	Female	58	T2DM, HT, DLP	Confirmed	IPD	33	HBOT	Mild headache, middle ear barotrauma grade II
2	Female	19	None	Confirmed	IPD	25	HBOT	Middle ear barotrauma grade II
3	Male	11	None	Confirmed	IPD	31	HBOT	Fully recovered
4	Female	40	None	Suspected	OPD	–	Supportive	Fully recovered
5	Male	62	T2DM, HT	Suspected	No	–	None	Mild fatigue
6	Female	54	None	Suspected	No	–	None	Fully recovered
7	Male	34	None	Suspected	No	–	None	Fully recovered
8	Female	28	None	Suspected	No	–	None	Fully recovered
9	Male	19	None	Suspected	No	–	None	Fully recovered
10	Male	19	Asthma	Suspected	No	–	None	Fully recovered
11	Female	2	None	Suspected	No	–	None	Fully recovered

COHb: carboxyhemoglobin; DLP: dyslipidaemia; HBOT: hyperbaric oxygen therapy; HT: chronic hypertension; IPD: inpatient department; OPD: outpatient department; T2DM: type II diabetes mellitus.

during which a module on CO poisoning was presented. An online public education campaign was launched to raise awareness of the risks of unintentional CO poisoning.

Unintentional, non-fire related carbon monoxidepoisoning in Thailand

Between 1 January 2019 and 30 June 2023, the Department of Disease Control's surveillance system showed 10 incidents of UNFR CO poisoning in Thailand, resulting in 23 cases and 2 deaths. The median number of cases per event was 1.5 (range 1–9). Nine incidents occurred in northern Thailand, and eight were caused by using gas water heaters in unventilated bathrooms in local resorts. Eight of the incidents occurred during the winter months. Notably, one incident involved the use of charcoal stoves for hotpot cooking in a camping tent. No prior reports of CO poisoning in restaurants had been documented.

DISCUSSION

We confirmed the first incident of CO poisoning in a food establishment in Thailand, which occurred at a Thai-style hotpot restaurant. The source of CO exposure was from charcoal stoves in which hotpots were cooked. Hotpot restaurants have been linked to multiple incidents of unintentional CO poisoning. Gaüzère et al. reported the mass CO intoxication of more than 50 people who dined in an unventilated Chinese hotpot restaurant.[17] Chua et al. reported another mass CO poisoning of 30 hotpot restaurant staff due to an exhaust fan malfunction.[18] Environmental studies in China found that nearly half of hotpot and barbeque restaurants studied had CO levels above the recommended indoor air quality standard. The CO levels were highest in hotpot restaurants that used charcoal as the main fuel.[19,20]

In the current incident, two children were the first to exhibit symptoms of CO poisoning. Children are more

Fig. 1. **Number of carbon monoxide poisoning cases in a hotpot restaurant by time of onset, central Thailand, 26 June 2023 (*N* = 11)**

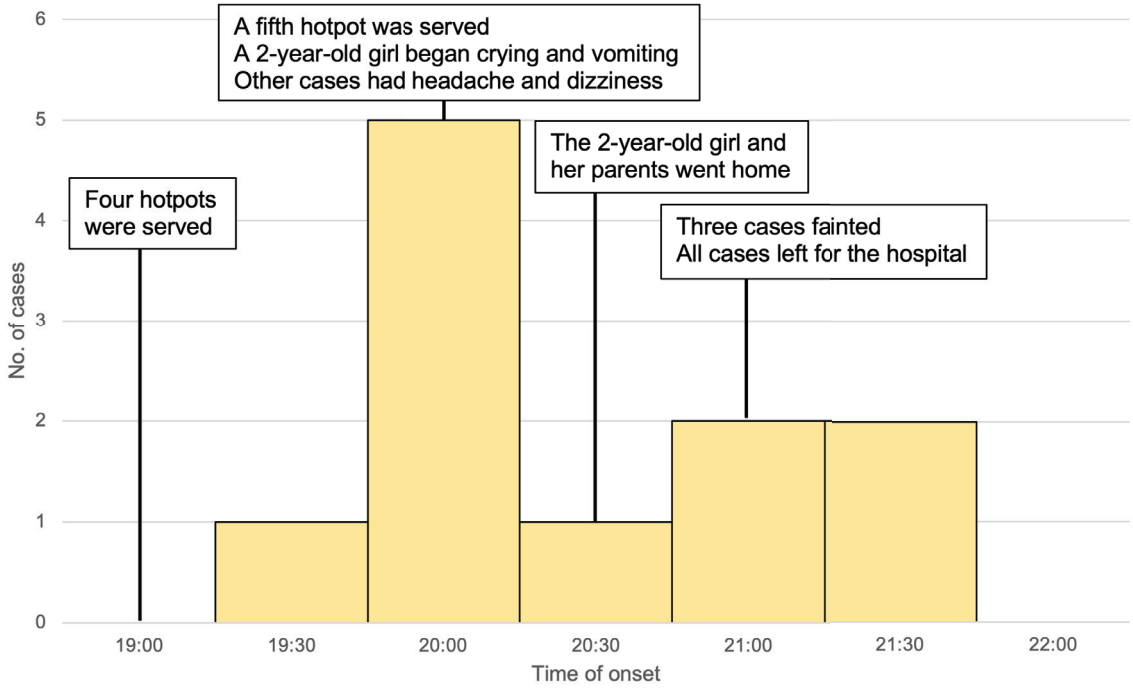

Table 2. **General information and air quality parameters of dining areas in the restaurant during the 60-minute simulation in Private Room B, central Thailand, 2023**

Parameter	Thai IAQ standards[14]	Dining Room A	Private Room B	Private Room C	Outdoor zone
Room volume (m^3)	–	58.29	99.26	43.12	–
Capacity	–	12–18 guests	18–28 guests	6–12 guests	150–200 guests
Ventilation system	–	1 exhaust fan, sized 0.10 × 0.10 m	2 wall exhaust fans, sized 0.22 × 0.22 m	1 wall exhaust fan, sized 0.22 × 0.22 m	–
Temperature (°C)	24–26	25.90 ± 0.41	26.38 ± 0.62	24.55 ± 0.33	28.96 ± 0.58
Relative humidity (%)	50–65	63.53 ± 3.63	57.93 ± 1.16	63.25 ± 0.72	80.25 ± 6.19
CO (ppm)	≤9	3.78 ± 0.22	0.08 ± 0.09	0.00 ± 0.00	0.01 ± 0.04
CO_2 (ppm)	≤1000	544.00 ± 6.12	500.94 ± 47.16	406.04 ± 14.15	361.98 ± 12.38
Air changes per hour	>10	0.25	3.15	4.19	–

°C: centigrade; CO: carbon monoxide; CO_2: carbon dioxide; IAQ: indoor air quality; ppm: parts per million.

Fig. 2. **Carbon monoxide and carbon dioxide concentrations during the 60-minute simulation in Private Room B, central Thailand, 2023**

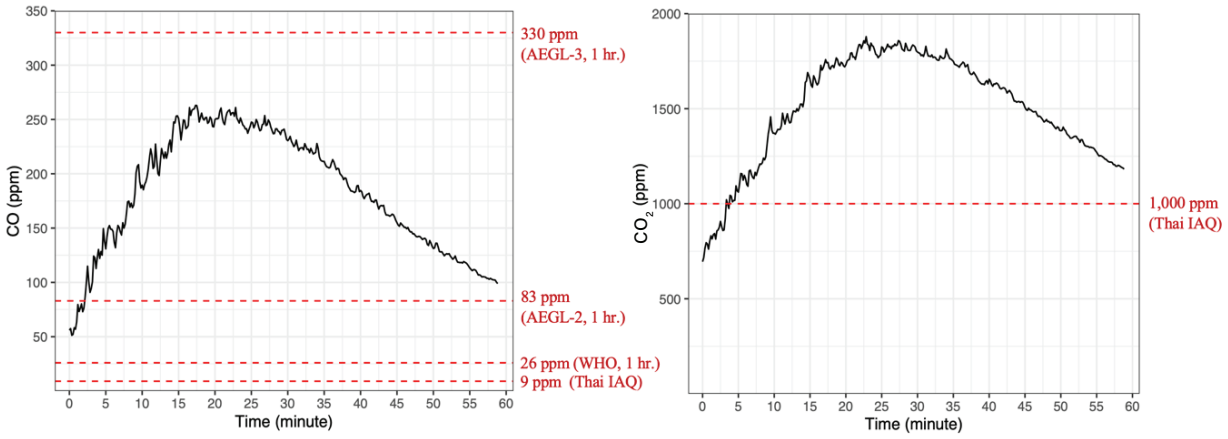

AEGL: acute exposure guideline level; CO: carbon monoxide; CO_2: carbon dioxide; IAQ: indoor air quality; ppm: parts per million; WHO: World Health Organization.

vulnerable to CO toxicity and experience symptoms much earlier than adults due to their elevated respiratory and metabolic rates, increased oxygen requirements and immature central nervous systems.[21,22] In a report by Klasner et al., children started having headache, dizziness and nausea at a COHb level as low as 7%.[23] In contrast, healthy adults would only feel occasional temporal headache at a COHb level of around 20%.[24] Additionally, children are prone to the neurotoxic effects of CO. According to studies in Taiwan (China) and the United States, approximately 60–80% of children who presented to the hospital with CO poisoning exhibited acute neurological manifestations, with symptoms ranging from varying degrees of consciousness changes and tremor to ataxia and seizures.[25–27]

From the environmental survey, we found that the air change rates of dining rooms were significantly below the standards set by the Department of Health.[14] Poor air changes together with the use of multiple charcoal stoves led to rapid accumulation of CO and other pollutants. During the simulation, the CO concentrations exceeded the AEGL-2 value in less than 5 minutes. CO exposure at this level could result in serious health damage, particularly in susceptible populations. For example, it could cause significant cardiac changes and reduce the time to onset of angina in patients with coronary artery disease.[28,29] As for CO_2, short-term exposure to concentrations above 1000 ppm is not immediately dangerous, but it can lead to a reduction in cognitive performance.[30] Our findings highlight the dangers of using charcoal in poorly ventilated areas.

The findings of this study should be interpreted with caution due to some limitations. First, for safety reasons, we were unable to simulate the exact event with people in the private room. Second, the environmental survey was conducted during the restaurant's closing hours. Therefore, the air pollution levels that were detected may have been lower than those that would have been present during the restaurant's operating hours, when cooking activities were taking place. Third, the lack of laboratory results for patients with mild symptoms limited our ability to confirm the diagnosis of CO poisoning.

Future policy should mandate routine inspections of all restaurants to ensure compliance with occupational and environmental health standards. These inspections should verify adequate ventilation of indoor dining areas and proper venting of fuel-burning appliances. Restaurants should also be required to train their staff on the hazards of CO poisoning and how to prevent it. By implementing these measures, the risk of unintentional CO poisoning in restaurants could be effectively reduced.

We reported a CO poisoning incident associated with a hotpot restaurant on 26 June 2023. All 11 cases were restaurant guests, aged 2–62 years. Three cases were hospitalized and received hyperbaric oxygen therapy. No deaths were reported. Charcoal stoves were the source of CO exposure. From an environmental survey, we found that the restaurant's indoor dining areas had very low air exchange rates, which contributed to the accumulation of CO. The use of indoor charcoal

stoves was prohibited. The restaurant floor plan and ventilation system were reviewed by local authorities and renovated. In addition, an online public awareness campaign on unintentional CO poisoning was launched. The routine inspection of restaurants and the provision of training sessions on CO poisoning are recommended as future policy interventions to mitigate the risk of CO poisoning in restaurants.

Acknowledgements

The authors thank the restaurant staff, staff of the local provincial public health office, health promotion hospital, town municipality office, Office of Disease Prevention and Control Region 4 Saraburi, Pathum Thani Hospital, and Department of Disease Control joint investigation team for their kind support.

Conflicts of interest

The authors have no conflicts of interest to declare.

Ethics statement

This study was conducted as part of normal outbreak surveillance and response activities of the Department of Disease Control, Ministry of Public Health, Thailand. No additional ethical approval was required.

Funding

None.

References

1. Wilbur S, Williams M, Williams R, Scinicariello F, Klotzbach JM, Diamond GL, et al. Toxicological profile for carbon monoxide. Atlanta (GA): United States Agency for Toxic Substances and Disease Registry; 2012. Available from: https://wwwn.cdc.gov/TSP/ToxProfiles/ToxProfiles.aspx?id=1145&tid=253, accessed 7 October 2023.
2. Gozubuyuk AA, Dag H, Kacar A, Karakurt Y, Arica V. Epidemiology, pathophysiology, clinical evaluation, and treatment of carbon monoxide poisoning in child, infant, and fetus. North Clin Istanb. 2017;4(1):100–7. doi:10.14744/nci.2017.49368 pmid:28752154
3. Eichhorn L, Thudium M, Jüttner B. The diagnosis and treatment of carbon monoxide poisoning. Dtsch Arztebl Int. 2018;115(51–52):863–70. doi:10.3238/arztebl.2018.0863 pmid:30765023
4. Environmental health criteria 13: carbon monoxide. Geneva: World Health Organization and International Programme on Chemical Safety; 1979. Available from: https://iris.who.int/handle/10665/336055, accessed 7 October 2023.
5. Raub JA, Mathieu-Nolf M, Hampson NB, Thom SR. Carbon monoxide poisoning–a public health perspective. Toxicology. 2000;145(1):1–14. doi:10.1016/S0300-483X(99)00217-6 pmid:10771127
6. Iqbal S, Law HZ, Clower JH, Yip FY, Elixhauser A. Hospital burden of unintentional carbon monoxide poisoning in the United States, 2007. Am J Emerg Med. 2012;30(5):657–64. doi:10.1016/j.ajem.2011.03.003 pmid:21570230
7. Close RM, Iqbal N, Jones SJ, Kibble A, Flanagan RJ, Crabbe H, et al. Fatal unintentional non-fire related carbon monoxide poisoning: data from narrative verdicts in England and Wales, 1998–2019. Int J Environ Res Public Health. 2022;19(7):4099. doi:10.3390/ijerph19074099 pmid:35409782
8. Dianat I, Nazari J. Characteristics of unintentional carbon monoxide poisoning in Northwest Iran—Tabriz. Int J Inj Contr Saf Promot. 2011;18(4):313–20. doi:10.1080/17457300.2011.589006 pmid:21827338
9. Non-fire carbon monoxide deaths associated with the use of consumer products 2019 annual estimates. Bethesda (MD): United States Consumer Product Safety Commission; 2023. Available from: https://www.cpsc.gov/content/Non-Fire-Carbon-Monoxide-Deaths-Associated-with-the-Use-of-Consumer-Products-2019-Annual-Estimates, accessed 7 October 2023.
10. Li M, Shan B, Peng X, Chang H, Cui L. An urgent health problem of indoor air pollution: results from a 15-years carbon monoxide poisoning observed study in Jinan City. Sci Rep. 2023;13(1):1619. doi:10.1038/s41598-023-28683-0 pmid:36709374
11. Fisher DS, Bowskill S, Saliba L, Flanagan RJ. Unintentional domestic non-fire related carbon monoxide poisoning: data from media reports, UK/Republic of Ireland 1986–2011. Clin Toxicol. 2013;51(5):409–16. doi:10.3109/15563650.2013.786833 pmid:23578111
12. Carbon monoxide poisoning 2019 case definition. Atlanta (GA): United States Centers for Disease Control and Prevention; 2021. Available from: https://ndc.services.cdc.gov/case-definitions/carbon-monoxide-poisoning-2019, accessed 14 July 2023.
13. Zhang Y, Cao G, Feng G, Xue K, Pedersen C, Mathisen HM, et al. The impact of air change rate on the air quality of surgical microenvironment in an operating room with mixing ventilation. J Build Eng. 2020;32:101770. doi:10.1016/j.jobe.2020.101770
14. Notification of the Department of Health regarding Indoor Air Quality Monitoring Standards in Public Building B.E. 2565 (2022). Nonthaburi: Department of Health, Thailand; 2022. Available from: https://enviliance.com/categories/southeast-asia/th, accessed 14 July 2023.
15. National Research Council (US) Committee on Acute Exposure Guideline Levels. Acute exposure guideline levels for selected airborne chemicals. Volume 8. Washington (DC): National Academies Press; 2010.
16. Penney D, Benignus V, Kephalopoulos S, Kotzias D, Kleinman M, Verrier A. Carbon monoxide. In: WHO guidelines for indoor air quality: selected pollutants. Copenhagen: WHO Regional Office for Europe; 2010. pp. 55–101. Available from: https://iris.who.int/handle/10665/260127, accessed 7 October 2023.

17. Gaüzère BA, Djardem Y, Bourdé A, Blanc P. A new chinese restaurant syndrome: the 'Chinese fondue' carbon monoxide mass intoxication. Crit Care. 1999;3(1):55. doi:10.1186/cc308 pmid:11094474

18. Chua ISY, Tan KBK, Ponampalam R. Carbon monoxide poisoning in a group of restaurant workers: lessons learnt and how to prevent future occurrences. Singapore Med J. 2024;65(5):288–90. doi:10.11622/smedj.2021217 pmid:34823325

19. Zhao Y, Tao P, Zhang B, Huan C. Contribution of Chinese hot pot and barbecue restaurants on indoor environmental parameters. Aerosol Air Qual Res. 2020;20(12):2920–40. doi:10.4209/aaqr.2020.04.0141

20. Zhang Z, Zhao Y, Zhou M, Tao P, Li R. Measurement of indoor air quality in Chinese charcoal barbecue restaurants. Procedia Eng. 2017;205:887–94. doi:10.1016/j.proeng.2017.10.088

21. Liebelt EL. Hyperbaric oxygen therapy in childhood carbon monoxide poisoning. Curr Opin Pediatr. 1999;11(3):259–64. doi:10.1097/00008480-199906000-00017 pmid:10349107

22. Martin JD, Osterhoudt KC, Thom SP. Recognition and management of carbon monoxide poisoning in children. Clin Pediatr Emerg Med. 2000;1(3):244–50. doi:10.1016/S1522-8401(00)90035-1

23. Klasner AE, Smith SR, Thompson MW, Scalzo AJ. Carbon monoxide mass exposure in a pediatric population. Acad Emerg Med. 1998;5(10):992–6. doi:10.1111/j.1553-2712.1998.tb02778.x pmid:9862591

24. Henderson Y, Haggard HW, Teague MC, Prince AL, Wunderlich RM. Physiological effects of automobile exhaust gas and standards of ventilation for brief exposures. J Ind Hyg. 1921;3(3):79–92.

25. Chang YC, Lee HY, Huang JL, Chiu CH, Chen CL, Wu CT. Risk factors and outcome analysis in children with carbon monoxide poisoning. Pediatr Neonatol. 2017;58(2):171–7. doi:10.1016/j.pedneo.2016.03.007 pmid:27502424

26. Cho CH, Chiu NC, Ho CS, Peng CC. Carbon monoxide poisoning in children. Pediatr Neonatol. 2008;49(4):121–5. doi:10.1016/S1875-9572(08)60026-1 pmid:19054917

27. Meert KL, Heidemann SM, Sarnaik AP. Outcome of children with carbon monoxide poisoning treated with normobaric oxygen. J Trauma. 1998;44(1):149–54. doi:10.1097/00005373-199801000-00020 pmid:9464764

28. Allred EN, Bleecker ER, Chaitman BR, Dahms TE, Gottlieb SO, Hackney JD, et al. Effects of carbon monoxide on myocardial ischemia. Environ Health Perspect. 1991;91:89–132. doi:10.1289/ehp.919189 pmid:2040254

29. Allred EN, Bleecker ER, Chaitman BR, Dahms TE, Gottlieb SO, Hackney JD, et al. Short-term effects of carbon monoxide exposure on the exercise performance of subjects with coronary artery disease. N Engl J Med. 1989;321(21):1426–32. doi:10.1056/NEJM198911233212102 pmid:2682242

30. Allen JG, MacNaughton P, Cedeno-Laurent JG, Cao X, Flanigan S, Vallarino J, et al. Airplane pilot flight performance on 21 maneuvers in a flight simulator under varying carbon dioxide concentrations. J Expo Sci Environ Epidemiol. 2019;29(4):457–68. doi:10.1038/s41370-018-0055-8 pmid:30089876

COVID-19 mortality in the Philippines: province-level ecological analysis, 2020–2023

Jimuel Celeste Jr,[a,b] Jesus Emmanuel Sevilleja,[c,d] Vena Pearl Bongolan,[a] Roselle Leah Rivera,[e] Salvador Eugenio Caoili[f] and Romulo de Castro[b,g]

Correspondence to Jimuel Celeste Jr (email: jimuelceleste@gmail.com)

Objective: To investigate COVID-19 mortality in Philippine provinces from 2020 to 2023.

Methods: Crude mortality rate (CMR), age-standardized mortality rate (ASMR) and age-specific mortality rate were computed for 84 areas (82 provinces and 2 cities) using COVID-19 surveillance data from the Philippine Department of Health, which captured data about confirmed deaths occurring between 20 January 2020 and 9 May 2023. Provinces were ranked by their ASMR. A correlation analysis was conducted to identify possible predictors of COVID-19 mortality. Among the factors investigated were the incidence of poverty, population density, proportion of the population considered elderly (aged ≥65 years), hospital bed density and COVID-19 testing rates.

Results: Eight of the 10 provinces that had the highest COVID-19 ASMRs were located in the Luzon island group. The province with the highest ASMR was Benguet in Northern Luzon (207.83 deaths/100 000 population), and the lowest rate was in Tawi-Tawi in Southwestern Mindanao (2.22 deaths/100 000 population). The incidence of poverty was negatively correlated with COVID-19 mortality, while hospital bed density and COVID-19 testing rates were positively correlated with CMRs and ASMRs.

Discussion: This analysis provides a starting point for investigating COVID-19 mortality in Philippine provinces. The ranking of provinces by their ASMR is useful for directing future epidemiological investigations and, coupled with the results of the correlation analysis, provides insight into the factors that may have impacted COVID-19 mortality in the Philippines. Our analysis suggests that COVID-19 mortality patterns can partly be explained by the streetlight effect and factors linked to the availability of and access to health care.

The COVID-19 pandemic caused millions of deaths globally. As of 29 December 2024, the cumulative total number of COVID-19 deaths reported to the World Health Organization (WHO) stood at just over 7.07 million.[1] The corresponding figure for the Philippines was 66 800 deaths.[1,2] Although the numbers of cases and deaths are not as high as they were when COVID-19 was a public health emergency of international concern, it is important to investigate what transpired during the pandemic, to look back and reflect, and to learn from the experience, given the risk of the emergence of new viruses.[3,4]

As a first step towards this goal, this study undertook a provincial-level investigation of COVID-19 mortality in the Philippines. The aims of the analysis were, first, to identify the provinces with the highest and lowest mortality rates, and, second, to identify possible drivers of high mortality rates. The study's objective was to add nuance to the understanding of COVID-19 mortality in the Philippines at the provincial level and to provide data to guide future epidemiological investigations and to inform future planning for pandemic preparedness and response, including surveillance.

[a] System Modeling and Simulation Laboratory, Department of Computer Science, College of Engineering, University of the Philippines Diliman, Quezon City, Philippines.
[b] Center for Informatics, University of San Agustin, Iloilo City, Philippines.
[c] Mental Health Research Unit, Office for Special Concerns, National Center for Mental Health, Mandaluyong City, Philippines.
[d] Hospital Epidemiology Surveillance Unit, Public Health Unit, National Center for Mental Health, Mandaluyong City, Philippines.
[e] Department of Women and Development Studies, College of Social Work and Community Development, University of the Philippines Diliman, Quezon City, Philippines.
[f] Biomedical Innovations Research for Translational Health Science (BIRTHS) Laboratory, Department of Biochemistry and Molecular Biology, College of Medicine, University of the Philippines Manila, Manila, Philippines.
[g] Health Informatics Program, Institute of Health Sciences and Nursing, Far Eastern University, Manila, Philippines.
Published: 25 March 2026
doi: 10.5365/wpsar.2026.17.1.1128

METHODS

Data sources

COVID-19 data

Data about confirmed deaths from COVID-19 compiled by the Department of Health's COVID-19 Case Tracker up until 27 May 2023 were analysed.[2] This dataset includes records of deaths of patients who were diagnosed with COVID-19 as confirmed by reverse transcription–polymerase chain reaction (RT–PCR) conducted by a certified laboratory.[2] The first confirmatory test for COVID-19 in the Philippines using RT–PCR was performed at the Research Institute for Tropical Medicine on 20 January 2020.[5] The latest death in the dataset was recorded on 9 May 2023.

Records were excluded if they did not contain data on the age, sex or province of the person tested. For records missing the date of infection, one of the following variables was used as a substitute, whichever had the first non-missing value: the date of disease onset, specimen collection, result release, report confirmation (i.e. the date when the Department of Health confirmed that the record was accurate) or death. Finally, case data were stratified by 84 administrative areas (82 provinces and 2 cities, the City of Isabela and Cotabato City) and 5-year age groups (0–4, 5–9, … ≥80 years).

Predictor variables

Possible predictors of COVID-19 mortality were selected depending on the availability of reliable provincial-level data from official government sources and a priori knowledge, with the latest year for the data also noted:

- population density (number of persons/km^2) (2020);[6]
- percentage of the population aged ≥65 years (2020);[7]
- incidence of poverty (2021);[8]
- hospital bed density (number of beds/100 000 population) (2022);[7,9] and
- COVID-19 testing rates (number of tests performed/100 000 population) (2020–2023).[7,10]

All of the predictors have been identified as possible determinants of the risk of mortality from COVID-19 in studies conducted in other countries.[11–15]

Population data and information about the incidence of poverty were from publicly available datasets from the Philippine Statistics Authority.[6–8] The Authority defines poverty incidence as "the proportion of Filipinos whose per capita income cannot sufficiently meet [their] individual basic food and non-food needs".[8] In 2021, this threshold was set at 12 030 Philippine pesos per month for a family of five.[8]

Data on the number of hospital beds and COVID-19 tests were extracted from publicly available datasets curated by the Department of Health.[2,9,10] Hospital bed density was computed as the number of hospital beds divided by the total population of the province, and multiplied by 100 000.[7,9] Similarly, the COVID-19 testing rate was computed as the number of COVID-19 RT–PCR tests performed divided by the total population of the province, multiplied by 100 000.[7,10] As the last recorded death occurred on 9 May 2023, RT–PCR testing data were also truncated at this date.

The number of COVID-19 tests performed by each province was estimated from the number of COVID-19 tests performed in all facilities in that province. Data about COVID-19 testing were available by facility, not by province, and people living in one province may have been tested in a neighbouring province. In such cases, their test would be counted in the total of the province where they were tested, not where they lived.

Statistical analysis

Mortality rates

The crude mortality rate (CMR), age-standardized mortality rate (ASMR) and age-specific mortality rate were calculated for each of the 84 administrative reporting units. The ASMR was computed through direct standardization to eliminate the confounding effect of age (i.e. the risk of COVID-19 mortality increases sharply with age) and to facilitate comparisons between provinces with varying age structures, in line with standard practice in global ranking studies.[11,16]

The following formulas were used to calculate the CMR and ASMR:

$$\text{CMR} = 100\,000 \times \sum_{i=1}^{n} \left(\frac{p_i}{\sum_{i'=1}^{n} p_{i'}}\right)\left(\frac{m_i}{p_i}\right) \text{ (Equation 1) and}$$

$$\text{ASMR} = 100\,000 \times \sum_{i=1}^{n} \left(\frac{s_i}{\sum_{i'=1}^{n} s_{i'}}\right)\left(\frac{m_i}{p_i}\right) \text{ (Equation 2),}$$

where i is the age group, m is the number of deaths, p is the provincial population, m/p is the age-specific mortality rate and s is the standard population. In this study, the standard population was the 2020 population.[7] Note that the age-specific mortality rate is different from the ASMR. The age-specific mortality rate is mortality in a specific age group, while the ASMR is calculated using the age-specific mortality rates from all age groups. The ASMR was used to rank the provinces from highest to lowest COVID-19 mortality.

Correlation analysis

A correlation analysis was performed to identify possible predictors of COVID-19 mortality and to investigate the relationships between selected possible predictors. Prior to the correlation analysis, the distributions of the CMR, ASMR and the five risk factor variables were explored. On the basis of this analysis, which revealed the presence of non-normal data distributions (**Supplementary Fig. 1**), Spearman's method was chosen to measure the strength of the relationship between pairs of variables. Spearman's correlation coefficient (r_s) is considered to be more robust to outliers than Pearson's correlation coefficient.[17] Mukaka's approach was adopted to aid in interpreting the correlation coefficients:[17] r_s values from -0.30 to 0.00 or 0.00 to 0.30 imply no or a negligible correlation; values from -0.50 to -0.30 or 0.30 to 0.50 imply a weak correlation; values from -0.70 to -0.50 or 0.50 to 0.70 imply a moderate correlation; values from -0.90 to -0.70 or 0.70 to 0.90 imply a strong correlation; and values from -1.00 to -0.90 or 0.90 to 1.00 imply a very strong or perfect correlation. Finally, P values were calculated to test the statistical significance of the correlations found.

Statistical analyses were conducted using Python Pandas software for the correlation coefficients and SciPy for the P values.[18–20]

RESULTS

Crude versus age-standardized mortality

The CMRs and ASMRs for the 84 administrative areas are reported in **Table 1** and **Supplementary Table 1**; also shown are the absolute differences between the CMRs and ASMRs. The median of the absolute difference is 1.26 deaths/100 000 population (interquartile range [IQR]: -2.35, 7.22). Compared with the ASMRs, the CMRs had a higher median value (48.36 vs 44.73 deaths/100 000 population, respectively) and a wider dispersion (IQR: 22.32, 73.08 vs 24.78, 67.48, respectively). These results confirm the presence of the confounding effect of population age on the CMRs. Thus, ranking the provinces by their CMR would be misleading, as this measure does not account for differences in the age structure of the provinces. For this purpose, the ASMR is more appropriate.[16]

COVID-19 deaths

A total of 66 566 records of COVID-19 death were available, of which 388 (0.6%) were excluded due to missing demographic data. A total of 66 178 complete records were retained for analysis and covered confirmed COVID-19 deaths that occurred between 18 January 2020 and 9 May 2023.

Age-standardized mortality

Provinces are ranked by their ASMRs in **Table 1**. The 10 provinces with the highest COVID-19 mortality rates, in decreasing order, were Benguet (207.83 deaths/100 000 population), Cagayan, Bataan, Nueva Vizcaya, Quirino, National Capital Region, Isabela, Cebu, Aurora and Davao del Sur (96.91 deaths/100 000 population). Eight of these 10 provinces are in the Luzon island group, the northern part of the country. Moreover, four of the top five are in northern Luzon, suggesting a clustering of provinces with high ASMRs, which is particularly evident in the heatmap visualization shown in **Fig. 1**.

The 11 provinces with the lowest rates, in increasing order, were Tawi-Tawi (2.22 deaths/100 000 population,

Table 1. **Crude and age-standardized COVID-19 mortality per 100 000 population, by province, Philippines, January 2020–May 2023**[a]

Province (geographical region/administrative region)[b]	Mortality		Difference (CMR - ASMR)
	CMR	ASMR	
Benguet (Northern Luzon/CAR)	211.03	207.83	3.20
Cagayan (Northern Luzon/R2)	163.17	139.28	23.90
Bataan (Central Luzon/R3)	136.30	137.88	-1.58
Nueva Vizcaya (Northern Luzon/R2)	132.31	121.07	11.24
Quirino (Northern Luzon/R2)	118.90	115.12	3.78
National Capital Region (NCR)	102.67	109.92	-7.25
Isabela (Northern Luzon/R2)	116.72	108.25	8.47
Cebu (Central Visayas/R7)	102.90	107.51	-4.61
Aurora (Central Luzon/R3)	98.30	97.25	1.05
Davao del Sur (Southern Mindanao/R11)	93.00	96.91	-3.91
Apayao (Northern Luzon/CAR)	106.51	93.98	12.53
Kalinga (Northern Luzon/CAR)	92.01	89.46	2.55
Guimaras (Western Visayas/R6)	102.89	82.65	20.24
Davao del Norte (Southern Mindanao/R11)	79.36	82.27	-2.91
Mountain Province (Northern Luzon/CAR)	97.59	81.97	15.62
Zambales (Central Luzon/R3)	90.93	81.34	9.59
Cotabato City (Southwestern Mindanao/BARMM)	47.45	78.79	-31.34
Agusan del Norte (Northeastern Mindanao/CARAGA)	78.85	77.65	1.20
South Cotabato (Central Mindanao/R12)	61.49	70.81	-9.32
Ifugao (Northern Luzon/CAR)	72.42	70.32	2.10
Pampanga (Central Luzon/R3)	68.65	68.55	0.10
Negros Occidental (Western Visayas/R6)	75.06	67.13	7.93
Surigao del Sur (Northeastern Mindanao/CARAGA)	70.57	67.02	3.55
Iloilo (Western Visayas/R6)	81.89	64.58	17.32
La Union (Northern Luzon/R1)	79.84	62.92	16.93
Surigao del Norte (Northeastern Mindanao/CARAGA)	66.01	62.47	3.54
Rizal (Southern Luzon/R4A)	53.65	61.75	-8.10
Bulacan (Central Luzon/R3)	59.67	59.84	-0.17
Ilocos Norte (Northern Luzon/R1)	83.15	58.17	24.99
Davao de Oro (Southern Mindanao/R11)	55.20	57.49	-2.29
City of Isabela (Western Mindanao/R9)	45.34	57.34	-12.00
Zamboanga del Sur (Western Mindanao/R9)	53.42	57.22	-3.80
Tarlac (Central Luzon/R3)	62.24	57.11	5.13
Oriental Mindoro (Southern Luzon/R4B)	56.91	56.55	0.36
Nueva Ecija (Central Luzon/R3)	60.60	55.42	5.18
Davao Oriental (Southern Mindanao/R11)	56.00	54.82	1.18
Laguna (Southern Luzon/R4A)	50.10	54.25	-4.15
Agusan del Sur (Northeastern Mindanao/CARAGA)	45.12	50.59	-5.47
Pangasinan (Northern Luzon/R1)	53.87	47.63	6.24
Abra (Northern Luzon/CAR)	62.32	47.37	14.95

Province (geographical region/administrative region)[b]	Mortality		Difference (CMR - ASMR)
	CMR	ASMR	
Capiz (Western Visayas/R6)	58.84	46.68	12.16
Negros Oriental (Central Visayas/R7)	53.27	45.74	7.53
Dinagat Islands (Northeastern Mindanao/CARAGA)	51.58	43.73	7.85
Lanao del Norte (Northern Mindanao/R10)	34.87	43.02	-8.15
Antique (Western Visayas/R6)	53.15	42.03	11.12
Lanao del Sur (Southwestern Mindanao/BARMM)	19.76	40.93	-21.17
Occidental Mindoro (Southern Luzon/R4B)	37.01	39.89	-2.87
Cavite (Southern Luzon/R4A)	37.14	39.60	-2.46
Davao Occidental (Southern Mindanao/R11)	33.45	38.77	-5.32
Batangas (Southern Luzon/R4A)	38.13	36.49	1.65
Palawan (Southern Luzon/R4B)	31.36	35.99	-4.63
Ilocos Sur (Northern Luzon/R1)	49.27	35.30	13.98
Marinduque (Southern Luzon/R4B)	46.06	34.57	11.48
Aklan (Western Visayas/R6)	41.11	33.99	7.12
Bohol (Central Visayas/R7)	42.93	32.92	10.02
Misamis Oriental (Northern Mindanao/R10)	28.65	29.82	-1.17
Biliran (Eastern Visayas/R8)	32.45	28.35	4.11
Siquijor (Central Visayas/R7)	41.74	27.56	14.18
Zamboanga del Norte (Western Mindanao/R9)	27.82	27.47	0.35
Camarines Sur (Southern Luzon/R5)	26.72	26.95	-0.23
Albay (Southern Luzon/R5)	27.03	25.47	1.56
Romblon (Southern Luzon/R4B)	30.19	25.37	4.82
Zamboanga Sibugay (Western Mindanao/R9)	22.58	24.93	-2.35
Maguindanao (Southwestern Mindanao/BARMM)	10.73	24.34	-13.61
Quezon (Southern Luzon/R4A)	23.70	23.20	0.50
Basilan (Southwestern Mindanao/BARMM)	11.53	21.32	-9.79
Samar (Western Samar) (Eastern Visayas/R8)	19.59	18.84	0.75
Leyte (Eastern Visayas/R8)	20.69	18.82	1.87
Sorsogon (Southern Luzon/R5)	18.88	17.56	1.32
Cotabato (North Cotabato) (Central Mindanao/R12)	16.17	17.48	-1.31
Bukidnon (Northern Mindanao/R10)	14.44	17.00	-2.56
Northern Samar (Eastern Visayas/R8)	14.76	14.83	-0.07
Eastern Samar (Eastern Visayas/R8)	15.76	14.13	1.63
Batanes (Northern Luzon/R2)	21.51	13.63	7.88
Catanduanes (Southern Luzon/R5)	14.77	12.77	2.00
Southern Leyte (Eastern Visayas/R8)	16.57	12.30	4.27
Sultan Kudarat (Central Mindanao/R12)	9.63	11.93	-2.30
Camiguin (Northern Mindanao/R10)	14.02	11.05	2.97
Sarangani (Central Mindanao/R12)	8.42	10.79	-2.37
Camarines Norte (Southern Luzon/R5)	8.59	8.70	-0.11
Misamis Occidental (Northern Mindanao/R10)	9.59	7.72	1.87
Masbate (Southern Luzon/R5)	4.41	4.82	-0.41

Province (geographical region/administrative region)[b]	Mortality		Difference (CMR - ASMR)
	CMR	ASMR	
Sulu (Southwestern Mindanao/BARMM)	1.40	2.63	-1.23
Tawi-Tawi (Southwestern Mindanao/BARMM)	1.37	2.22	-0.85

ASMR: age-standardized mortality rate; BARMM: Bangsamoro Autonomous Region in Muslim Mindanao; CAR: Cordillera Administrative Region; CARAGA: Caraga Administrative Region (Region 13); CMR: crude mortality rate; R: administrative region.

[a] Data are presented in descending order of age-standardized mortality.

[b] The designations in the Province column link each province to its location in the heatmap in Fig. 1. For instance, the province of Benguet is in CAR, in the geographical region of Northern Luzon.

less than 1% of Benguet's rate), Sulu, Masbate, Misamis Occidental, Camarines Norte, Sarangani, Camiguin, Sultan Kudarat, Southern Leyte, Catanduanes and Batanes (13.6/100 000 population). The geographical distribution of these provinces was more varied: Tawi-Tawi and Sulu provinces are in Southwestern Mindanao; Misamis Occidental and Camiguin are in northern Mindanao; Sarangani and Sultan Kudarat are in central Mindanao; Masbate, Camarines Norte and Catanduanes are in southern Luzon; Southern Leyte is in eastern Visayas; and Batanes is in Northern Luzon (**Fig. 1**).

Age-specific mortality

Age-specific mortality is plotted in **Fig. 2** and demonstrates a J-shaped pattern. The lowest mortality was recorded in children aged 5–9 years (median: 0.53 deaths/100 000 population; IQR: 0, 1.95), but mortality rose steeply with increasing age. The highest mortality (640.90 deaths/100 000 population; IQR: 347.27, 1046.65) was recorded in the oldest age group (≥80 years). Interestingly, the median mortality in the youngest age group, 0–4 years (4.79 deaths/100 000 population; IQR: 2.15, 9.61), was higher than that for the adjacent age groups of 5–9, 10–14 and 15–19 years (**Supplementary Table 2**).

Correlation analysis

Three predictor variables were found to be correlated with both the CMR and the ASMR, namely poverty incidence, hospital bed density and COVID-19 testing rate (**Table 2**, **Supplementary Table 3**). Poverty incidence was negatively correlated with the CMR and ASMR (CMR: r_s = -0.55 [moderate], $P < 0.001$; and ASMR: r_s = -0.34 [weak], $P < 0.001$), implying that provinces with a high incidence of poverty tended to have lower mortality from COVID-19. Conversely, hospital bed density and COVID-19 testing rates exhibited weak positive correlations with the CMR and ASMR (for hospital bed density, CMR: $r_s = 0.35$, $P < 0.05$ and ASMR: $r_s = 0.33$, $P < 0.05$; for testing rates, CMR: $r_s = 0.44$, $P < 0.001$ and ASMR: $r_s = 0.46$, $P < 0.001$), suggesting that mortality was higher in provinces with better availability of and access to health care.

Furthermore, evidence was found of correlations between several pairs of the predictor variables (**Table 2**, **Supplementary Table 3**). First, poverty incidence was weakly negatively correlated with COVID-19 testing rates (r_s = -0.35, $P < 0.05$) and likewise with hospital bed density (r_s = -0.45, $P < 0.001$). Second, population density showed a moderate positive correlation with COVID-19 testing rates ($r_s = 0.52$, $P < 0.001$) and a weak positive correlation with hospital bed density ($r_s = 0.32$, $P < 0.05$). Lastly, there was a very weak negative correlation between population density and poverty incidence (r_s = -0.29, $P < 0.05$). Collectively, these pairwise correlations indicate that the more densely populated provinces with lower levels of poverty tended to have better access to, and better availability of, health-care services, including COVID-19 testing.

DISCUSSION

COVID-19 mortality

Two noteworthy findings emerged from our province-level ecological analysis of COVID-19 mortality in the Philippines. First, we observed a J-shaped pattern in age-specific mortality, with the lowest rates occurring in children aged 5–9 years. Similar patterns have been seen in several other countries, including Spain, the United Kingdom of Great Britain and Northern Ireland and the United States of America, indicating that while children were generally at low risk of developing COVID-19 disease, newborns and children aged <1 year experienced slightly elevated risks.[21] Our results add the Philippines to the list of countries where such a pattern was observed.

Fig. 1. **Heatmap of province-level, age-standardized COVID-19 mortality per 100 000 population, Philippines, January 2020–May 2023**[a]

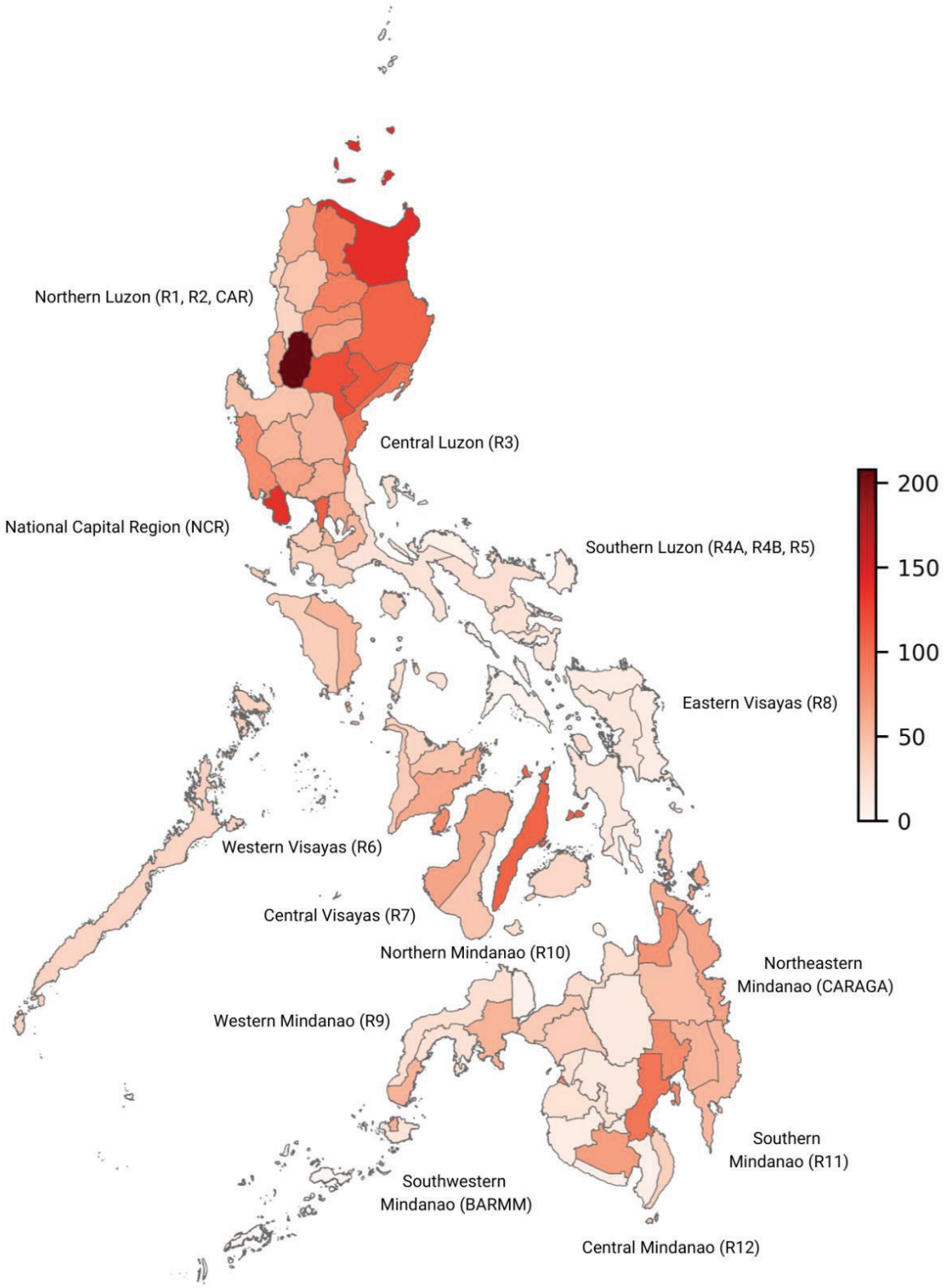

BARMM: Bangsamoro Autonomous Region in Muslim Mindanao; CAR: Cordillera Administrative Region; CARAGA: Caraga Administrative Region (Region 13); R: administrative region.

[a] The designations next to the names of the geographical regions correspond to the administrative regions in Table 1.

Table 2. **Spearman's rank correlation coefficients for associations between crude and age-standardized COVID-19 mortality and five predictor variables, Philippines, January 2020–May 2023**

Variable	Mortality		Predictor variable (data year)				
	Crude	Age-standardized	Poverty incidence (2021)	Hospital bed density (2022)	Population density (2020)	% population aged ≥65 years (2020)	COVID-19 test rate (2020–2023)
Crude mortality	1.00	0.97[a]	-0.55[a]	0.35[b]	0.10	0.21	0.44[a]
Age-standardized mortality		1.00	-0.49[a]	0.33[b]	0.11	-0.01	0.46[a]
Poverty incidence (2021)			1.00	-0.45[a]	-0.29[b]	-0.25[a]	-0.35[b]
Hospital bed density (2022)				1.00	0.32[b]	0.15[b]	0.52[a]
Population density (2020)					1.00	0.00	0.52[a]
% population aged ≥65 years (2020)						1.00	-0.01
COVID-19 test rate (2020–2023)							1.00

[a] $P < 0.001$.

[b] $P < 0.05$.

Fig. 2. **Age-specific COVID-19 mortality per 100 000 population presented as strip plots with medians, Philippines, January 2020–May 2023**

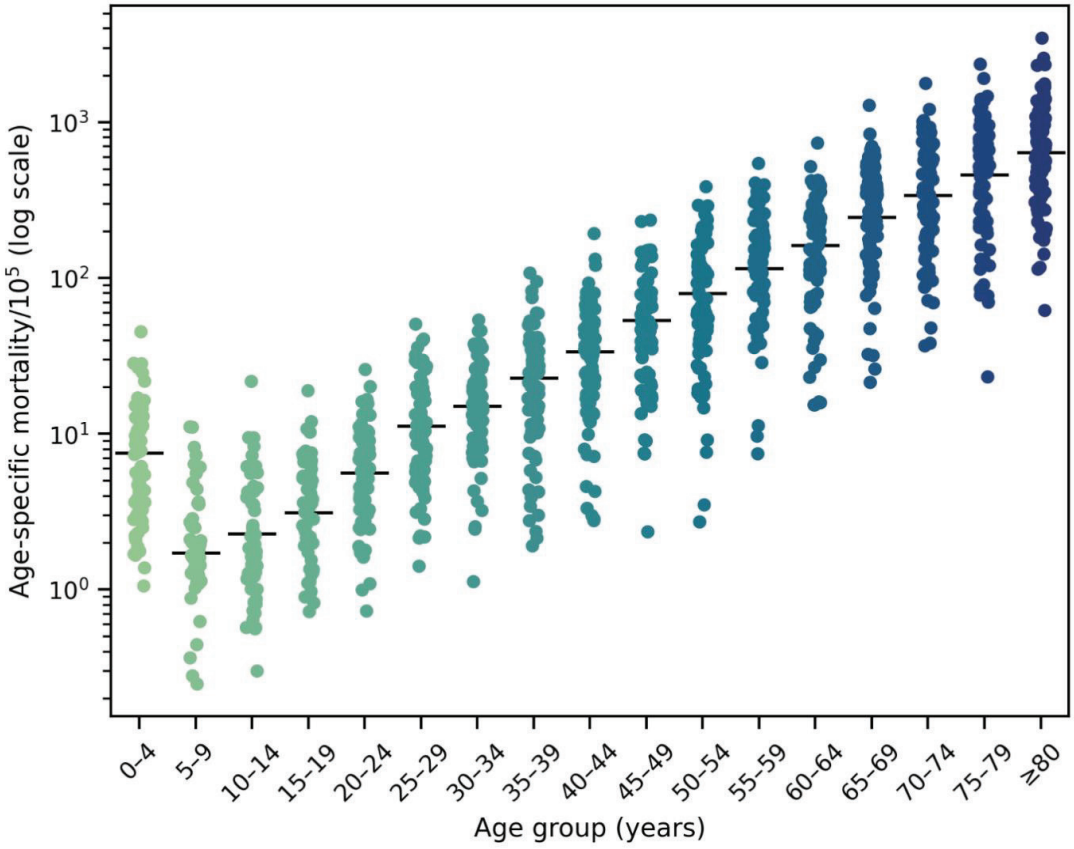

Second, ranking and mapping provinces by their ASMRs revealed a clustering of provinces with high COVID-19 mortality, particularly in the Northern and Central Luzon regions, but also in the National Capital Region and the Central and Western Visayas and Southern Mindanao regions. It is noteworthy that 4 of the 10 provinces with the highest rates have densely populated cities: Benguet in northern Luzon is home to Baguio City; the National Capital Region has 16 major cities; Cebu province in central Visayas has three large cities; and Davao del Sur in southern Mindanao has one major conurbation. In contrast, some of the provinces with low mortality, such as Tawi-Tawi, Sulu, Camiguin and Batanes, are remote and/or composed of small islands.

Therefore, it seems likely that geographical connectedness and population density were instrumental in driving up COVID-19 mortality in parts of the Philippines. Worldwide, COVID-19 spread faster among populations with high rates of social interaction, which is much more likely to occur in densely populated areas. Furthermore, mobility was harder to constrain in geographically connected provinces and provinces linked by established transportation routes (i.e. land or sea). It is also worth noting that in this analysis, more remote, less densely populated island provinces tended to have much lower COVID-19 mortality. However, we found no evidence of a correlation between population density and COVID-19 mortality at the provincial level, suggesting that other factors also possibly played a role.

Predictors of COVID-19 mortality

The observed positive correlations between COVID-19 mortality and hospital bed density and between COVID-19 mortality and testing rates represent another interesting finding and indicate that mortality may have been influenced by the availability of health-care services and capacity for disease surveillance. During the pandemic, hospitals and testing centres served as data collection and reporting sites. Thus, it follows that COVID-19 deaths that occurred in hospitals or health-care facilities with RT–PCR testing capacity were more likely to have been recorded than those that occurred in provinces with fewer resources, where a higher percentage of deaths may have occurred outside health-care facilities and were not confirmed as COVID-19 deaths.

The study also found a negative correlation between COVID-19 mortality and poverty. This relationship could be interpreted in terms of immunity, but this would imply that low-income communities had greater immunity against COVID-19. A wealth of published evidence suggests that this is unlikely. Numerous studies have consistently shown that COVID-19 disproportionately affected low-income populations,[13] including one study from Sweden that found having a lower socioeconomic status was linked to a higher risk of COVID-19 mortality.[14] Explanatory factors implicated in this relationship have included overcrowding, employment that did not allow people to work from home, financial uncertainty, reduced health-care access, and a higher burden of undiagnosed or untreated comorbidities. Evidence of negative correlations between the incidence of poverty and hospital bed density – and between poverty and COVID-19 testing – add further weight to the case against immunity.

Instead, we hypothesize that a more likely explanation for the observed correlations stems from what is widely referred to as the streetlight effect, a phenomenon whereby the number of cases is higher in populations with better surveillance.[22] Support for our hypothesis comes from an earlier study, conducted in 2020, in the Western Visayas region.[23] The authors of the Western Visayas study analysed data about testing, infection and contact tracing and found that the highest number of cases was recorded in Iloilo City, which housed the only regional COVID-19 testing facility at that time.

We further hypothesize that in the Philippines, the streetlight effect may have been exacerbated by patterns of health-seeking behaviour. Cross-sectional surveys conducted in low-income households in the Philippines, initially from 20 February to 13 March 2020, and again from 12 November to 12 December 2020, showed an increase in the practice of preventive measures (e.g. avoiding crowded places, handwashing, using disinfectants and mask-wearing). According to these repeated surveys, there was also a drop in the intention to seek care from public hospitals when exhibiting symptoms of COVID-19 and an increase in self-medication with stored medications and antibiotics.[24] Among the reasons cited by participants to explain their low levels of seeking health care during the

pandemic were concerns about discrimination at public health-care facilities due to their socioeconomic status, high transportation costs due to mobility restrictions, stigma around contracting the virus and mistrust in control protocols.[24] Therefore, it seems plausible to assume that low-income households, which already had disproportionately poorer access to health care before the pandemic, were even less likely to seek treatment for COVID-19 symptoms and less likely to have been tested. Consequently, fewer deaths would have been attributed to COVID-19, further depressing rates of COVID-19 mortality relative to wealthier provinces.

The case of Benguet

Benguet, with 207.83 deaths/100 000 population, had by far the highest computed ASMR, but it also ranked high in terms of testing capacity and coverage of contact tracing. Indeed, in 2020, Baguio City and the province of Benguet overall were commended by WHO for their exceptional COVID-19 pandemic response, which included surveillance.[25] It is highly likely that this level of response meant that COVID-19 deaths were more likely to be recorded in Benguet than in other provinces. However, this is not to say that high rates of testing and contact tracing were the only factors that contributed to Benguet's extremely high COVID-19 mortality.

A high population density was likely a contributory factor, given that Benguet is home to Baguio City, one of the more densely populated cities in the Philippines. Another possible factor is Benguet's climate. Baguio City has a mean annual temperature of 18 °C, making it the coldest city in the Philippines.[26] Several ecological studies[27–29] have reported associations between temperature, humidity and COVID-19 mortality, in which areas with colder and more humid weather – where people typically spend more time indoors – have consistently recorded more cases and deaths.

Limitations and recommendations for future work

Ecological studies have inherent limitations, including an inability to account for local dynamics within a province. A fuller understanding of the drivers of COVID-19 mortality and the effectiveness of public health measures and interventions would require closer, more detailed investigation of individual provinces. Nevertheless, this analysis, by identifying provinces with very high and very low mortality, represents a useful first step. Moreover, Benguet has emerged as a good candidate for further epidemiological investigation, given its high mortality and unique combination of drivers of COVID-19 mortality, including a pronounced streetlight effect.

We were unable to include several important variables in our analysis, namely government policies, such as travel restrictions and lockdowns, climate variables, comorbidities and immunization status. Nor were we able to assess the impact of temporality; this is likely an important consideration for certain factors, such as testing rates, which will have changed through time. To overcome some of these shortcomings, future investigations should consider using alternative study designs, such as multivariate correlation analysis, multivariate regression and causal inference. Alternative means for estimating COVID-19 mortality, such as excess deaths, might also be useful.[30]

Conclusions

This study is the first to present a province-level analysis of COVID-19 mortality in the Philippines and, in addition to identifying provinces with high and low rates, found evidence of clustering of provinces with high rates. The study also found evidence of a so-called streetlight effect and concluded that the rankings of mortality, at least in part, are influenced by unequal surveillance capacity among provinces. We recommend further investigation of local dynamics within individual provinces to better understand the drivers of mortality and the impact of the interventions and control measures that were implemented during the pandemic to reduce mortality. These findings pave the way for future work by identifying some of the factors that will need to be considered and more closely investigated to get a clearer picture of what happened during the pandemic and to inform decision-making for future pandemic preparedness and response, and thereby safeguard millions of lives in communities across the Philippines.

Acknowledgements

The authors thank the Office of the Vice Chancellor for Research and Development, University of the Philippines

Diliman, for its support of our COVID-19 studies through Project/Grant No. 232301.

Conflicts of interest

The authors have no conflicts of interest to declare.

Ethics statement

This study did not require ethical approval as it utilized publicly available datasets from the Philippine Statistics Authority and the Department of Health. The COVID-19 dataset is anonymized, and no personally identifiable information was included in the analysis. No additional data were collected and no direct interaction with human participants occurred. However, ethical guidelines for data usage were followed.

Funding

This study was funded through Project/Grant No. 232301 SOS (Mathematical Modeling and Equity: Informing and Influencing the Covid-19 Response) from the Office of the Vice Chancellor for Research and Development, University of the Philippines Diliman.

References

1. COVID-19 dashboard: deaths [online database]. Geneva: World Health Organization; 2025. Available from: https://data.who.int/dashboards/covid19/deaths, accessed 18 January 2025.
2. COVID-19 case tracker [online database]. Manila: Department of Health; 2025. Available from: https://doh.gov.ph/diseases/covid-19/covid-19-case-tracker/, accessed 26 October 2023.
3. Statement on the fifteenth meeting of the IHR (2005) Emergency Committee on the COVID-19 pandemic [website]. Geneva: World Health Organization; 2023. Available from: https://www.who.int/news/item/05-05-2023-statement-on-the-fifteenth-meeting-of-the-international-health-regulations-(2005)-emergency-committee-regarding-the-coronavirus-disease-(covid-19)-pandemic, accessed 13 December 2023.
4. WHO chief declares end to COVID-19 as a global health emergency [website]. New York (NY): United Nations; 2023. Available from: https://news.un.org/en/story/2023/05/1136367, accessed 13 December 2023.
5. 2020–2021 RITM COVID-19 achievement report. Manila: Research Institute for Tropical Medicine, Department of Health, Philippines; 2023. Available from: https://ritm.gov.ph/ritm-covid-19-achievement-report/, accessed 2 February 2025.
6. Highlights of the population density of the Philippines 2020 census of population and housing (2020 CPH) [dataset]. Manila: Philippine Statistics Authority; 2021. Available from: https://psa.gov.ph/content/highlights-population-density-philippines-2020-census-population-and-housing-2020-cph, accessed 13 December 2023.
7. Age and sex distribution in the Philippine population (2020 census of population and housing) [dataset]. Manila: Philippine Statistics Authority; 2022. Available from: https://psa.gov.ph/content/age-and-sex-distribution-philippine-population-2020-census-population-and-housing, accessed 13 December 2023.
8. Proportion of poor Filipinos was recorded at 18.1 percent in 2021 [website]. Manila: Philippine Statistics Authority; 2022. Available from: https://psa.gov.ph/poverty-press-releases/nid/167972, accessed 13 December 2023.
9. List of regulated health facilities and services [dataset]. Manila: Department of Health, Philippines; 2022. Available from: https://hfsrb.doh.gov.ph/list-of-licensed-health-facilities/, accessed 13 December 2023.
10. Covid-19 testing laboratory – HFSRB – Department of Health [dataset]. Manila: Department of Health, Philippines; 2022. Available from: https://hfsrb.doh.gov.ph/covid-19-testing-laboratory/, accessed 27 October 2024.
11. Hong D, Lee S, Choi YJ, Moon S, Jang Y, Cho YM, et al. The age-standardized incidence, mortality, and case fatality rates of COVID-19 in 79 countries: a cross-sectional comparison and their correlations with associated factors. Epidemiol Health. 2021;43:e2021061. doi:10.4178/epih.e2021061 pmid:34525501
12. Hashim MJ, Alsuwaidi AR, Khan G. Population risk factors for COVID-19 mortality in 93 countries. J Epidemiol Glob Health. 2020;10(3):204–8. doi:10.2991/jegh.k.200721.001 pmid:32954710
13. Patel JA, Nielsen FBH, Badiani AA, Assi S, Unadkat VA, Patel B, et al. Poverty, inequality and COVID-19: the forgotten vulnerable. Public Health. 2020;183:110–1. doi:10.1016/j.puhe.2020.05.006 pmid:32502699
14. Drefahl S, Wallace M, Mussino E, Aradhya S, Kolk M, Brandén M, et al. A population-based cohort study of socio-demographic risk factors for COVID-19 deaths in Sweden. Nat Commun. 2020;11(1):5097. doi:10.1038/s41467-020-18926-3 pmid:33037218
15. Bongolan VP, Minoza JMA, de Castro R, Sevilleja JE. Age-stratified infection probabilities combined with a quarantine-modified model for COVID-19 needs assessments: model development study. J Med Internet Res. 2021;23(5):e19544. doi:10.2196/19544 pmid:33900929
16. Garcia-Calavaro C, Paternina-Caicedo A, Smith AD, Harrison LH, De la Hoz-Restrepo F, Acosta E, et al. COVID-19 mortality needs age adjusting for international comparisons. J Med Virol. 2021;93(7):4127–9. doi:10.1002/jmv.27007 pmid:33837989
17. Mukaka MM. Statistics corner: a guide to appropriate use of correlation coefficient in medical research. Malawi Med J. 2012;24(3):69–71. pmid:23638278
18. Python v3.0.1 documentation [website]. Hampton (NH): Python Software Foundation; 2009. Available from: https://docs.python.org/3.0/index.html, accessed 13 December 2023.
19. pandas-dev/pandas: Pandas [software programme]. Geneva: Zenodo; 2024. Available from: https://zenodo.org/doi/10.5281/zenodo.3509134, accessed 2 February 2025.
20. Virtanen P, Gommers R, Oliphant TE, Haberland M, Reddy T, Cournapeau D, et al.; SciPy 1.0 Contributors. SciPy 1.0: fundamental algorithms for scientific computing in Python. Nat Methods. 2020;17(3):261–72. doi:10.1038/s41592-019-0686-2 pmid:32015543
21. Khera N, Santesmasses D, Kerepesi C, Gladyshev VN. COVID-19 mortality rate in children is U-shaped. Aging (Albany NY). 2021;13(16):19954–62. doi:10.18632/aging.203442 pmid:34411000

22. Freedman DH. Why scientific studies are so often wrong: the streetlight effect. [website]. Wilmington (DE): Discover; 2010. Available from: https://www.discovermagazine.com/why-scientific-studies-are-so-often-wrong-the-streetlight-effect-1055, accessed 8 April 2025.

23. Zamora PRF, Rico JA, Bolinas DK, Sevilleja JE, de Castro R. Early COVID-19 pandemic response in Western Visayas, Philippines. medRxiv [Preprint]. 2022;2022.07.21.22277909. doi:10.1101/2022.07.21.22277909

24. Lau LL, Hung N, Go DJ, Choi M, Dodd W, Wei X. Dramatic increases in knowledge, attitudes and practices of COVID-19 observed among low-income households in the Philippines: a repeated cross-sectional study in 2020. J Glob Health. 2022;12:05015. doi:10.7189/jogh.12.05015 pmid:35596944

25. WHO field visit to Baguio City and Benguet Province: models for contact tracing and COVID-19 response in the Philippines. Geneva: World Health Organization; 2020. Available from: https://www.who.int/philippines/news/detail/29-07-2020-who-field-visit-to-baguio-city-and-benguet-province-models-for-contact-tracing-and-covid-19-response-in-the-philippines, accessed 13 December 2023.

26. Climate of the Philippines [website]. Quezon City: Philippine Atmospheric, Geophysical and Astronomical Services Administration; 2025. Available from: https://www.pagasa.dost.gov.ph/information/climate-philippines, accessed 13 December 2023.

27. Kifer D, Bugada D, Villar-Garcia J, Gudelj I, Menni C, Sudre C, et al. Effects of environmental factors on severity and mortality of COVID-19. Front Med (Lausanne). 2021;7:607786. doi:10.3389/fmed.2020.607786 pmid:33553204

28. Meo SA, Abukhalaf AA, Alomar AA, Al-Beeshi IZ, Alhowikan A, Shafi KM, et al. Climate and COVID-19 pandemic: effect of heat and humidity on the incidence and mortality in world's top ten hottest and top ten coldest countries. Eur Rev Med Pharmacol Sci. 2020;24(15):8232–8. doi:10.26355/eurrev_202008_22513 pmid:32767355

29. Quilodrán CS, Currat M, Montoya-Burgos JI. Air temperature influences early Covid-19 outbreak as indicated by worldwide mortality. Sci Total Environ. 2021;792:148312. doi:10.1016/j.scitotenv.2021.148312 pmid:34144236

30. Adam D. The pandemic's true death toll: millions more than official counts. Nature. 2022;601(7893):312–5. doi:10.1038/d41586-022-00104-8 pmid:35042997

Acute haemorrhagic conjunctivitis outbreak attributed to coxsackievirus A24 in Ratanakiri, Cambodia, 2023

Kimhour Lay,[a,b] Kossama Chukmol,[a,b] Guechlaing Chea,[a] Leng Un,[a] Kimhong Moch,[c] Seiha Do,[d,e] Lykheang Lou,[a] Meng Ngy[d,e] and Piseth Kong[a]

Correspondence to Kimhour Lay (email: laykimhour@gmail.com)

Objective: To determine the causative agent, clinical manifestations and risk factors for infection during a September 2023 outbreak of acute haemorrhagic conjunctivitis (AHC) in Pak Touch village, Ratanakiri province, Cambodia.

Methods: A retrospective case-control study was conducted. Cases were age-matched to controls (1:1), who were randomly selected from the village population. Twenty-one conjunctival samples were analysed using real-time reverse transcription–polymerase chain reaction (RT–PCR). RNA sequencing was additionally performed to identify the causative agent of the outbreak. Logistic regression models were used to identify significant risk factors.

Results: A total of 73 cases and 73 controls were included in the analysis. Cases had a median age of 20 years (range: 1–70, mean and standard deviation: 27.7 ± 20.0), and 46.6% (34/73) were male. The overall attack rate was 12.3% (73 cases/594 residents). Clinical presentations included conjunctival hyperaemia (100%), subconjunctival haemorrhage (82.2%, 60), pain and discharge (64.4%, 47 each), eyelid swelling (57.5%, 42) and tearing (54.8%, 40). RT–PCR identified enterovirus in 52.4% (11/21) of conjunctival swabs, with RNA sequencing confirming the coxsackievirus A24 variant as the causative agent in five swabs. Statistical analysis identified significant risk factors, including physical contact with patients with acute haemorrhagic conjunctivitis (adjusted odds ratio [aOR]: 4.42, 95% confidence interval [CI]: 1.90–10.10), frequent eye rubbing (aOR: 4.56, 95% CI: 2.00–10.37) and poor hand hygiene (aOR: 3.70, 95% CI: 1.64–8.43).

Discussion: The outbreak of acute haemorrhagic conjunctivitis in Pak Touch village was primarily caused by coxsackievirus A24. Significant risk factors included physical contact with infected individuals, frequent eye rubbing and poor hand hygiene. Effective hygiene measures are crucial to prevent the spread of AHC.

Acute haemorrhagic conjunctivitis (AHC) was initially reported in Ghana in 1969 and rapidly spread across Africa, South-East Asia and Japan.[1] It was nicknamed "Apollo 11 disease" due to its emergence coinciding with the Apollo 11 moon landing.[2] This highly contagious viral disease is characterized by the sudden onset of a red eye, eyelid swelling, tearing and subconjunctival haemorrhage. These symptoms typically appear after an incubation period of 12–48 hours and resolve spontaneously within 1–2 weeks. While AHC is not usually a serious condition, it can cause discomfort and disrupt daily life, and in rare cases it can lead to ocular and systemic complications.[3–5]

Outbreaks of AHC are often linked to enteroviruses, particularly *Enterovirus D 70* (EV-D70) and coxsackievirus A24 variant (CV-A24v), along with certain adenovirus strains.[6–10] EV-D70 was responsible for pandemics from the early 1970s to the mid-1980s, but its role in causing AHC declined significantly after 1994.[3,11–13] CV-A24v, a variant of the Joseph prototype strain within the *Enterovirus C* species first isolated in Singapore in 1970, has since gained recognition as the leading cause of AHC outbreaks worldwide.[14–16]

AHC spreads mainly through direct contact with contaminated fingers, objects and tears. However, in the case of CV-A24v – which uses sialic acids as receptors,

[a] Preah Ang Duong Hospital, Phnom Penh, Cambodia.
[b] Cambodian Ophthalmological Society, Phnom Penh, Cambodia.
[c] Provincial Referral Hospital of Ratanakiri, Ratanakiri, Cambodia.
[d] National Program for Eye Health, Phnom Penh, Cambodia.
[e] Khmer–Soviet Friendship Hospital, Phnom Penh, Cambodia.
Published: 23 February 2026
doi: 10.5365/wpsar.2026.17.1.1226

binding α2,3 on the cornea and α2,6 in the respiratory tract – transmission also occurs via airborne secretions.[17,18] Factors such as crowded environments and poor hygiene, and practices such as sharing towels and reusing bathing water further accelerate transmission.[19]

Rapid diagnosis and virological confirmation are essential for differentiating AHC from other eye infections and triggering appropriate treatment and control strategies to prevent epidemics. However, virus identification remains a challenging and time-consuming process. Initial isolation from conjunctival samples involves inoculation onto human cell lines (MRC5 or Hep-2) to detect cytopathic effects, with specificity confirmed using real-time reverse transcription–polymerase chain reaction (RT–PCR), immunofluorescence or seroneutralization assays.[11,20,21] However, CV-A24v cannot be identified through these conventional methods, necessitating *VP1* sequencing, which requires several days to yield results.[22–25] While effective, these methods still face sensitivity challenges and high costs, limiting accessibility in developing countries.

In Cambodia, the first major outbreak of AHC was reported in July 1980 and was attributed to EV-D70. It occurred 1 year after the fall of the Khmer Rouge, when the disease was prevalent in refugee camps and designated transit centres.[26] Since then, Cambodia had not had any reported cases of AHC. However, on 23 September 2023, the director of Soam Thom Health Center reported a surge in cases of conjunctivitis in a village in Ratanakiri province. On 24 September, the Communicable Disease Control Department of the Cambodian Ministry of Health assigned a rapid response team to investigate the outbreak, which was later confirmed to be AHC. The outbreak was linked to four cases occurring among eight individuals who had recently returned to Pak Touch village from a funeral in Viet Nam on 14 September 2023. A public health education campaign was promptly initiated by the Ministry of Health and the National Program for Eye Health to reduce further spread.

A retrospective study was conducted using data collected during the investigation of the outbreak, and this study aimed to characterize the AHC epidemic in Pak Touch village, Ratanakiri province, Cambodia. The objectives were to describe the clinical manifestations and to identify the causative agent and risk factors for infection.

METHODS

Study design and setting

This retrospective study used a case-control design. Pak Touch village is situated in Pak Nhai commune, O'yadav district, Ratanakiri province. It is 23 km from Soam Thom Health Center, 73 km from Ban Lung City, and 15 km from the Viet Nam border. The village is predominantly inhabited by people of the Charay ethnic group; the village faces challenges related to hygiene and sanitation,[27] and farming is the main occupation. It is home to 164 families, comprising a total population of 594 residents, including 297 males and 297 females.

Outbreak investigation

The initial investigation started on 24 September 2023, following a report from the director of the Soam Thom Health Center about a significant rise in the number of cases of acute conjunctivitis. The investigation protocol is illustrated in **Fig. 1**. The following case definitions were employed:

- suspected AHC case – any individual presenting with eye redness, eye pain or eyelid swelling on or after 14 September 2023, in Pak Touch village;
- confirmed AHC case – any clinical case of conjunctivitis that was diagnosed by an ophthalmologist and characterized by eye redness, eye pain, eyelid swelling and/or subconjunctival haemorrhage, occurring on or after 14 September 2023, in Pak Touch village.

Identification of cases and controls

For this case-control study, cases were identified through a review of medical records and the line lists compiled by local health authorities on 24 September 2023, the day of the investigation. Individuals who had been clinically confirmed as having AHC by an ophthalmologist on 24 September 2023 were included in the study as cases. Patients diagnosed with conjunctivitis before 14 September 2023 were excluded from the case-control analysis. Each case was matched to a control of the same age (i.e. year of birth ±2 years) selected at random from the population registry for the village. Potential controls were excluded if their medical records were incomplete or missing.

Fig. 1. **Schematic of the investigation of the outbreak of acute haemorrhagic conjunctivitis in Pak Touch village, Ratanakiri province, Cambodia, 2023**

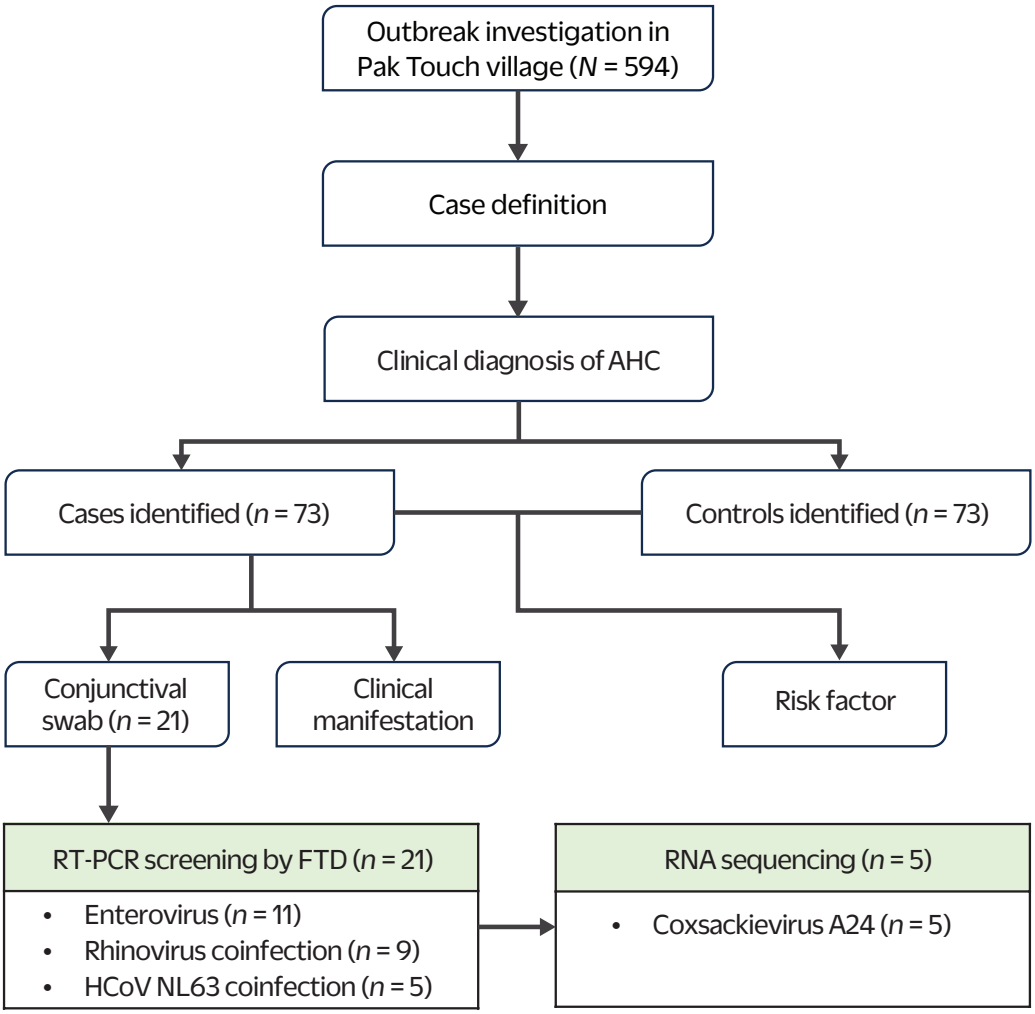

AHC: acute haemorrhagic conjunctivitis; FTD: Fast Track Diagnostics; HCoV NL63: human coronavirus NL63; RT-PCR: reverse transcription–polymerase chain reaction.

Definitions of risk factor variables

Demographic data (age and sex) were obtained from medical records, and data about the date of symptom onset among cases and potential risk factors were obtained from records of face-to-face interviews conducted during the field investigation by the response team. Nine risk factor variables were included in the analysis: having an AHC patient in the family, meeting with an AHC patient, having physical contact with an AHC patient, sharing eye drops, using the same toilet, rubbing eyes frequently, drinking from the same source (e.g. sharing cups), sharing a towel and having poor hand hygiene. Poor hand hygiene was defined as the absence of regular handwashing with soap and water, particularly before eating and after using the toilet.

Laboratory investigation

Sample collection

During the initial investigation, conjunctival swabs were collected from 21 patients with clinical signs of AHC. After aseptic collection, specimens were placed in test tubes containing 2 mL of minimal essential medium, stored at 4 °C and transported to the National Public Health Laboratory of Cambodia. The cold chain was maintained for 24 hours for further analysis. Real-time RT–PCR was

used to identify the viral pathogen; its genomic properties were identified using RNA sequencing.

Testing for respiratory pathogens

Real-time RT–PCR testing was conducted at the National Public Health Laboratory using Fast Track Diagnostics' Respiratory Pathogens 21 multiplex assay (Fast Track Diagnostics, Esch-sur-Alzette, Luxembourg), designed to identify 20 viruses and one bacterium.

RNA sequencing

To confirm the causative agent of the outbreak, the samples underwent comprehensive genomic sequencing using the Illumina RNA Prep with Enrichment tagmentation kit for targeted RNA sequencing, according to the manufacturer's instructions (Illumina, San Diego, CA, USA). The sequencing results were analysed using CZ ID, a cloud-based platform (Chan Zuckerberg Initiative).

Statistical analysis

For this case-control study, the characteristics of cases were described using frequencies and percentages for categorical variables, and the median and range, and mean and standard deviation (SD) for continuous variables (age). The attack rate was calculated using the following formula:

$$\text{Attack rate} = \text{number of new cases/total population at risk} \times 100$$

where the population at risk was 594, the number of people living in Pak Touch.

Chi-squared tests were performed to compare the distribution of categorical variables between cases and controls. Simple logistic regression was used to estimate the association between an individual risk factor variable and AHC infection, with results presented as crude odds ratios (cORs) and corresponding 95% confidence intervals (CIs). Multiple logistic regression was then conducted to identify factors independently associated with the outcome after adjusting for potential confounders. Final model results are reported as adjusted odds ratios (aORs) with 95% CIs and corresponding *P* values. Data analysis was conducted using STATA version 18 (StataCorp, College Station, TX, USA).

RESULTS

Demographic characteristics and risk factor prevalence

On the date of the investigation, 73 cases were identified, representing an attack rate of 12.3%. For the risk factor analysis, 73 controls were subsequently recruited. The median age of cases was 20.0 years (range: 1–70, mean ± SD: 27.7 ± 20.0). Due to age-matching, the age distribution between cases and controls was not statistically significant. Nor was there a significant difference in the sex distribution between cases and controls (cases: 53.4% female, 39/73; controls: 52.1% female, 38/73; $P = 0.868$) (**Table 1**).

Cases and controls differed in terms of the proportion who reported having met with AHC patients (69.9% [51/73] for cases vs 35.6% [26/73] for controls, $P < 0.001$) and who had physical contact with AHC patients (78.1% [57] vs 31.5% [23], $P < 0.001$) (**Table 1**). Having an AHC patient in the family was also more common among cases than controls (57.5% [42] vs 28.8% [21], $P < 0.001$). The prevalence of risk factors related to hygiene and sharing practices was also higher in cases than in controls. A higher proportion of cases reported sharing eye drops (31.5% [23] vs 13.7% [10], $P = 0.001$); drinking from the same cup was reported by 63.0% (46) of cases but only 37.0% (27) of controls ($P = 0.002$). Frequent eye rubbing was more common among cases (75.3% [55] vs 31.5% [23], $P < 0.001$), as was poor hand hygiene (72.6% [53] vs 34.2% [25], $P < 0.001$).

Clinical presentation

Conjunctival hyperaemia was the most common clinical manifestation of AHC, observed in all 73 cases (100%). Subconjunctival haemorrhage was experienced by 82.2% (60/73), while pain and discharge were each reported by 64.4% (47/73 each). Eyelid swelling was observed in 57.5% (42/73) and tearing in 54.8% (40/73) (**Table 2**). During the investigation, none of the patients developed systemic manifestations or subsequent complications.

The propagated epidemic curve, shown in **Fig. 2**, revealed a steady rise in the number of individuals presenting with symptoms between 16 and 23 September

Table 1. **Sociodemographic characteristics of cases of acute haemorrhagic conjunctivitis and controls (*N* = 146), Pak Touch village, Cambodia, 2023**

Characteristic	Cases (*n* = 73)	Controls (*n* = 73)	X^2	*P*
Demographic variables				
Median age (range, mean ± SD)	20.00 (1–70, 27.7 ± 20.0)	22.00 (2–70, 29.4 ± 19.9)		
Age group (years)				
<6	7 (9.6)	4 (5.5)		
6–18	19 (26.0)	31 (42.5)		
19–30	13 (17.8)	11 (15.1)		
31–50	19 (26.0)	16 (21.9)		
≥51	15 (20.5)	11 (15.1)		
Sex				
Male	34 (46.6)	35 (47.9)		
Female	39 (53.4)	38 (52.1)	0.0275	0.868
Risk factors				
Met with AHC patient				
No	22 (30.1)	47 (64.4)		
Yes	51 (69.9)	26 (35.6)	17.1749	**<0.001**
Physical contact with AHC patient				
No	16 (21.9)	50 (68.5)		
Yes	57 (78.1)	23 (31.5)	31.9652	**<0.001**
Had AHC patient in family				
No	31 (42.5)	52 (71.2)		
Yes	42 (57.5)	21 (28.8)	12.3133	**<0.001**
Used the same toilet				
No	29 (39.7)	35 (48.0)		
Yes	44 (60.3)	38 (52.0)	1.0015	0.317
Shared eye drops				
No	50 (68.5)	63 (86.3)		
Yes	23 (31.5)	10 (13.7)	6.6168	**0.001**
Shared cups for drinking				
No	27 (37.0)	46 (63.0)		
Yes	46 (63.0)	27 (37.0)	9.8904	**0.002**
Shared towel				
No	48 (65.8)	54 (74.0)		
Yes	25 (34.2)	19 (26.0)	1.1711	0.279
Rubbed eyes frequently				
No	18 (24.7)	50 (68.5)		
Yes	55 (75.3)	23 (31.5)	28.1870	**<0.001**
Poor hand hygiene				
No	20 (27.4)	48 (65.8)		
Yes	53 (72.6)	25 (34.2)	21.5807	**<0.001**

AHC: acute haemorrhagic conjunctivitis; SD: standard deviation; χ^2: chi-squared test.

Values are *n* (%) unless otherwise indicated. Bold *P* values are statistically significant (<0.05).

2023. The earliest case presentation, on 16 September 2023, occurred 2 days after the individuals returned from Viet Nam. Reported case numbers increased thereafter, peaking at 31 new cases on 23 September 2023.

Risk factor regression

As shown in **Table 3**, seven of nine potential risk factors had a statistically significant association with increased odds of AHC in an unadjusted logistic regression analysis. Those with the strongest associations included direct physical contact with AHC patients (cOR: 7.74, 95% CI: 3.70–16.30, $P < 0.001$), frequent eye rubbing (cOR: 6.64, 95% CI: 3.20–13.70, $P < 0.001$) and poor hand hygiene (cOR: 5.10, 95% CI: 2.50–11.30, $P < 0.001$). Using the same toilet and sharing a towel were not found to be significantly associated with AHC in the univariable models.

The three factors with the highest crude ORs remained significantly associated with increased odds of an AHC infection in the multivariable analysis (**Table 3**). Having physical contact with an AHC patient and frequent eye rubbing both increased the odds of AHC more than fourfold (aOR: 4.42, 95% CI: 1.90–10.10, $P < 0.001$; aOR: 4.56, 95% CI: 2.00–10.37, $P < 0.001$, respectively). Poor hand hygiene was also independently associated with AHC infection (aOR: 3.70, 95% CI: 1.64–8.43, $P = 0.002$). All other factors including meeting with an AHC patient, having an AHC patient in the family, and the other sharing and hygiene-related behaviours were not significantly associated with infection after adjusting for confounders.

Laboratory findings

Among the 21 conjunctival swabs tested, real-time RT–PCR detected enterovirus in 11 samples. Nine of these showed coinfection with rhinovirus, and five were also positive for human coronavirus NL63 (HCoV NL63). Further RNA sequencing of five samples that were positive for enterovirus revealed the highest similarity to CV-A24v, confirming it as the cause of the AHC outbreak.

DISCUSSION

AHC, or "pink eye," a highly contagious viral infection with a short incubation period, has caused several global outbreaks over the past four decades. In recent years, most notably in 2023, large-scale epidemics occurred across Asia, mainly due to infection with CV-A24v. Because of its high infectivity, AHC remains a significant public health risk, with potential medical, social and economic impacts.[28,29] Recent outbreaks highlight the need for robust surveillance and targeted response strategies.

Table 2. **Clinical presentation of cases with acute haemorrhagic conjunctivitis, Pak Touch village, Cambodia, 2023 ($N = 73$)**

Clinical presentation	No. (%) of cases
Eyelid swelling	42 (57.5)
Discharge	47 (64.4)
Pain	47 (64.4)
Tearing	40 (54.8)
Conjunctival hyperaemia	73 (100.0)
Subconjunctival haemorrhage	60 (82.2)

Enterovirus infections can occur year-round, but tend to peak in spring and autumn.[30] In the autumn of 2023, India, Nepal, Pakistan and Viet Nam all reported surges in cases of infectious conjunctivitis.[31] Multiple outbreaks also occurred during Thailand's rainy season (September–October).[32] Thus, Cambodia's spike in AHC cases in September 2023, at the end of its rainy season, is unsurprising. However, it was Cambodia's first outbreak of AHC since 1980.[26] This does not necessarily mean that such outbreaks have not occurred during the past 43 years. The lack of investigations and limited emphasis on surveillance for eye health may have led to cases being overlooked or misidentified, suggesting that the extent of the presence of AHC in the country may have been underreported.

The wide age range of cases (1–70 years) and the lack of a significant gender predisposition highlight the disease's ability to affect people of all ages and genders. However, this analysis showed that individuals aged 6–18 years accounted for 26% of cases, a proportion similar to that in those aged 31–50 years. While this does not confirm increased susceptibility, the involvement of school-aged children may reflect exposure patterns associated with communal settings, such as schools and social gatherings. Similar trends were observed in a 1972 outbreak in Tunisia and a July 2023 outbreak in India, both of which saw a higher proportion of cases among

Fig. 2. **Epidemic curve of outbreak of acute haemorrhagic conjunctivitis in Pak Touch village (*N* = 73), Ratanakiri province, Cambodia, 14–24 September 2023, based on the first day of clinical presentation as reported by the patient**

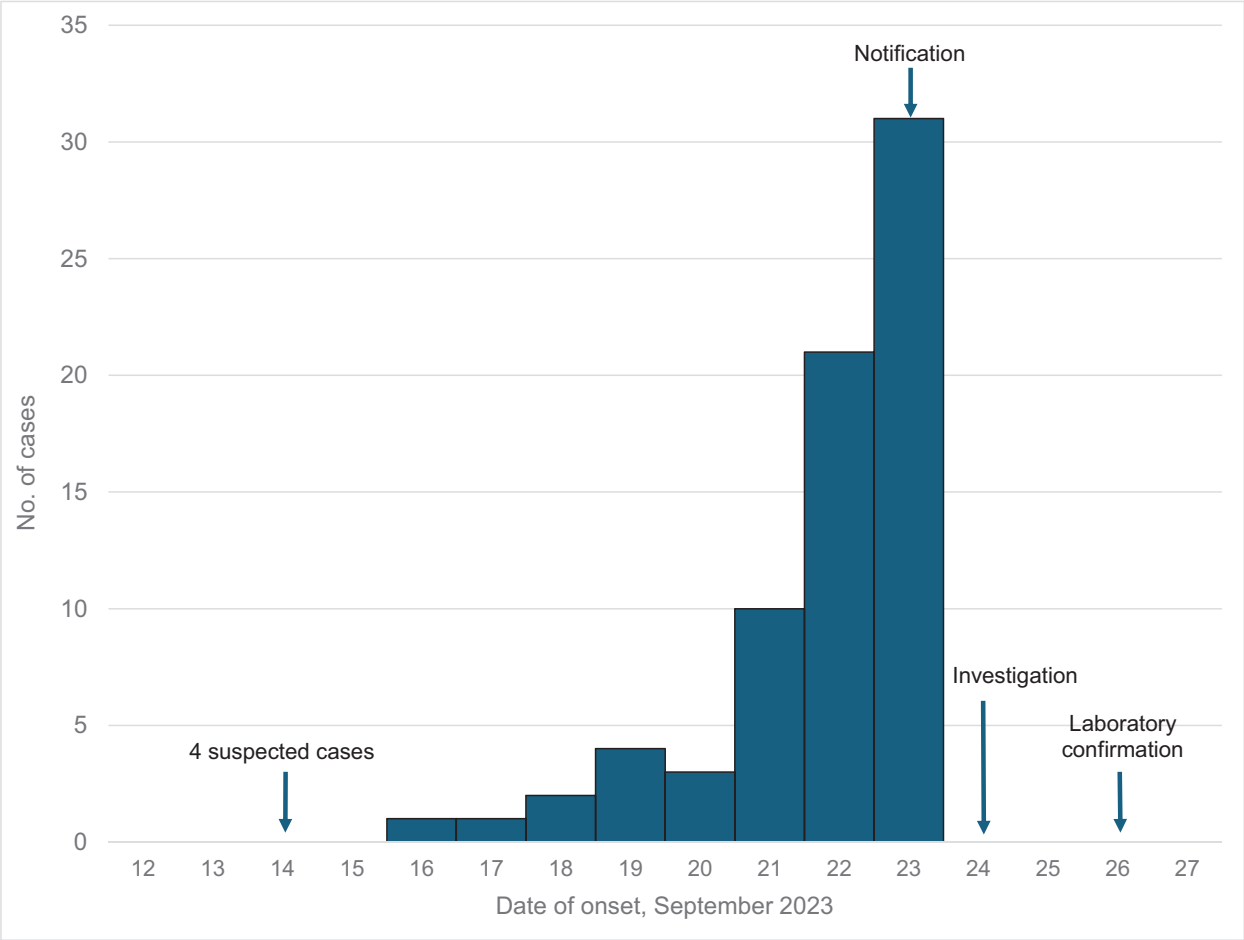

school-aged children, although older individuals were also affected.[33,34]

This retrospective case-control study identified several key risk factors for AHC transmission including physical contact with an AHC patient, frequent eye rubbing and poor hand hygiene. Similar risk factors have been reported in previous outbreaks, including the 1985 outbreak in Singapore and the 2003 outbreak in Melaka, Malaysia, in both of which close contact and the sharing of personal items played major roles in transmission.[6,35] These findings underscore the importance of focusing on personal hygiene and avoiding sharing items as a basis for developing control and prevention strategies.

Immediately following the initial investigation, the Ministry of Health, in collaboration with the National Program for Eye Health, initiated a comprehensive public health education campaign to alert the public to the symptoms and modes of transmission of and preventive measures for AHC, such as practising good hand hygiene and avoiding contact with infected individuals. The public health education programme targeted schools, health-care facilities and community leaders, and used multiple communication channels, including local media and social media platforms, to deliver its messaging.

The propagated epidemic curve in this study showed a rapid increase in cases within 1 week, reflecting the characteristically swift transmission of AHC during outbreaks. Clinically, the individuals affected by the outbreak presented with typical signs, such as conjunctival hyperaemia, subconjunctival haemorrhage, discharge, eyelid swelling, pain and tearing. The high prevalences of subconjunctival haemorrhage (82.2%) and conjunctival hyperaemia (100%) highlight the

Table 3. **Crude and adjusted odds ratios for the association between behavioural risk factor and acute haemorrhagic conjunctivitis for cases and controls (*N* = 146), Pak Touch village, Cambodia, 2023**

Variable	Crude OR (95% CI)	*P*	Adjusted OR (95% CI)	*P*
Age group (years)				
<6	Reference		Reference	
6–18	2.85 (0.70–11.00)	0.129	2.91 (0.56–15.03)	0.201
19–30	1.48 (0.34–6.42)	0.600	4.80 (0.70–22.30)	0.112
31–50	1.47 (0.34–6.42)	0.586	4.57 (0.80–26.80)	0.092
≥51	1.28 (0.30–5.50)	0.737	2.5 (0.40–13.90)	0.347
Sex				
Male	Reference			
Female	1.05 (0.50–2.00)	0.868	–	–
Met with AHC patient				
No	Reference		Reference	
Yes	4.19 (2.10–8.40)	<0.001	1.30 (0.30–5.55)	0.738
Physical contact with AHC patient				
No	Reference		Reference	
Yes	7.74 (3.70–16.30)	<0.001	4.42 (1.90–10.10)	**<0.001**
Had AHC patient in family				
No	Reference		Reference	
Yes	3.35 (1.70–6.70)	0.001	1.05 (0.15–7.10)	0.957
Used the same toilet				
No	Reference			
Yes	1.40 (0.70–2.70)	0.318	–	–
Shared eye drops				
No	Reference		Reference	
Yes	2.90 (1.26–6.65)	0.012	2.50 (0.90–7.20)	0.083
Shared cups for drinking				
No	Reference		Reference	
Yes	2.90 (1.50–5.70)	0.002	1.30 (0.50–3.10)	0.570
Shared towel				
No	Reference			
Yes	1.50 (0.70–3.00)	0.280	–	–
Rubbed eyes frequently				
No	Reference		Reference	
Yes	6.64 (3.20–13.70)	<0.001	4.56 (2.00–10.37)	**<0.001**
Poor hand hygiene				
No	Reference		Reference	
Yes	5.10 (2.50–11.30)	<0.001	3.70 (1.64–8.43)	**0.002**

AHC: acute haemorrhagic conjunctivitis; CI: confidence interval; OR: odds ratio.
Bold *P* values are statistically significant (<0.05).

distinct and severe presentation of AHC compared with other types of conjunctivitis. In most respects, clinical manifestations were similar to those reported in the 2023 outbreak in India, in which conjunctival hyperaemia was also observed in all cases.[34] However, this study observed higher rates of subconjunctival haemorrhage

than in outbreaks in Viet Nam in 2023 and India in 2022, which reported prevalences of 4% and 17%, respectively.[30,31] The high prevalence of subconjunctival haemorrhage in the cases in this study might be linked to a high prevalence of frequent eye rubbing, which can cause subconjunctival haemorrhage secondary to AHC. Other signs, such as eyelid swelling, tearing, pain and discharge, had prevalences comparable to those in both earlier and more recent investigations.[34,36]

The AHC surge in Pak Touch village began with the four cases observed among eight individuals who returned home from Viet Nam on 14 September 2023. Therefore, it is possible that the Pak Touch outbreak may be linked to the outbreak of CV-A24v infection in Viet Nam in 2023, as reported by Tran et al.[31] News reports from early September 2023 indicated that the Viet Nam outbreak may well have contributed to the rise in AHC cases observed in Cambodia, but further investigation would be needed to confirm this.[37,38] Nevertheless, these events highlight how quickly diseases can spread globally and underscore the need for effective surveillance systems to detect and respond to outbreaks promptly. Consequently, international coordination is crucial for sharing information and implementing unified public health strategies to control cross-border infections.

The advanced PCR methods used in this study allowed for rapid identification of the virus and revealed the presence of enterovirus in 11 of 21 conjunctival swab samples. Interestingly, nine of these positive samples showed coinfection with rhinovirus, and five had additional coinfection with HCoV NL63. These findings are consistent with those from a study conducted in Madurai, India, in 2021 during the COVID-19 Delta surge, during which many AHC cases caused by CV-A24v infection also involved coinfections with *Human adenovirus D* (HAdV-D) and severe acute respiratory syndrome coronavirus 2 (SARS-CoV-2).[39] Similarly, the 2023 AHC outbreak in Viet Nam, which was linked to CV-A24v, revealed coinfections, including three cases also with HAdV-D, two with herpes simplex virus type 1, and one each with Epstein–Barr virus and cytomegalovirus.[31] This similarity highlights the recurring nature of coinfections during viral outbreaks and underscores the importance of implementing comprehensive viral screening to manage and understand AHC. The first-line test for virological confirmation is the real-time RT–PCR assay, as it can yield results in a few hours.[22] However, due to a lack of sensitivity, more advanced gene sequencing techniques, such as RNA sequencing with next-generation sequencing, are required to fully characterize the responsible pathogen.[22] Although considered the gold standard for virus isolation,[22] these methods pose challenges for timely diagnosis, particularly in resource-limited settings such as Cambodia. In this study, the use of unbiased RNA sequencing analysis confirmed the presence of CV-A24v in all five cases who tested positive for enterovirus, but it took approximately 16 days to yield definitive results.

Effectively managing AHC outbreaks in resource-limited settings such as Cambodia requires addressing several public health challenges. Currently, eye health diseases are not included in Cambodia's case-based, event-based and sentinel surveillance systems, which often leads to delayed reporting.[40] However, while extending these systems to remote areas, such as Pak Touch village, may be desirable, it may be difficult for systems that rely on digital tools – such as CamEwarn (a case-based surveillance system for seven epidemic-prone diseases) and Hotline-115 (for reporting diseases) – because local health centres often lack the necessary computers, reliable internet connections and technical skills. A more feasible way forward may be to implement enhanced community-based syndromic surveillance, which would require training local health-care workers and volunteers to recognize early symptoms of AHC and to report via a mobile app or SMS integrated with Hotline-115.

Limitations

This study had several limitations. Its retrospective design and reliance on historical and self-reported data risk introducing bias due to recall inaccuracies and missing or incomplete records. The epidemic curve, for example, was based on patients' recollections of the date of symptom onset, which may have affected the accuracy of the outbreak timeline. Data collection ceased on 24 September, potentially resulting in missed cases and an underestimation of the true attack rate. The small number of conjunctival swabs and samples for sequencing limited the ability to draw more robust conclusions about the viral strains and their transmission dynamics. Furthermore, the lack of phylogenetic analysis limited insights into the genetic diversity and evolutionary changes of the virus. Finally, the findings from the risk factor analysis may

not be generalizable to other areas, given the specific sociodemographic and environmental characteristics of Pak Touch village.

Conclusions

The AHC outbreak in Pak Touch village, Ratanakiri province, Cambodia, was attributed to infection with CV-A24v. Critical risk factors for infection in this setting included physical contact with AHC patients, frequent eye rubbing and poor hand hygiene. These findings are essential for developing targeted public health interventions to control and prevent future outbreaks of AHC in Cambodia. Continual surveillance and public education remain crucial to manage AHC and reduce its public health impact in the future.

Acknowledgements

The authors gratefully acknowledge The University of Edinburgh, as this manuscript was prepared as the final project for the Master of Surgery degree in the Clinical Ophthalmology Programme. The authors also extend their appreciation to the rapid response team, assigned by the Communicable Disease Control Department of the Ministry of Health, for their invaluable contributions to the outbreak investigation, including providing critical information and facilitating access to the documentation necessary for this study. Laboratory testing of clinical specimens was performed at the National Public Health Laboratory of Cambodia. The authors also thank Assistant Professor Chau Darapheak, Head of the Laboratory Bureau at the National Institute of Public Health of Cambodia, for expert guidance and detailed information about Fast Track Diagnostics' Respiratory Pathogens 21 assay and RNA sequencing.

Conflicts of interest

The authors have no conflicts of interest to declare.

Ethics statement

This study was conducted in accordance with the ethical standards of the National Ethics Committee for Health Research of Cambodia. Ethical approval was granted under Non-Clinical Trials of Investigational Medicinal Products Study Protocol QA001-T01/V1.0 on 7 March 2024.

Funding

None.

References

1. Wairagkar NS. Acute hemorrhagic conjunctivitis 077.4 (epidemic hemorrhagic conjunctivitis, Apollo 11 disease). In: Roy FH, Fraunfelder FW, Fraunfelder FT, Tindall R, Jensvold B, editors. Roy and Fraunfelder's current ocular therapy. 6th ed. Edinburgh: WB Saunders; 2008. pp. 10–1. Available from: https://doi.org/10.1016/B978-1-4160-2447-7.50009-8, accessed 10 January 2024.
2. Chatterjee S, Quarcoopome C, Apenteg A. An epidemic of acute conjunctivitis in Ghana. Ghana Med J. 1970;9(1):9–11.
3. Romero JR, Modlin JF. Coxsackieviruses, echoviruses, and numbered enteroviruses. In: Bennett JE, Dolin R, Blaser MJ, editors. Mandell, Douglas, and Bennett's principles and practice of infectious diseases. 8th ed. Philadelphia: WB Saunders; 2015. pp. 2080–90.e4. Available from: https://doi.org/10.1016/B978-1-4557-4801-3.00174-0, accessed 18 February 2024.
4. Medina NH, Haro-Muñoz E, Pellini AC, Machado BC, Russo DH, Timenetsky MD, et al. Acute hemorrhagic conjunctivitis epidemic in São Paulo state, Brazil, 2011. Rev Panam Salud Publica. 2016;39(2):137–41. pmid:27754516
5. Ghendon Y. Ocular enterovirus infections in the world. In: Ishii K, Uchida Y, Miyamura K, Yamazaki S, editors. Acute hemorrhagic conjunctivitis: etiology, epidemiology and clinical manifestation. Basel: Karger; 1989. pp. 3–9. Available from: https://doi.org/10.1159/000417539, accessed 18 February 2024.
6. Ghazali O, Chua KB, Ng KP, Hooi PS, Pallansch MA, Oberste MS, et al. An outbreak of acute haemorrhagic conjunctivitis in Melaka, Malaysia. Singapore Med J. 2003;44(10):511–6. pmid:15024454
7. Oh MD, Park S, Choi Y, Kim H, Lee K, Park W, et al. Acute hemorrhagic conjunctivitis caused by coxsackievirus A24 variant, South Korea, 2002. Emerg Infect Dis. 2003;9(8):1010–2. doi:10.3201/eid0908.030190 pmid:12967504
8. Palacios G, Oberste MS. Enteroviruses as agents of emerging infectious diseases. J Neurovirol. 2005;11(5):424–33. doi:10.1080/13550280591002531 pmid:16287683
9. Kaufman HE. Adenovirus advances: new diagnostic and therapeutic options. Curr Opin Ophthalmol. 2011;22(4):290–3. doi:10.1097/ICU.0b013e3283477cb5 pmid:21537185
10. Wu D, Ke CW, Mo YL, Sun LM, Li H, Chen QX, et al. Multiple outbreaks of acute hemorrhagic conjunctivitis due to a variant of coxsackievirus A24: Guangdong, China, 2007. J Med Virol. 2008;80(10):1762–8. doi:10.1002/jmv.21288 pmid:18712817
11. Lévêque N, Huguet P, Norder H, Chomel JJ. [Enteroviruses responsible for acute hemorrhagic conjunctivitis]. Med Mal Infect. 2010;40:212–8 (in French). doi:10.1016/j.medmal.2009.09.006 pmid:19836177
12. Shulman LM, Manor Y, Azar R, Handsher R, Vonsover A, Mendelson E, et al. Identification of a new strain of fastidious enterovirus 70 as the causative agent of an outbreak of hemorrhagic conjunctivitis. J Clin Microbiol. 1997;35(8):2145–9. doi:10.1128/jcm.35.8.2145-2149.1997 pmid:9230400
13. Uchio E, Yamazaki K, Ishikawa H, Matsunaga I, Asato Y, Aoki K, et al. An epidemic of acute haemorrhagic conjunctivitis caused by enterovirus 70 in Okinawa, Japan, in 1994. Graefes Arch Clin Exp Ophthalmol. 1999;237(7):568–72. doi:10.1007/s004170050280 pmid:10424307

14. Yin-Murphy M, Lim KH, Ho YM. A coxsackievirus type A24 epidemic of acute conjunctivitis. Southeast Asian J Trop Med Public Health. 1976;1(1):1–5. pmid:1027096
15. Mirkovic RR, Schmidt NJ, Yin-Murphy M, Melnick JL. Enterovirus etiology of the 1970 Singapore epidemic of acute conjunctivitis. Intervirology. 1974;4(2):119–27. doi:10.1159/000149850 pmid:4217326
16. Lim KH, Yin-Murphy M. An epidemic of conjunctivitis in Singapore in 1970. Singapore Med J. 1971;12(5):247–9. pmid:5134044
17. Nilsson EC, Jamshidi F, Johansson SM, Oberste MS, Arnberg N. Sialic acid is a cellular receptor for coxsackievirus A24 variant, an emerging virus with pandemic potential. J Virol. 2008;82(6):3061–8. doi:10.1128/JVI.02470-07 pmid:18184708
18. Nokhbeh MR, Hazra S, Alexander DA, Khan A, McAllister M, Suuronen EJ, et al. Enterovirus 70 binds to different glycoconjugates containing α2,3-linked sialic acid on different cell lines. J Virol. 2005;79(11):7087–94. doi:10.1128/JVI.79.11.7087-7094.2005 pmid:15890948
19. Messacar K, Modlin JF, Abzug MJ. Enteroviruses and parechoviruses. In: Long SS, Prober CG, Fischer M, editors. Principles and practice of pediatric infectious diseases. 5th ed. Philadelphia: Elsevier; 2018. pp. 1205–13.e3. Available from: https://www.sciencedirect.com/science/chapter/edited-volume/abs/pii/B978032340181400236X, accessed 20 March 2024.
20. Lina B, Pozzetto B, Andreoletti L, Beguier E, Bourlet T, Dussaix E, et al. Multicenter evaluating of a commercially available PCR assay for diagnosing enterovirus infection in a panel of cerebrospinal fluid specimens. J Clin Microbiol. 1996;34(12):3002–6. doi:10.1128/jcm.34.12.3002-3006.1996 pmid:8940438
21. Melnick JL, Schmidt NJ, Hampil B, Ho HH. Lyophilized combination pools of enterovirus equine antisera: preparation and test procedures for the identification of field strains of 19 group A coxsackievirus serotypes. Intervirology. 1977;8(3):172–81. doi:10.1159/000148892 pmid:558177
22. Lévêque N, Lahlou Amine I, Tcheng R, Falcon D, Rivat N, Dussart P, et al. Rapid diagnosis of acute hemorrhagic conjunctivitis due to coxsackievirus A24 variant by real-time one-step RT-PCR. J Virol Methods. 2007;142(1-2):89–94. doi:10.1016/j.jviromet.2007.01.009 pmid:17328967
23. Centers for Disease Control and Prevention (CDC). Acute hemorrhagic conjunctivitis outbreak caused by Coxsackievirus A24–Puerto Rico, 2003. MMWR Morb Mortal Wkly Rep. 2004;53(28):632–4. pmid:15269699
24. Park SW, Lee CS, Jang HC, Kim EC, Oh MD, Choe KW. Rapid identification of the coxsackievirus A24 variant by molecular serotyping in an outbreak of acute hemorrhagic conjunctivitis. J Clin Microbiol. 2005;43(3):1069–71. doi:10.1128/JCM.43.3.1069-1071.2005 pmid:15750062
25. Xiao XL, Wu H, Li YJ, Li HF, He YQ, Chen G, et al. Simultaneous detection of enterovirus 70 and coxsackievirus A24 variant by multiplex real-time RT-PCR using an internal control. J Virol Methods. 2009;159(1):23–8. doi:10.1016/j.jviromet.2009.02.022 pmid:19442840
26. Bernard KW, Hierholzer JC, Dugan JB, DeLay PR, Helmick CG. Acute hemorrhagic conjunctivitis in Southeast Asian refugees arriving in the United States–isolation of enterovirus 70. Am J Trop Med Hyg. 1982;31(3 Pt 1):541–7. doi:10.4269/ajtmh.1982.31.541 pmid:6282147
27. Lim S, Kem K. Indigenous people: political rights, culture, education and health care. Phnom Penh: Parliamentary Institute of Cambodia; 2015. Available from: https://pcasia.org/pic/wp-content/uploads/simple-file-list/20160407_Indigeneous-Peoples-Political-Rights-Culture-Education-and-Health-Care_EN.pdf, accessed 23 January 2025.
28. Zhang L, Zhao N, Huang X, Jin X, Geng X, Chan TC, et al. Molecular epidemiology of acute hemorrhagic conjunctivitis caused by coxsackie A type 24 variant in China, 2004–2014. Sci Rep. 2017;7(1):45202. doi:10.1038/srep45202 pmid:28332617
29. Chu PY, Ke GM, Chang CH, Lin JC, Sun CY, Huang WL, et al. Molecular epidemiology of coxsackie A type 24 variant in Taiwan, 2000–2007. J Clin Virol. 2009;45(4):285–91. doi:10.1016/j.jcv.2009.04.013 pmid:19473877
30. Prajna NV, Prajna L, Teja V, Gunasekaran R, Chen C, Ruder K, et al. Apollo rising: acute conjunctivitis outbreak in India, 2022. Cornea Open. 2023;2(2):e0009. doi:10.1097/coa.0000000000000009 pmid:37719281
31. Tran H, Ha T, Hoang L, Tran Y, Ruder K, Zhong L, et al. Coxsackievirus A24 causing acute conjunctivitis in a 2023 outbreak in Vietnam. Int J Infect Dis. 2024;146:107133. doi:10.1016/j.ijid.2024.107133 pmid:38876162
32. Chansaenroj J, Vongpunsawad S, Puenpa J, Theamboonlers A, Vuthitanachot V, Chattakul P, et al. Epidemic outbreak of acute haemorrhagic conjunctivitis caused by coxsackievirus A24 in Thailand, 2014. Epidemiol Infect. 2015;143(14):3087–93. doi:10.1017/S0950268815000643 pmid:25824006
33. Nabli B. Acute hemorrhagic conjunctivitis in Tunisia. In: Ishii K, Uchida Y, Miyamura K, Yamazaki S, editors. Acute hemorrhagic conjunctivitis: etiology, epidemiology and clinical manifestation. Basel: Karger; 1989. pp. 105–9. Available from: https://doi.org/10.1159/000417548, accessed 15 June 2024.
34. Boro P, Gongo T, Ori K, Kamki Y, Ete N, Jini M, et al. An outbreak of acute hemorrhagic conjunctivitis due to coxsackievirus A24 in a residential school, Naharlagun, Arunachal Pradesh: July 2023. Indian J Med Microbiol. 2024;48:100549. doi:10.1016/j.ijmmb.2024.100549 pmid:38395257
35. Yin-Murphy M, Baharuddin-Ishak, Phoon MC, Chow VT. A recent epidemic of Coxsackie virus type A24 acute haemorrhagic conjunctivitis in Singapore. Br J Ophthalmol. 1986;70(11):869–73. doi:10.1136/bjo.70.11.869 pmid:3024697
36. Kosrirukvongs P, Kanyok R, Sitritantikorn S, Wasi C. Acute hemorrhagic conjunctivitis outbreak in Thailand, 1992. Southeast Asian J Trop Med Public Health. 1996;27(2):244–9. pmid:9279984
37. Pink eye likely to be epidemic [website]. Saigon: Sàigòn Giai Phong News; 2023. Available from: https://en.sggp.org.vn/pink-eye-likely-to-be-epidemic-post104764.html, accessed 21 June 2024.
38. Harp MD. Conjunctivitis (pink eye) sees a spike in cases in Vietnam, India and Pakistan [website]. Cranbury (NJ): Ophthalmology Times; 2023. Available from: https://www.ophthalmologytimes.com/view/conjunctivitis-pink-eye-sees-a-spike-in-cases-in-vietnam-india-and-pakistan, accessed 21 June 2024.
39. Lalitha P, Prajna NV, Gunasekaran R, Teja GV, Sharma SS, Hinterwirth A, et al. Deep sequencing analysis of clinical samples from patients with acute infectious conjunctivitis during the COVID-19 delta surge in Madurai, India. J Clin Virol. 2022;157:105318. doi:10.1016/j.jcv.2022.105318 pmid:36242841
40. Suy Lan C, Sok S, Chheang K, Lan DM, Soung V, Divi N, et al. Cambodia national health hotline – participatory surveillance for early detection and response to disease outbreaks. Lancet Reg Health West Pac. 2022;29:100584. doi:10.1016/j.lanwpc.2022.100584 pmid:36605884

Implementation of fireworks-related injury surveillance in Metro Manila, Philippines, 2023–2024

Kenneth Paul S Ong[a,b]

Correspondence to Kenneth Paul S Ong (email: kong0031@student.monash.edu / ksong2@alum.up.edu.ph)

Many countries record high rates of fireworks-related injuries, especially during national celebrations. In the Philippines, increases in the number of injuries reported around the New Year period in recent years have highlighted the importance of continued strengthening of national fireworks-related injury surveillance. The Philippines' regional epidemiology and surveillance units play a significant role in surveillance by linking its key stakeholders, the sentinel hospitals and the Department of Health's Central Office. More specifically, these units promote compliance with reporting standards among sentinel hospitals and support case data validation. Approximately half of the sentinel hospitals that contribute data to the surveillance system are in the nation's capital, Metro Manila. This concentrated coverage prompted the Regional Epidemiology and Surveillance Unit staff in Metro Manila to implement low-cost, digital strategies to improve the quality and timeliness of fireworks-related injury reporting. During the 2023–2024 surveillance period (21 December to 5 January), the use of virtual coordination spaces and data dashboards contributed to reducing turnaround times for generating surveillance reports from 31 minutes to 8 minutes. Moreover, at least 80% of sentinel hospitals provided timely reports on 11 of the 16 days of the surveillance period. Staff commitment was a major contributing factor in overcoming the time and human resource constraints encountered during implementation of these strategies. However, it is important to recognize that beyond these digital innovations, policy reforms that increase funding are needed to enhance fireworks-related injury surveillance and secure its long-term sustainability and scalability in the Philippines.

Fireworks-related injuries (FWRIs) are increasing across the Philippines, following a decline during the first year of the COVID-19 pandemic.[1,2] Injury prevalence is greatest during December and January, when fireworks are traditionally enjoyed as part of New Year's celebrations. Injuries rose from 188 cases in December 2021–January 2022 to 291 cases in December 2022–January 2023, an increase of 55%.[1,2] A further increase was observed the following year, with cases in December 2023–January 2024 roughly doubling the number recorded in December 2022–January 2023.[3] Despite policies prohibiting their use, approximately 40% of FWRIs have been attributed to illegal firecrackers.[1,3] These trends underscore the continuing importance of FWRI surveillance as a basis for targeted interventions to reduce these injuries.

In the Philippines, FWRI surveillance is overseen by the Department of Health (DOH) and runs annually from 21 December to 5 January.[4] Throughout this period, the DOH conducts campaigns to remind the public of the dangers associated with fireworks and to promote injury prevention.[1,3,5,6] Central to FWRI surveillance is the Online National Electronic Injury Surveillance System (ONEISS), which collates data on identified FWRI cases submitted by a nationwide network of 61 sentinel hospitals using standardized case investigation forms (DOH Department Memorandum 2023–0427).[3,7] All patients who seek treatment for injuries caused by fireworks at sentinel hospitals are classified as FWRI cases and are further subclassified as fireworks injury, fireworks ingestion, stray bullet injury or fireworks-related tetanus. If no FWRIs are seen on a given day during the

[a] Monash University, Melbourne, Victoria, Australia.
[b] Center for Health Development, Department of Health, Manila, Philippines.
Published: 16 March 2026
doi: 10.5365/wpsar.2026.17.1.1272

surveillance period, sentinel hospitals are required to submit zero reports to ensure completeness of reporting and data integrity (DOH Department Memorandum 2023–0427). The DOH Central Office (CO) reviews and validates all submitted case investigation forms and generates national FWRI reports.

FWRI surveillance is supported by 17 regional epidemiology and surveillance units (RESUs), one for each region of the country. RESUs promote compliance with reporting standards and disseminate FWRI reports to internal and external regional stakeholders. Requests to sentinel hospitals for action on missing, incomplete or unclear data relating to FWRIs are coursed through RESUs.

Almost half of the FWRI sentinel hospitals (n = 30) are in Metro Manila,[4] making the city a critical focal point for FWRI surveillance reporting and a natural candidate for trialling innovations in surveillance practice. This article documents the operationalization of two digital innovations aimed at improving coordination and reporting efficiency – a virtual coordination space (VCS) and a data dashboard (**Box 1**). Both were implemented by RESU staff in Metro Manila during the 2023–2024 FWRI surveillance period.

METHODS

Pre-implementation activities

Approximately 3 weeks before the start of the surveillance period, 35 RESU staff were divided into groups of two or three and matched with sentinel hospitals. Due to human resource constraints, some staff were part of more than one group, and some groups were matched with more than one hospital. Two individuals were assigned as co-heads and tasked with liaising directly with the DOH CO and with managing the new email account dedicated to coordinating FWRI surveillance.

After a virtual orientation on liaising with sentinel hospitals, each group gave its assigned sentinel hospital an overview of the FWRI surveillance system and briefed hospital staff on the importance of submitting complete and timely case investigation forms. Hospital staff's contact details were registered in an online directory. A VCS was created using a free online messaging application, accessible to all involved staff via a mobile phone or computer.

Development of the data dashboard for visualization of FWRI data involved several steps:

1. consideration of dashboard objectives and its intended users;
2. design of dashboard elements; and
3. addition of filters for data customization.

The main objective of the dashboard was to provide the Regional Director of the DOH Metro Manila Center for Health Development and other regional stakeholders with access to the latest FWRI statistics within an hour of the end of each reporting day (06:00 to 05:59 the following day). The dashboard was developed using the free-to-use Google Looker Studio. Looker Studio files were linked to a Google Sheets spreadsheet, into which ONEISS data were uploaded. Data visualizations in the form of tables and graphs were then created using the chart function of Looker Studio. The completed dashboard consisted of the following components:

1. epidemiologic curve of FWRI cases, by date of injury and comparisons with 2022–2023 data and a 5-year average;
2. number of FWRI cases by age, sex, local government unit, reporting sentinel hospital, place of injury, patient disposition (treated and sent home, admitted, refused admission) and outcome (alive, died);
3. anatomic sites affected; and
4. types of fireworks implicated.

Data filters enabled the generation of granular data by date of injury, local government unit, sentinel hospital and legal status of the implicated fireworks. The ONEISS was cited as the reference for all dashboard visualizations.

Implementation

Project outputs included an updated online directory of sentinel hospitals, a VCS and a data dashboard. Deliverables included promoting sentinel hospital reporting timeliness; addressing requests for action on missing, incomplete or unclear data; and generating daily FWRI surveillance reports. **Fig. 1** illustrates the process flow for handling requests for action on missing,

Box 1. **Use of the virtual coordination space: (a) updates on FWRI cases; (b) case validation; (c) zero reporting; and (d) staff feedback**

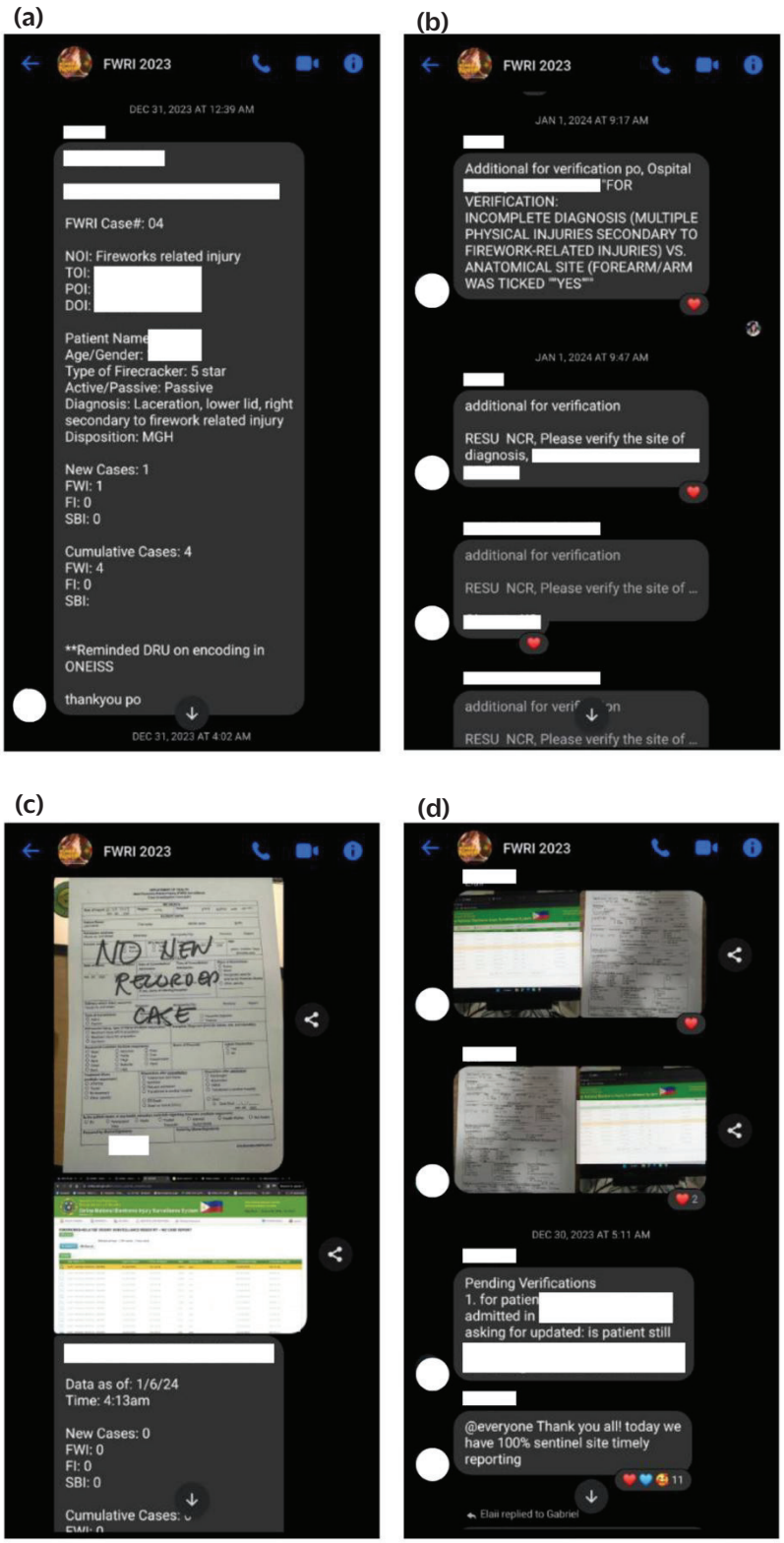

FWRI: fireworks-related injury.

Fig. 1. **Process flows for FWRI surveillance: (a) general process flow illustrating major activities; and (b) steps for case data validation[a]**

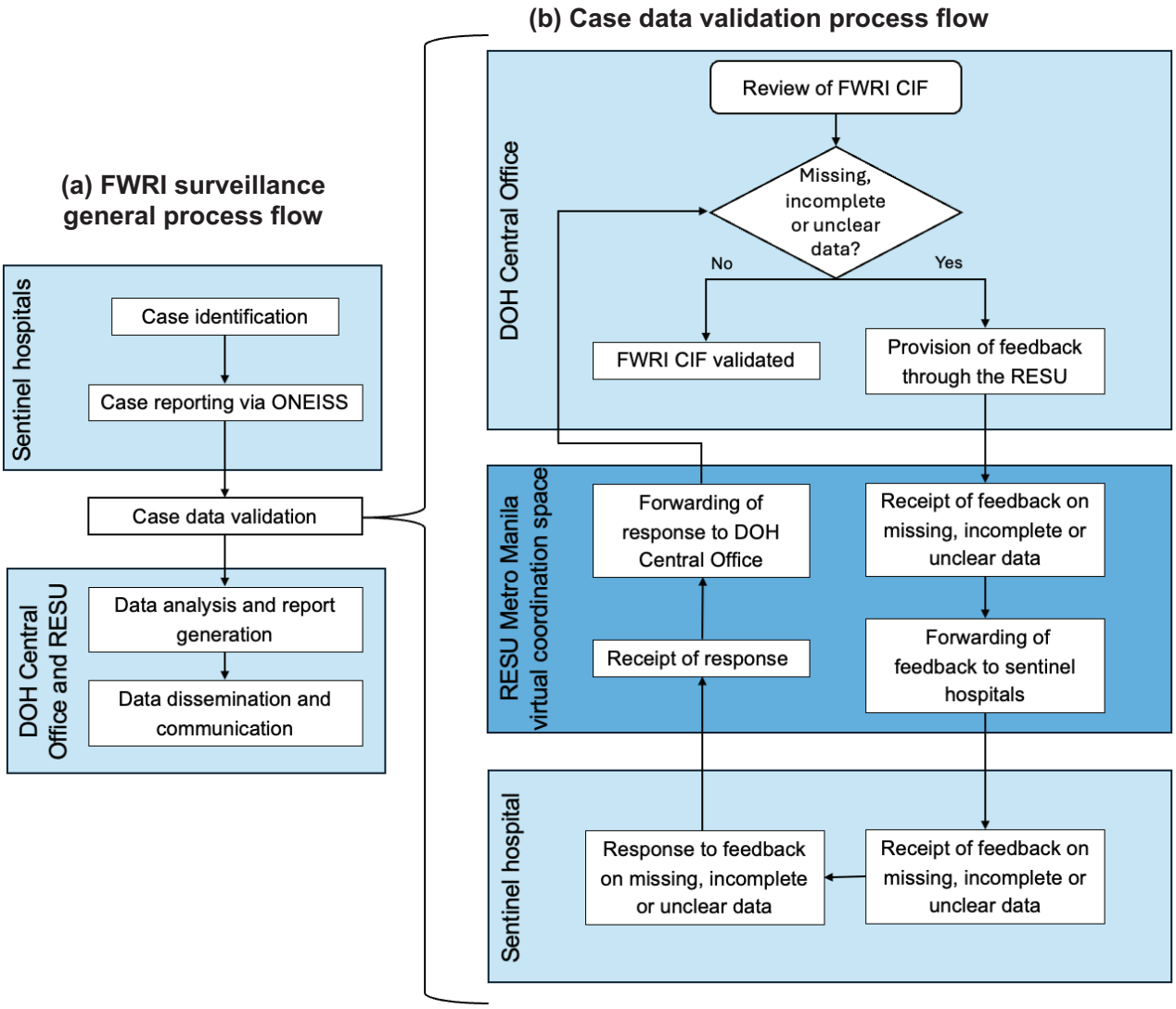

CIF: case investigation form; DOH: Department of Health; FWRI: fireworks-related injury; ONEISS: Online National Electronic Injury Surveillance System; RESU: regional epidemiology and surveillance unit.

[a] Use of the virtual coordination space is highlighted in dark blue.

incomplete or unclear injury data via the VCS as part of data validation. Action requests from the DOH CO were relayed to the co-heads, who posted them in the VCS. RESU staff read the requests and forwarded them to sentinel hospitals. Responses from sentinel hospitals were likewise relayed back through the same mechanism.

At around 02:30, RESU staff issued reminders to sentinel hospitals that had not reported an FWRI for that day to submit a zero report. Proof of hospital compliance with zero reporting was then uploaded to the VCS. Sentinel hospitals that did not submit a zero report were classified as a non-reporting facility. RESU staff were able to contest at the national level any erroneous classification of the facility as non-reporting by taking screenshots of their zero reports.

After the end of each reporting day, RESU staff posted daily and cumulative FWRI statistics for each sentinel hospital in the VCS. In addition, a summary of sentinel hospital timeliness was shared via the VCS, and RESU staff provided sentinel hospitals with appropriate

Fig. 2. **FWRI cases and sentinel hospitals with timely reports for each day of the FWRI surveillance period, Metro Manila, Philippines, 2023–2024**

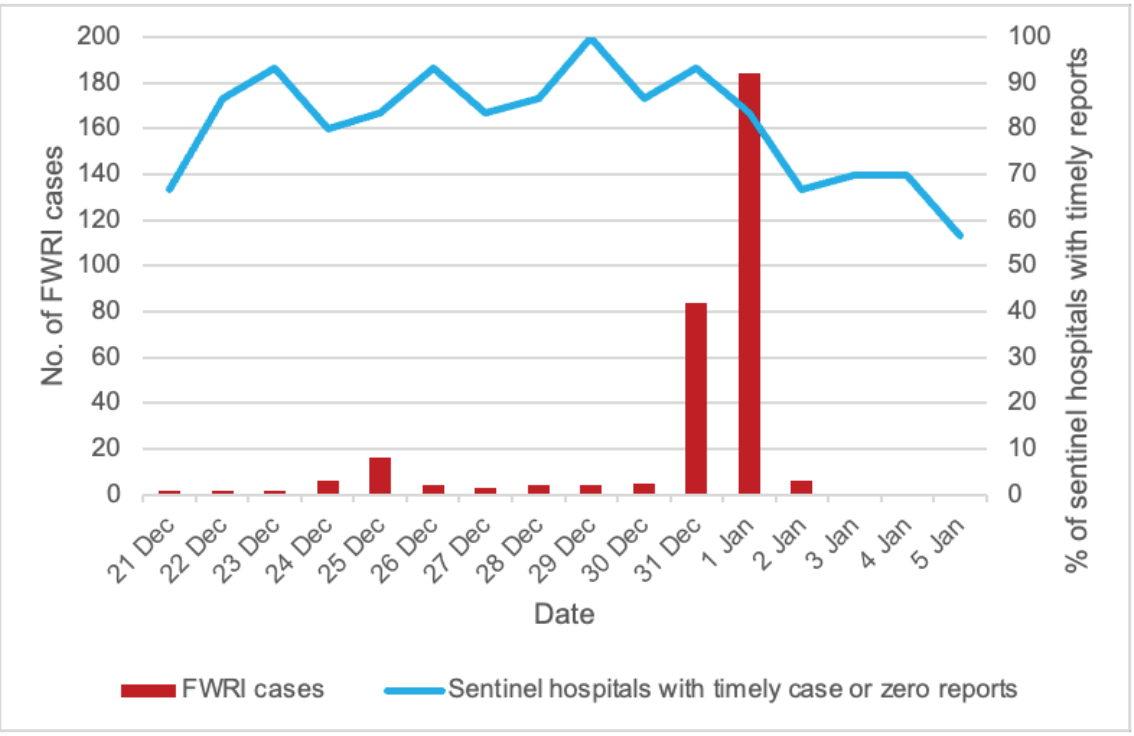

FWRI: fireworks-related injury.

Source: Fireworks-related injury surveillance, DOH MMCHD RESU daily update 2023, Update No. 16. Mandaluyong City: Department of Health (DOH), Metro Manila Center for Health Development; 2024.

feedback. Sentinel hospitals were considered timely if they submitted FWRI reports on the same day as the date of injury or submitted a zero report before 05:00, whichever criterion applied. Hospitals that did not meet these conditions were classified as late.

To generate daily FWRI surveillance reports, validated case data for Metro Manila were extracted from ONEISS and copied into the online spreadsheet. The dashboard page was refreshed, and the updated report was exported and disseminated to internal and external stakeholders. The link to the dashboard was also shared with stakeholders within the DOH Metro Manila Center for Health Development.

Post-implementation and evaluation

At the end of the FWRI surveillance period, a final report comprising cumulative FWRI surveillance statistics and a summary of reporting compliance by sentinel hospitals was generated and submitted for dissemination.

For internal evaluation purposes, we estimated three performance metrics: the proportion of action requests resolved, the proportion of sentinel sites achieving timely reporting and the process flow (the time between ONEISS data download and surveillance report creation).

RESULTS

A total of 322 FWRI cases were captured by ONEISS during the 2023–2024 surveillance period. The number of FWRIs reported per day ranged from 0 to 6 cases, except on 25 and 31 December and 1 January when 16, 84 and 184 cases were reported, respectively (**Fig. 2**). A total of 77 action requests were coursed through RESU staff, all of which were posted in the VCS and then relayed to sentinel hospitals. Likewise, responses from sentinel hospitals to all 77 action requests were relayed to the DOH CO.

The proportion of sentinel sites that submitted timely reports for each day of the surveillance period ranged from 56.7% (n = 17/30) to 100% (n = 30/30), with a median of 83.3% (n = 25/30). On 11 consecutive days of the 16-day surveillance period, reporting was timely for at least 80% of sentinel hospitals (**Fig. 2**).

Fig. 3. **The original and new process flows for generating FWRI surveillance reports**

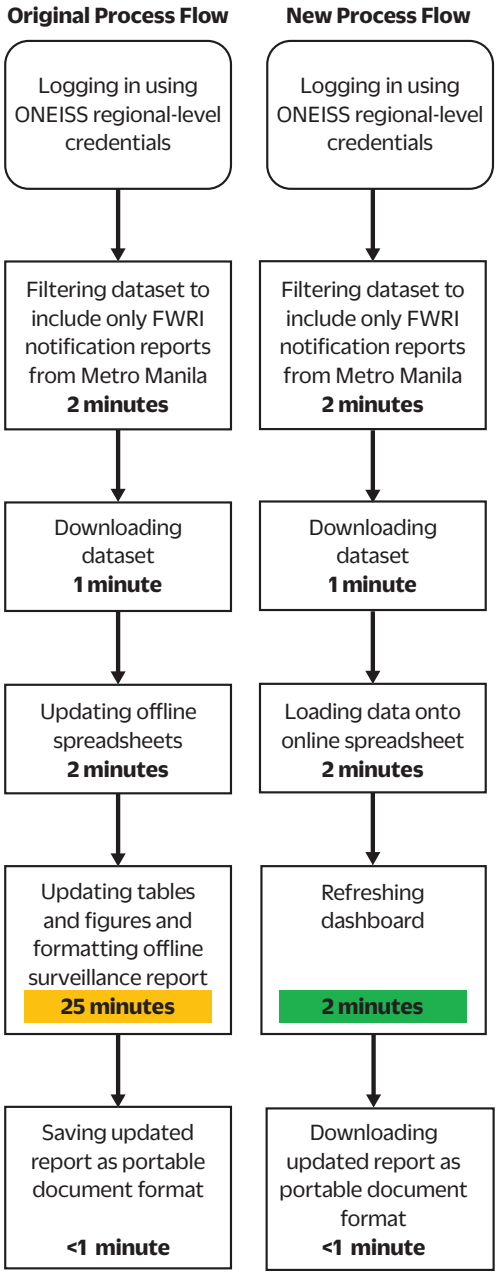

FWRI: fireworks-related injury; ONEISS: Online National Electronic Injury Surveillance System.

The process flow for generating an FWRI surveillance report using the dashboard took approximately 8 minutes, which was faster than the original workflow of 31 minutes (**Fig. 3**).

DISCUSSION

The VCS and data dashboard contributed to improvements in FWRI surveillance process flows in Metro Manila. RESU staff were able to liaise continuously with the 30 sentinel hospitals and the DOH CO, resulting in high levels of timely reporting during the surveillance period. Data dashboards reduced the turnaround time for generating surveillance reports. While these tools are neither novel nor unique, to the best of our knowledge, their use at the regional level for FWRI surveillance has not previously been described.

The VCS delivered greater interconnectedness across the FWRI surveillance system; it facilitated connections between the DOH CO and sentinel hospitals and enabled RESU staff working in different locations across Metro Manila to coordinate their efforts. The VCS was most active during 03:00–05:00, especially on the nights of 24 and 31 December and 1 January, when the most FWRI cases were reported, indicating RESU staff's high levels of commitment to their nightly coordination roles. There were several undocumented instances of sleep deprivation among staff who often had to work the following day. However, within their respective groupings, staff rotated nightly coordination duties to sustain the round-the-clock demands of FWRI surveillance whenever possible. The commitment shown by RESU staff, many of whom worked well beyond their normal hours, was a key factor behind the 100% response rate in processing requests from the DOH CO and the high levels of case validation. This dedication built not only a strong, lasting collaborative network of FWRI surveillance stakeholders, but also trust – which is essential for surveillance systems to thrive.

The human resource demands created by the VCS were to some extent offset by the dashboard, which relieved staff of the repetitive processes involved in manual data visualization. Dashboards are increasingly being used for process improvement, and in this setting demonstrably reduced workload by reducing turnaround time for generating reports.[8,9] Previous institutional experience in developing dashboards, in particular to support the COVID-19 response, helped with building the FWRI dashboard.[10] However, formal training on its use and management was not feasible due to time constraints. Staff responded by helping stakeholders familiarize themselves with the dashboard as needed, and one staff member took responsibility for its maintenance.

The main challenge encountered during implementation of the VCS and the dashboard was human resource constraints. Compared with other

regions, which typically have fewer than four sentinel hospitals, FWRI surveillance in Metro Manila has a relatively greater complement of human resources and level of coordination covering all 30 sentinel hospitals. Even so, staff delegated to FWRI surveillance tasks were already either managing other surveillance systems or assigned as field staff in hospitals or local government units. Furthermore, most staff contracts ended on 31 December, affecting follow-up with sentinel hospitals for reporting and data validation during the last 5 days of FWRI surveillance. While the VCS and dashboard helped overcome this constraint, greater sustainability in FWRI surveillance requires solutions beyond process improvement, such as policy reforms allocating greater funding.

While we believe we have demonstrated that it is possible to operationalize regional dashboards, we acknowledge that further improvements in the VCS and the FWRI dashboard are needed to address evolving challenges and strengthen FWRI surveillance in Metro Manila. Data quality issues, such as missed and misclassified FWRIs, and underreporting at both sentinel and non-sentinel sites, have yet to be fully understood and addressed. Given that around 29% of all FWRIs in Metro Manila during the 2023–2024 surveillance period were reported by non-sentinel sites, the expansion of the surveillance network is key to future development, one where the VCS can play a role in facilitating stakeholder engagement and sustaining coordination. Additionally, the inclusion of visualizations of operational performance indicators (for example, the proportion of unreported and misclassified FWRI cases, and validated zero reports) in the dashboard would improve data quality and strengthen FWRI surveillance. There is also an opportunity to transform the FWRI dashboard into a public-facing dashboard, thereby helping raise public awareness of the risks of FWRIs.

Conclusion

The implementation of FWRI surveillance is unique in Metro Manila primarily because of the concentration of sentinel sites. Significant improvements in turnaround time for generating surveillance reports were achieved through the adoption of innovative digital tools such as the VCS and data dashboards. These strategies can be scaled up to other surveillance systems and adopted by other organizations facing similar challenges. While continued use and development of such tools can contribute to stronger FWRI surveillance, it should be noted that policy reforms that increase funding would further strengthen FWRI surveillance and its sustainability in the Philippines.

Acknowledgements

The author wishes to thank the RESU staff of the Center for Health Development, Department of Health, Metro Manila, for their unwavering support during 2023. In particular, the author wishes to acknowledge staff who were involved in FWRI surveillance in 2023–2024, in alphabetical order:

Ivy Madelle Andres,[a] Leah Mae Arce,[a] Ramon Bajan,[a] Ellaine Ballester,[a] Janezza Christine Batino,[a] Jose Ruiz Belicano,[a] Amelia Bustos,[a] Michael Cagaoan,[a] Mary Zes Carreon,[a] Catrina Mira Cerneo,[a] Franchesca Chavez,[a] Nico Antonio Cortez,[a] Eden Dangngay,[a] Elizabeth Del Rosario,[a] Ysabelle Louie Dela Cruz,[a] Kimberly Dela Pacion,[a] Junelin Deocampo Jr,[a] Catherine Allyson Diaz,[a] Dave Chester Febrio,[a] Gayle Fernandez,[b] Kclyn Gregorio,[a] Analize Marie Jacob,[a] Junito Julio Jr,[a] Mary Grace Labayen,[c] Alyanna Leaño,[a] Gabriel Lukban,[d] Charo Mahilum,[a] Athina Manzano,[a] Michael Mojica,[a] Grace Omac,[a] Vanezza Ann Pascual,[a] Mary Coleen Rivera,[c] Adrian Rafael Rodriguez,[a] Frances Catherine Rosario,[a] Shaima Jacinta Sotero[a] and Herbert Valencia.[a]

[a] Health Program Officer II

[b] Health Program Researcher

[c] Medical Technologist II

[d] Medical Officer III

Conflicts of interest

The author has no conflicts of interest to declare.

Ethics statement

This study received an exemption from ethics review issued by the Department of Health Single Joint Research Ethics Board on 19 February 2025 (protocol code: SJREB-2025-15).

Funding

None.

References

1. DOH reports 85% decrease in fireworks injuries for 2021. Philippine News Agency; 1 January 2021. Available from: https://www.pna.gov.ph/articles/1126103, accessed 24 October 2025.
2. Dela Peña K. Increase in firecracker injuries shows lessons never learned. Cebu Daily News; 31 December 2024. Available from: https://cebudailynews.inquirer.net/614901/increase-in-firecracker-injuries-shows-lessons-never-learned, accessed 22 October 2025.
3. Cabato L. Fireworks-related injuries post 50% increase, says DOH. Inquirer.net; 6 January 2024. Available from: https://newsinfo.inquirer.net/1884763/fireworks-related-injuries-post-50-increase-says-doh, accessed 12 December 2024.
4. Roca JB, de los Reyes VC, Racelis S, Deveraturda I, Sucaldito MN, Tayag E, et al. Fireworks-related injury surveillance in the Philippines: trends in 2010–2014. Western Pac Surveill Response J. 2015;6(4):1–6. doi:10.5365/wpsar.2015.6.1.014 pmid:26798555
5. Montemayor MT, Caliwan CL, Agoot L. DOH reports 443 firecrackers, stray bullet victims. Philippine News Agency; 2 January 2024. Available from: https://www.pna.gov.ph/articles/1216231, accessed 12 December 2024.
6. Jaymalin M, Lazaro RE. Fireworks-related injuries up 39% – DOH. Philstar.com; 29 December 2022. Available from: https://www.philstar.com/nation/2022/12/29/2233881/fireworks-related-injuries-39-doh, accessed 12 December 2024.
7. Rivera AS, Lam HY, Macalino JU. Epidemiology of injuries in the Philippines: an analysis of secondary data. Acta Med Philipp. 2018;52(2):180–6. doi:10.47895/amp.v52i2.442
8. Wahi MM, Dukach N. Visualizing infection surveillance data for policymaking using open source dashboarding. Appl Clin Inform. 2019;10(3):534–42. doi:10.1055/s-0039-1693649 pmid:31340399
9. Weir BS, Vordtriede C, Lee JE, Metter EJ, Talbot LA. An interdisciplinary dashboard to streamline medication processing at patient discharge: a quality improvement initiative. Mil Med. 2023;188(7-8):usab526. doi:10.1093/milmed/usab526 pmid:34950952
10. Ong KPS. Optimizing and automating aggregation and visualization of COVID-19 data in Metro Manila, Philippines, through the use of a free dashboard software: a case study. J Public Health Manag Pract. 2025;31(6):E361–7. doi:10.1097/PHH.0000000000002215 pmid:40779696

World Health Organization
Western Pacific Region

WPSAR
Western Pacific Surveillance and Response Journal

wpsar@who.int | https://ojs.wpro.who.int/